

2007

The Expression and Function of PPAR and HIF-1 in Human Melanoma

Caroline Mills

Follow this and additional works at: <http://mds.marshall.edu/etd>

 Part of the [Cancer Biology Commons](#), [Cell Biology Commons](#), [Cells Commons](#), [Integumentary System Commons](#), and the [Medical Cell Biology Commons](#)

Recommended Citation

Mills, Caroline, "The Expression and Function of PPAR and HIF-1 in Human Melanoma" (2007). *Theses, Dissertations and Capstones*. Paper 757.

THE EXPRESSION AND FUNCTION OF PPAR AND HIF-1 IN HUMAN MELANOMA

DISSERTATION

Submitted to the Graduate School

Of

Marshall University

In Partial Fulfillment of the Requirement for

The Degree of Doctor of Philosophy

By

Caroline Mills

Huntington

West Virginia

2007

©COPYRIGHT 2007

APPROVAL OF EXAMINING COMMITTEE

TO MY FAMILY, FRIENDS, and COWORKERS

ACKNOWLEDGEMENTS

First and foremost, I would like to thank my grandmother, Angeline Legg, for all of her support, love, and guidance. She made me who I am, and inspired who I will become. I love you always and forever. Thank you so much. I also have to thank my mother, Barbara Mathis, who worked most of her life away to give me a wonderful and happy life. She always believes in me and is always on my side, and I love her for this. I need to thank my father, Theodore R. Mills, for his unwavering support of my goals. He always made sure that I knew I had his love and that he truly wanted nothing more than for me to accomplish this milestone. My extended family was always supportive and helpful in so many ways. I could have never made this journey without the help of all of these people. I hope that I can continue to make all of you proud.

My coworkers have been an indispensable part of this as well. I know that I could not have made a better choice for a mentor than Dr. Richard Niles. He has always had my best interests at heart. He has given me the strength, confidence, and skill that I will need to be an excellent mentor when my time comes. Thank you so much. Dr. Beverly Delidow has been such a positive influence on my journey as well. She has shown me the character and determination that it takes to be a woman of science. Many thanks for all of the advice and conversation. All of my committee members have been there for me at one time or another to help me through a seemingly impossible situation. I can not even begin to thank you all enough for all that you have done for me. All of my lab mates have been excellent

to learn from and work with. I know that I could have never made it this far without the guidance of Linda Eastham. She has helped me through so many problems and difficulties. I can never thank you enough, Linda. She, too, will make an excellent mentor soon. To all the other people I have had the joy of working with, thank you, thank you, thank you. I will never forget it. Now, let's go find a cure...

ABSTRACT

The first part of my dissertation focuses on the expression and function of PPARs in human melanoma. I found that the A375 cells were significantly growth inhibited in response to PGJ₂ and troglitazone treatment. HEMn-LP showed significant growth inhibition in response to troglitazone. I found that PPAR γ and PPAR δ mRNA is present in both the SK-Mel 28 and A375 cells. The relative level of PPAR α mRNA expression is highest in SK-Mel 28 cells, ~3 fold higher relative to both the normal human melanocytes and A375 cells. PPAR γ protein was ~50% higher in both SK-Mel 28 and A375 cells relative to the HEMn-LP. PPAR α protein levels were highest in the A375 cells. Consistent 80% knockdown of PPAR α was achieved through siRNA treatment; however, there was no change in cellular morphology. There was also no decrease in expression of a direct PPAR α target, MCAD. Therefore, a reasonable conclusion is that the increased expression of PPAR α in SK-Mel28 cells is not contributing to its *in vitro* transformed phenotype.

Hypoxia inducible factor 1 α , HIF-1 α , is a transcription factor that has been shown to be a master regulator of oxygen homeostasis. A splice variant of HIF-1 α , HIF-1 α 785, is missing exon 11 from its oxygen dependent degradation domain. This region encodes the lysine that is critical for enhancing HIF-1 α degradation. The role of HIF-1 α in the progression of human melanoma has not been fully elucidated. Here, I show for the first time that in human melanoma, HIF-1 α is expressed endogenously with no external stimuli under normoxic conditions. In cell lines derived from RGP, VGP, and metastatic phases of human melanoma progression,

the relative amounts of HIF-1 α and HIF-1 α 785 mRNA increase as a function of malignant progression. The expression levels have been verified by qPCR and western blot. Overexpression of HIF-1 α or HIF-1 α 785 in SbCl₂ cells leads to increased anchorage independent growth, with HIF-1 α 785 having the greater impact. In WM9 cells, inhibition of HIF-1 α by siRNA significantly inhibits matrigel invasion and anchorage independent growth in soft agar. These results show that in human melanoma, HIF-1 α and HIF-1 α 785 seem to function to increase tumorigenicity.

TABLE OF CONTENTS

TITLE PAGE	i
NOTICE OF COPYRIGHT	ii
APPROVAL OF EXAMINING COMMITTEE.....	iii
DEDICATION PAGE.....	iv
ACKNOWLEDGEMENTS.....	v
ABSTRACT	vii
TABLE OF CONTENTS.....	ix
LIST OF FIGURES.....	xiii
LIST OF ABBREVIATIONS.....	xv
REVIEW OF THE LITERATURE - PART I	1
MELANOMA.....	1
NUCLEAR RECEPTORS.....	4
PEROXISOME PROLIFERATOR ACTIVATED RECEPTORS	5
PPAR γ	7
Natural Ligands of PPAR γ	7
Synthetic Ligands of PPAR γ	11
PPAR γ Antagonists.....	13
PPAR γ is required for development.....	15
REGULATION OF PPAR γ	16
Transcriptional level.....	16
Post-translational Regulation.....	17
Corepressors and Coactivators.....	19
Role of PPAR γ in Disease.....	19
Role of PPAR γ in melanoma.....	21
PPAR α	22
Natural Ligands of PPAR α	22
Synthetic ligands for PPAR α	23
PPAR α Antagonists	23

PPAR α Knockouts.....	24
Regulation of PPAR α	24
Post – translational PPAR α control.....	24
Role of PPAR α in disease.....	26
PPAR δ	27
Natural ligands of PPAR δ	27
Synthetic ligands of PPAR δ	28
PPAR δ knockouts	28
Regulation of PPAR δ	29
Transcriptional Regulation of PPAR δ	29
Role of PPAR δ in disease.....	29
REVIEW OF THE LITERATURE - PART II	30
HIF-1	30
Structure of HIF-1	31
Regulation of HIF-1	32
Transcriptional regulation	32
Post translational regulation of HIF-1 α	34
Control of HIF-1 α protein stability by acetylation	38
Control of HIF-1 α activity by hydroxylation.....	38
Control of HIF-1 α by growth factor stimulation.....	38
Control of HIF-1 α activity by phosphorylation	39
Control of HIF-1 α activity by sumoylation	39
Control of HIF-1 α activity by heterodimerization	40
HIF-1 antagonists	40
Physiological Roles of HIF-1	41
Role of HIF-1 in development.....	42
Role of HIF-1 in ischemia.....	42
Role of HIF-1 in cancer.....	43
Role of HIF-1 in melanoma	45
EXPERIMENTAL OBJECTIVE.....	46
CHAPTER I.....	48

Function of PPARs in human melanoma progression.....	48
INTRODUCTION.....	49
MATERIALS AND METHODS.....	50
Cell and Culture Conditions	50
PGJ ₂ , Ciglitazone, Troglitazone, WY-14643, and LTB ₄	50
Anchorage-Dependent Growth.....	51
Relative Melanin Content.....	52
RT-PCR	52
Quantigene® assay	53
Western Blotting	54
RESULTS	56
Anchorage-Dependent growth in human melanoma and normal human melanocyte cell lines treated with PPAR agonists.....	56
Expression of PPAR subtype mRNA	57
Expression of PPAR subtype protein	89
Decrease in SK-Mel 28 cell PPAR α by siRNA knockdown	89
DISCUSSION – Part I.....	101
INTRODUCTION TO DISSERTATION PART II.....	106
CHAPTER II.....	110
Function of HIF-1 in human melanoma progression.....	110
MATERIALS AND METHODS.....	111
Cell lines and cell culture conditions.....	111
Western Blot analysis of HIF-1 α	111
RT-PCR for HIF-1 α and HIF-1 α 785.....	112
Quantitative PCR for HIF-1 α and HIF-1 α 785	112
Overexpression of HIF-1 α or HIF-1 α 785 in SbCl ₂ cells	113
siRNA inhibition of HIF-1 α in WM9 human metastatic cells.....	114
Matrigel invasion assay	114
Anchorage-independent growth assay.....	115
RESULTS	116

Expression of HIF-1 α in human melanoma cells.....	116
Expression of HIF-1 α mRNA.....	116
HIF-1 α and HIF-1 α 785 gain of function in radial growth phase SbCl ₂ cells	117
HIF-1 α loss-of-function in human metastatic melanoma WM9 cells.....	118
DISCUSSION – Part II	136
SUMMARY AND CONCLUSIONS.....	142
REFERENCES.....	144
Curriculum Vitae.....	165

LIST OF FIGURES

Figure 1	Progression from normal human melanocytes to metastatic melanoma	3
Figure 2	Structural diagram of nuclear hormone receptor domains	9
Figure 3	Schematic representation of the functional domains of both HIF-1 α full length and HIF-1 α 785	37
Figure 4	Anchorage-dependent growth study in SK-Mel 28 treated with PGJ ₂	60
Figure 5	Melanin production in SK-Mel 28 treated with PGJ ₂	62
Figure 6	Anchorage-dependent growth study in SK-Mel 28 treated with ciglitazone	64
Figure 7	Anchorage-dependent growth study in SK-Mel 28 treated with WY-14643	66
Figure 8	Anchorage-dependent growth study in SK-Mel 28 treated with troglitazone	68
Figure 9	Anchorage-dependent growth study in A375 treated with PGJ ₂	70
Figure 10	Anchorage-dependent growth study in A375 treated with ciglitazone	72
Figure 11	Anchorage-dependent growth study in A375 treated with WY-14643	74
Figure 12	Anchorage-dependent growth study in A375 treated with LTB ₄	76
Figure 13	Anchorage-dependent growth study in A375 treated with troglitazone	78
Figure 14	Anchorage-dependent growth study in HEMn-LP treated with troglitazone	80
Figure 15	Melanin production in HEMn-LP treated with troglitazone	82
Figure 16	Anchorage-dependent growth study in HEMn-LP treated with PGJ ₂	84
Figure 17	RT-PCR for PPARs in human melanoma cells	86
Figure 18	Quantigene® analysis to determine relative expression of PPAR α mRNA	88
Figure 19	PPAR α protein expression in human melanoma and normal melanocytes	92

Figure 20	PPARγ protein expression in human melanoma and HEMn-LP	94
Figure 21	Quantigene® analysis to determine siRNA knockdown of PPARα	96
Figure 22	MCAD protein expression in SK-Mel 28 cells	98
Figure 23	A. Image of SK-Mel 28 cells treated with control siRNA	100
	B. Image of SK-Mel 28 cells treated with PPARα siRNA	100
Figure 24	A. HIF-1α protein expression in A375 and HEMn-LP	120
	B. HIF-1α protein expression in HEMn-LP, SbCl₂, WM1366, and WM9	120
Figure 25	RT-PCR for HIF-1α and HIF-1α785 in HEMn-LP, SbCl₂, WM1366, and WM9	122
Figure 26	A. qPCR for HIF-1α and HIF-1α785 in HEMn-LP, SbCl₂, WM1366, and WM9 at 24h	124
	B. qPCR for HIF-1α and HIF-1α785 in HEMn-LP, SbCl₂, WM1366, and WM9 at 72h	124
Figure 27	Representation of the pLenti-V5-D-TOPO vector	126
Figure 28	Expression of HIF-1α785 tagged with the V5 epitope in SbCl₂ cells	128
Figure 29	Anchorage-independent growth of SbCl₂ cells expressing HIF-1α or HIF-1α785	130
Figure 30	Matrigel invasion assay in WM9 cells treated with HIF-1α siRNA	132
Figure 31	Anchorage independent growth of WM9 cells treated with HIF-1α siRNA – Day 4	134
Figure 32	Anchorage independent growth of WM9 cells treated with HIF-1α siRNA – Day 5	136

LIST OF ABBREVIATIONS

15-S-HETE	15-S-hydroxyeicosatetraenoic acid
ABCA1	ATP binding cassette transporter 1
ADD-1	Adipocyte Differentiation and Determination factor 1
AF-1	activation function – 1
AF-2	activation function – 2
Akt	RAC serine/threonine-protein kinase
AP-1	activating protein 1
ARD1	ADP-ribosylation factor domain protein 1
Arnt	Ah receptor nuclear translocator protein
BADGE	bisphenol-A-diglycidyl ether
BCL-6	B-cell lymphoma gene 6
BCS	bovine calf serum
bHLH	basic helix loop helix
C/EBP	CCAAT/enhancer core binding protein
CBP	creb binding protein
CDK	cyclin dependent kinase
c-Ets-1	erythroblastosis virus E26 oncogene homolog 1
CREB	cAMP response element-binding protein
DBD	DNA – binding domain
ddH ₂ O	Double distilled H ₂ O
dH ₂ O	Distilled H ₂ O
DMBA	7,12-dimethylbenz[a]anthracene
DMEM	Dulbecco's Modified Eagle's Medium
DMSO	dimethylsulfoxide
DNA	deoxyribonucleic acid
DR	direct repeat
Egr-1	early growth response 1

ERK	extracellular signal-regulated protein kinase
ES	embryonic stem cells
FABP	fatty acid binding protein
FIH1	factor inhibiting HIF-1
FLIP	FLICE-inhibitory protein
GAPDH	glyceraldehyde 3-phosphate dehydrogenase
HASMC	human aortic smooth muscle cells
HDL	high density lipoprotein
HIF-1	Hypoxia-inducible factor 1 heterodimer
HIF-1 α	hypoxia-inducible factor 1 subunit α
HIF-1 α 785	Hypoxia-inducible factor 1 subunit α splice variant 785
HMGS	human melanocyte growth serum
HNF4	hepatocyte nuclear factor 4
HRE	hypoxia response element
IBMX	3-isobutyl-1-methylxanthine
IL-6	interleukin 6
IPAS	inhibitory PAS molecule
JNK	c-Jun N-terminal kinase
KRAB	Kruppel-Associated Box domain
LBD	ligand binding domain
LDL	low density lipoproteins
LPA	lysophosphatidic acid
LTB ₄	leukotriene B4
LXR α	liver X receptor α
M (in figures)	Molecular marker
MAPK	mitogen activated protein kinase
MCAD	medium chain acyl dehydrogenase
MM	metastatic melanoma

mTOR	mammalian target of rapamycin
NAB2	nuclear polyadenylated RNA-binding protein 2
NCoR	nuclear receptor corepressor
NF-1	nuclear factor 1
NF-KB	nuclear factor KB
NHM	normal human melanocytes
ODDD	oxygen dependent degradation domain
PAS	per-arnt-sim
PBS	phosphate buffered saline
Per	period circadian protein
PGD2	prostaglandin D2
PGJ ₂	15-deoxy-D-12,14-prostaglandin J2
PGJ ₂	15-deoxy-D-12,14-prostaglandin J2
PHD	prolyl hydroxylase
PI3K	phosphoinositide-3-kinase
PKA	protein kinase A
PKC	protein kinase c
PMA	phorbol 12-myristate 13-acetate
PPAR	peroxisome proliferator activated receptor
PPRE	peroxisome proliferator activated receptor response element
pRb	phospho-retinoblastoma protein
PUFA	polyunsaturated fatty acids
RGP	radial growth phase
RT-PCR	reverse transcriptase-polymerase chain reaction
RXR	retinoid X receptor
SDS-PAGE	sodium dodecyl sulfate-polyacrylamide gel electrophoresis
Sim	single-minded protein
SMRT	silencing mediator of retinoic acid and thyroid hormone receptor

SR-202	dimethyl α -(dimethoxyphosphinyl)-p-chlorobenzyl phosphate
SRC-1	steroid receptor coactivator-1
SREBP-1	Sterol Regulatory Element Binding Protein 1
TBS	tris-buffered saline
TBST	tris-buffered saline with Tween-20
TCF-4	T cell factor 4
TGF β	transforming growth factor β
TNF α	tumor necrosis factor α
TRAIL	TNF-related apoptosis inducing ligand
TZD	thiazolidinedione
VEGF	vascular endothelial growth factor
VGP	vertical growth phase
VHL	von Hippel Lindau tumor suppressor
VLDL	very low density lipoprotein
ZFP	zinc finger proteins

REVIEW OF THE LITERATURE – PART I

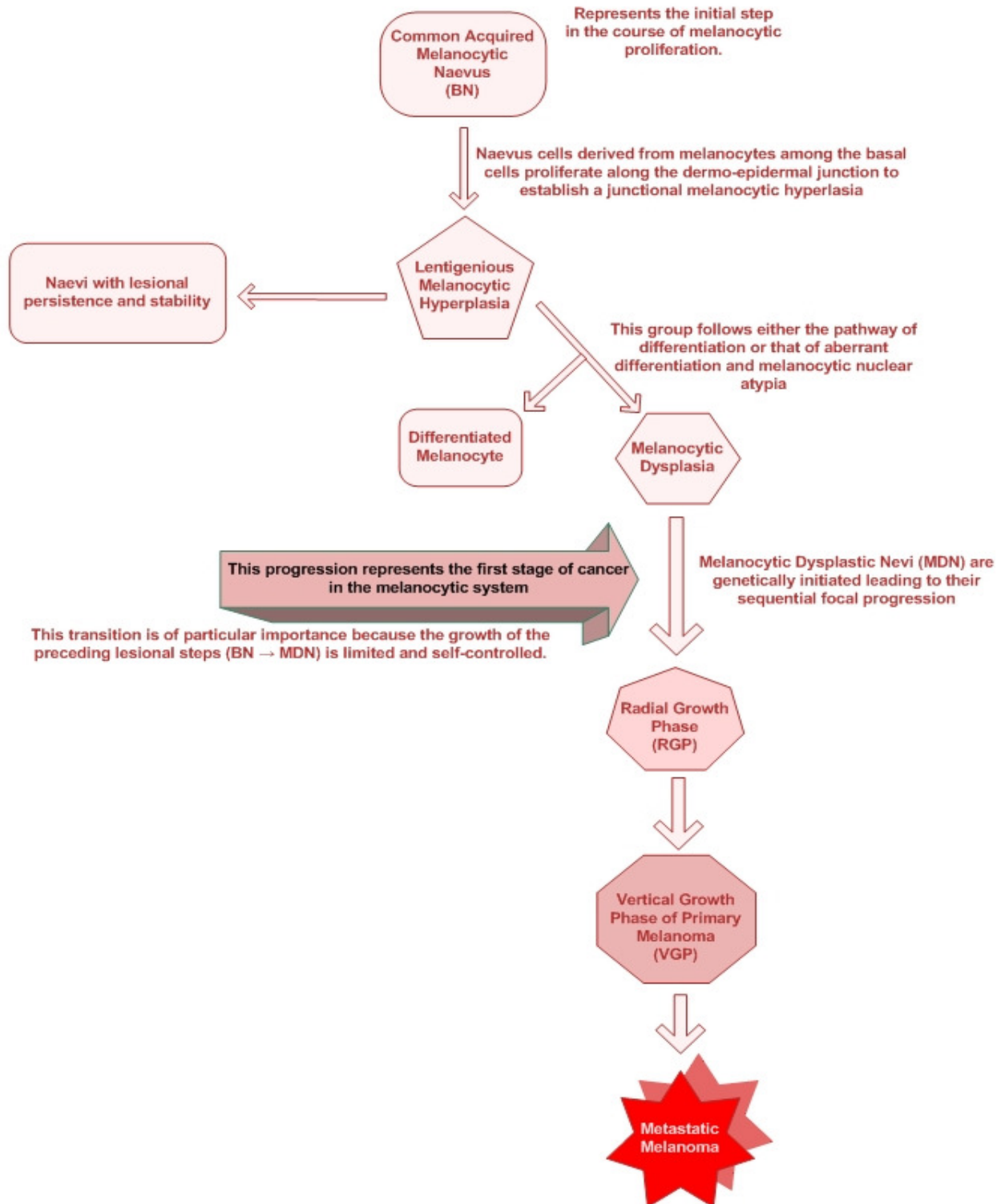
MELANOMA

Melanoma is the most serious form of skin cancer. Melanoma cells derive from the skin's natural defense system to UV light, the melanocyte. Melanocytes absorb UV light and in response, produce the pigment, melanin. To defeat the stresses of this unique function, the melanocytes are inherently and naturally resistant to apoptosis (Soengas and Lowe 2003). Melanoma incidence is increasing at an alarming rate in the U.S. Melanoma accounts for 4% of all skin cancers, but for 79% of all skin cancer-related deaths in the United States (Melanoma Research Foundation fact sheet 2006).

Melanoma has several clinical stages. These range from a radial growth phase (RGP) → vertical growth phase (VGP) → metastatic melanoma (MM). Radial growth phase cells have the ability to grow without differentiation; however, they are non-tumorigenic in patients and animal models (Satyamoorthy *et al.*, 1999). They have partial growth autonomy (Hussein MR, 2005). After the accumulation of more genetic changes such as overexpression of oncogenes and loss of certain tumor suppressor genes, RGP melanoma cells progress to VGP cells. Vertical growth phase cells have acquired the ability to invade into the dermis (Satyamoorthy *et al.*, 1999). Metastatic cells not only have the ability to invade but to also travel to distant sites resulting in secondary tumors (**Figure 1**). The later stages of the disease are notoriously resistant to chemo- and radiotherapy. More investigation is needed to determine targets allowing circumvention of survival mechanisms inherent not only to melanoma cells, but also to melanocytes (Soengas and Lowe 2003).

Figure 1: Diagram showing the progression from normal human melanocytes to metastatic melanoma. The progression from melanocytic dysplasia to radial growth phase represents the initial stage of cancer in human melanoma progression. Radial growth phase cells have very limited anchorage-independent growth capabilities and little to no invasion capacity. Vertical growth phase cells are able to form tumors in mice, have increased anchorage-independent growth capabilities and a high level of invasion. Metastatic melanoma cells have acquired the ability to travel to secondary sites to form secondary tumors.

Figure 1: Progression from normal human melanocytes to metastatic melanoma.



NUCLEAR RECEPTORS

Nuclear receptors are a superfamily of transcription factors that regulate the expression of hundreds of important target genes. These genes can be involved in a variety of processes including cell division, organogenesis, homeostasis, and reproduction (Wu *et al.*, 2005). This superfamily includes the vitamin D receptors, thyroid hormone receptors, retinoid receptors, steroid receptors and several orphan receptors (no endogenous ligand known). Nuclear receptors are ligand activated and require the sequential recruitment of coactivators to fully induce gene transcription. Nuclear receptors allow cells to respond to extracellular signals via the binding of their respective ligands (Friedmann *et al.*, 2005). Nuclear receptors have several conserved functional domains (**Figure 2**). Progressing from the N- to the C- terminus are the first activation function (AF-1) domain, the DNA-binding domain, a hinge region, as well as a ligand-binding domain that includes the second activation function (AF-2) domain (Wu *et al.*, 2005). The AF-1 domain, sometimes referred to as the A/B domain, has transactivation activity. It has highly variable sequences and lengths among nuclear receptors and is often the origin of multiple splice variants resulting in different isoforms of the same nuclear receptor. The DNA-binding domain (DBD) is the most highly conserved region of the nuclear receptors and is responsible for recognizing and binding the receptor's cognate DNA response element in the target gene's promoter region. The DBD is also responsible for nuclear receptor homo- or heterodimerization. The ligand binding domain (LBD) of nuclear receptors also varies between nuclear receptors, but the structure of the LBD is common to nearly all of the nuclear receptors.

The LBD has 11-13 alpha helices that form a hydrophobic binding pocket to accommodate the nuclear receptor ligand. The residues at the bottom of the LBD pocket confer specificity, determining whether or not the nuclear receptor will bind its specific ligands such as all-trans retinoic acid, vitamin D₃, estrogen, etc. The LBD also accommodates binding of the nuclear receptor to heat shock proteins as well as coactivators or corepressors and is also responsible for nuclear localization of the receptor. The second activation function (AF-2 domain) at the C-terminal end of the nuclear receptor is thought to act as a "flap" that closes back onto the LBD inducing a conformational change inhibiting further ligand binding and allowing interaction with coactivators (McAdara J., 2000).

PEROXISOME PROLIFERATOR ACTIVATED RECEPTORS

Peroxisome Proliferator Activated Receptors (PPARs) are ligand-activated nuclear receptors. They belong to the subfamily of nuclear receptors termed orphan receptors. They were first shown to be responsive to a class of chemicals called peroxisome proliferators. Peroxisomes are cellular organelles that are involved in the removal of molecular O₂ and the breakdown of H₂O₂. Other functions of peroxisomes include fatty acid oxidation, cholesterol biosynthesis, and glycerolipid synthesis (Vamecq *et al.*, 1999). Peroxisome proliferators were shown to cause an expansion of the population of peroxisomes in the livers of rats (Issemann and Green 1990). The PPARs have been shown to regulate a myriad of target genes involved in several biological processes such as inflammation and the immune response, cell proliferation, cell differentiation, angiogenesis, and lipid and glucose metabolism (Friedmann *et al.*, 2005).

There are 3 isotypes of PPAR: PPAR γ , PPAR α , and PPAR β/δ . Each isotype is encoded by a different gene, and has specific functions as well as specific patterns of tissue distribution. PPARs have been localized mainly to the liver where there is a high fatty acid metabolism, but have also been reported to be expressed in heart, B and T lymphocytes (Jones *et al.*, 2002), fat, kidney, vascular smooth muscle and in keratinocytes (Westergaard *et al.*, 2001). PPARs have the typical nuclear receptor functional domains; however, each isotype has a distinctive ligand binding domain. PPAR ligand binding induces conformational changes which stabilize their interaction with coactivators and destabilize their interactions with corepressors. The three PPARs have ligand binding domains that are significantly larger than that of other ligand-activated nuclear receptors. The length of the ligand binding domain of the PPARs is ~1300 Å. Of this 1300 Å, only 30-40% is occupied by ligand (Xu *et al.*, 2001). It is thought that the large size of the ligand binding domain explains why the PPARs can bind to multiple natural and synthetic ligands. Even though promiscuous, there still remain structural determinants of each PPAR isotype in their respective ligand binding domains.

The ligand binding domain of the PPARs also facilitates their heterodimerization with the receptor for 9-cis retinoic acid, retinoid X receptor (RXR). Once ligand is bound to the PPAR, there is a conformational change that enables this heterodimerization (Friedmann *et al.*, 2005). This heterodimerization is necessary for the PPARs to recognize and bind to their DNA response elements within their target genes' promoter regions. The PPAR:RXR heterodimer recognizes a Peroxisome Proliferator Response Element (PPRE) consisting of a direct repeat (DR) of the hexameric sequence

AGGTCA with 1 nucleotide between the repeats. The ligand for the RXR is not required for the transcriptional activation of the PPAR:RXR heterodimer; however if present, it has been shown to have a synergistic effect in combination with a PPAR ligand (Kliewer, S.A. 1992). In the absence of ligand, the PPAR:RXR heterodimer is associated with corepressors which inhibit its ability to activate gene transcription (Wahli W., 2002).

PPAR γ

Peroxisome Proliferator Activated Receptor γ has a molecular weight of ~56kD. The gene encoding PPAR γ is located on human chromosome 3p25. There are two isoforms, PPAR γ 1 and PPAR γ 2, resulting from 4 splice variants of the PPAR γ gene. Splice variants 1, 3, and 4 encode the same PPAR γ 1 isoform. Splice variant 2 encodes the PPAR γ 2 isoform. PPAR γ 2 has a longer and distinct N-terminus relative to PPAR γ 1.

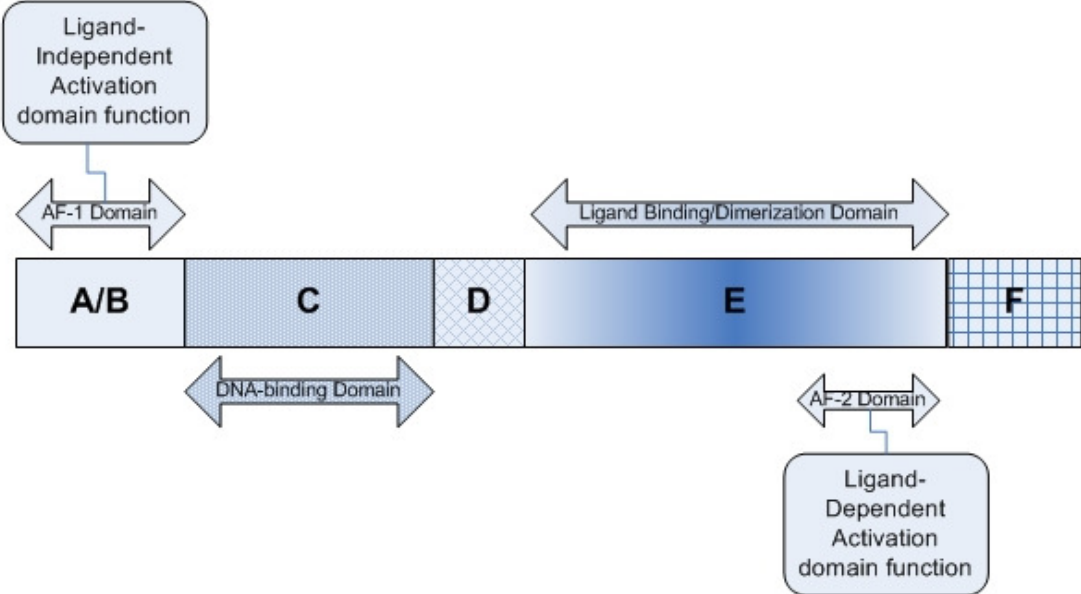
Natural Ligands of PPAR γ

Essential fatty acids are required in the human diet and can neither be synthesized nor derived from other fatty acids. There are two families of essential fatty acids: Omega-3 (ω -3) and Omega-6 (ω -6). These essential fatty acids are modified to form lipoxins, resolvins, lipid rafts, and the eicosanoid family of oxygenated hydrophobic molecules.

Most human eicosanoids are derived from arachidonic acid, a metabolite of linoleic acid. Arachidonic acid can feed into either the 5-lipoxygenase pathway or into the cyclooxygenase (prostanoid) pathway. The 5-lipoxygenase pathway results in the

Figure 2: Structural diagram of nuclear hormone receptor domains. The variable NH₂-terminal region (A/B) consists of the ligand-independent AF-1 transactivation domain. The highly conserved DNA-binding domain (C) is responsible for response element recognition and binding. A variable linker region (D) is connected to the conserved E/F region that contains the ligand-binding domain, the dimerization surface, and the ligand-dependent AF-2 transactivation domain.

Figure 2: Structural diagram of nuclear hormone receptor domains.



formation of the leukotriene family of eicosanoid lipid molecules. The cyclooxygenase pathway results in the formation of prostaglandin, prostacyclin, and thromboxane lipid molecules.

PPAR γ can be activated by long chain polyunsaturated fatty acids (PUFAs), fatty acid components of oxidized low density lipoproteins (LDLs), as well as certain metabolites derived from the cyclooxygenase and lipoxygenase pathways i.e., 15-deoxy-D-12,14-prostaglandin J₂ (PGJ₂) and 15-S-hydroxyeicosatetraenoic Acid (15-S-HETE), respectively. PGJ₂, a metabolite of the PGD₂ branch of the cyclooxygenase pathway, is thought to be the most potent endogenous ligand for PPAR γ (Forman *et al.*, 1995). PGJ₂ was shown to directly interact with PPAR γ in 1995 by Kliewer *et al.* (Kliewer *et al.*, 1995). Leukemia cell lines (HL-60) treated with PGJ₂ showed a significant decrease in cellular proliferation and DNA synthesis (Yamakawa-Karakida *et al.*, 2002). In lung cancer cell lines, A549, H345, and N417, 72-hour 4 μ mol/L PGJ₂ treatment was shown to inhibit their growth by 50%, 90%, and 85% respectively (Avis *et al.*, 2005). However, PGJ₂ has also been reported to be non-specific for PPAR γ . Co-treatment experiments in macrophages were conducted with a competitive inhibitor (a thiazolidinedione (TZD) compound, AD-5075) which could bind PPAR γ but not induce any anti-inflammatory effects. When this inhibitor was used at a concentration that would have all but completely displaced any PGJ₂ binding, PGJ₂ treatment exhibited the same anti-inflammatory effects as those seen in control cells lacking the competitive inhibitor (Thieringer *et al.*, 2000). It was also shown that in PPAR γ -deficient

macrophages, PGJ₂ treatment inhibited PMA-induced IL-6 production at similar levels compared to the PPAR_γ-wild type macrophages (Moore *et al.*, 2001).

15-S-HETE was shown to activate PPAR_γ-dependent transcription in PC3 prostate cancer cells as well as in DU-145 cells (Shappell *et al.*, 2001). Also, when compared to a known synthetic PPAR_γ agonist, BRL49653 (rosiglitazone), 15-S-HETE was also able to induce a dose-dependent inhibition of soft-agar colony formation of PC3 cells (Shappell *et al.*, 2001).

Lysophosphatidic acid (LPA), a lipid mediator which controls mobility, differentiation, and cellular growth, is another natural ligand of PPAR_γ. In competitive binding studies, LPA was able to displace [3H]-rosiglitazone (a synthetic ligand for PPAR_γ) from immobilized PPAR_γ (McIntyre *et al.*, 2003). LPA was also shown to be able to stimulate a luciferase reporter gene controlled by a PPRE in RAW264.7 cells, a macrophage-like cell line. Co-transfection with PPAR_γ enhanced the effect of LPA on the PPRE reporter gene luciferase activity (McIntyre *et al.*, 2003). LPA has been shown to induce the atherosclerotic plaque precursor, neointimas. This LPA-induced neointima production in rat carotid artery tissue was abolished by treatment with the irreversible PPAR_γ antagonist, GW9662 (Zhang *et al.*, 2004).

Synthetic Ligands of PPAR_γ

Synthetic ligands for PPAR_γ include the thiazolidinedione (TZD) class of anti-diabetic drugs, i.e. Rezulin® (troglitazone) as well as some newly discovered non-thiazolidinedione compounds. TZD derivatives include BRL49653 (rosiglitazone),

pioglitazone, ciglitazone, and englitazone, and troglitazone (Houseknecht *et al.*, 2002; Lehmann *et al.*, 1995). TZDs, which are used as insulin sensitizers, are high-affinity ligands for PPAR γ . It has been found that the most potent of the synthetic ligands for PPAR γ is rosiglitazone followed by troglitazone, pioglitazone, ciglitazone, and finally englitazone (Lehmann *et al.*, 1995). Rezulin® has been shown to bind to PPAR γ with very high affinity $K_d = 40\text{nM}$ (Spiegelman B., 1998). Rezulin®'s effects on insulin sensitivity in humans has been shown to be mediated through PPAR γ interactions by Wilson and Cobb in 1996 (Wilson *et al.*, 1996). While Rezulin® was used to treat type 2 diabetes mellitus, it was determined by the FDA in March 2000 that it had toxic effects on the liver, relative to other thiazolidinedione derivatives rosiglitazone (Avandia®) and pioglitazone (Actos®) and was subsequently pulled from the market.

RWJ-348260 is a very potent non-TZD synthetic ligand for PPAR γ . Using a PPAR γ -Gal4 chimera reporter assay, RWJ-348260 induced PPAR γ reporter gene transcription with similar effectiveness to rosiglitazone (Rybczynski *et al.*, 2004). RWJ-348260 was shown to bind to PPAR γ with a binding affinity of $K_d = 216 \pm 99 \text{ nM}$, similar to that of rosiglitazone, $K_d = 242 \pm 22 \text{ nM}$. *In vivo*, this compound is an insulin sensitizer. It improved glucose tolerance as well as reduced glucose, insulin, and HbA1c levels in diabetic animals (Rybczynski *et al.*, 2004).

Recently, a new synthetic non-TZD PPAR γ agonist has been found. T33, formerly called T11, is a benzopyran derivative. T33 was shown to be able to activate a human PPAR γ based reporter gene assay with an EC50 value of 19 nmol/L (Hu *et al.*, 2006). There was a dose dependent reduction in blood glucose levels which was even

more significant than what rosiglitazone was able to accomplish in *ob/ob* mice (Hu *et al.*, 2006). This study also showed that T33 treatment resulted in a marked improvement in oral glucose tolerance and insulin tolerance in the *ob/ob* mice.

PPAR γ Antagonists

The most extensively studied aspect of PPAR γ has certainly been its ability to treat type II diabetes via the TZD agonists' ability to enhance insulin sensitivity and lower blood glucose and lipid levels. However, there are negative side-effects to these treatments. PPAR γ activation can increase adipocyte differentiation and therefore weight gain in these patients. There are PPAR γ modulators that can potentially have both anti-obesity as well as anti-diabetic effects. These modulators are more often than not PPAR γ antagonists.

There have been a number of PPAR γ antagonists synthesized to date including GW9662, bisphenol-A-diglycidyl ether (BADGE), PD 068235, LG 100641, GW0072 (partial agonist/antagonist), and recently SR-202 [dimethyl α -(dimethoxyphosphinyl)-p-chlorobenzyl phosphate]. GW9662 is an irreversible antagonist for PPAR γ (Gupta *et al.*, 2001). The mechanism of GW9662 antagonism is covalent modification of a cysteine residue (#285) in the LBD of PPAR γ (Leesnitzer *et al.*, 2002). GW9662 has been shown to have a 10-fold more potent binding to PPAR γ than to PPAR α , and a 600-fold more potent binding to PPAR γ than to PPAR δ (Leesnitzer *et al.*, 2002).

Another PPAR γ antagonist is BADGE (Yamauchi *et al.*, 2001). BADGE was shown to inhibit the transactivation of PPAR γ by 70% and to significantly decrease the

expression of PPAR γ target genes such as CD36 (Yamauchi *et al.*, 2001).

PD 068235 is a PPAR γ specific antagonist shown to cause a dose-dependent decrease in rosiglitazone-stimulated PPAR γ transactivation with an IC₅₀ of 0.82 μ M (Camp *et al.*, 2001). Co-incubation of rosiglitazone with increasing concentrations of PD 068235 resulted in a dose-dependent decrease in the recruitment of the coactivator SRC-1 to the PPAR γ receptor (Camp *et al.*, 2001). A hallmark of TZD-induced PPAR γ activation is the adipocyte differentiation which has been demonstrated in several preadipocyte cell lines. PD 068235 was able to antagonize rosiglitazone-stimulated adipocyte differentiation *in vitro* (Camp *et al.*, 2001).

LG100641 binds to PPAR γ and displaces the TZDs from the receptor but does not activate transcription of its target genes. LG100641 antagonizes TZD-induced adipocyte differentiation while retaining the ability to stimulate insulin-mediated glucose uptake in the adipocytes (Mukherjee *et al.*, 2000). It is thought that this antagonism is a result of LG100641 binding inhibiting the recruitment of the coactivator SRC-1 to the PPAR γ LBD (Mukherjee *et al.*, 2000).

GW0072 is a partial agonist/antagonist for PPAR γ (Oberfield *et al.*, 1999). GW0072 was shown to activate up to 15-20% of rosiglitazone-induced levels of reporter activity of a PPAR γ -Gal4 chimera plasmid. GW0072 was also shown to be able to displace the corepressor NCoR from the PPAR γ LBD, but was unable to adequately recruit the coactivators SRC-1 or CBP. Even though GW0072 is able to partially induce PPAR γ -Gal4 chimera reporter gene activity, it does not allow PPAR γ to induce adipocyte differentiation in preadipocyte cell lines that were either treated or untreated

with rosiglitazone; hence it is termed a partial agonist/antagonist specific for PPAR γ (Oberfield *et al.*, 1999).

SR-202 was shown to be a specific antagonist of PPAR γ that could have both antidiabetic as well as antiobesity activity. SR-202 selectively modulated PPAR γ transcriptional activity measured in HeLa cells using a PPRE-based transcriptional reporter assay (Rieusset *et al.*, 2002). SR-202 is able to block adipocyte differentiation induced by either TZDs, dexamethasone, insulin, or 3-isobutyl-1-methylxanthine (IBMX). *In vivo*, SR-202 has been shown to block PPAR γ activity, thus resulting in a decrease in fat deposits and an increase in insulin sensitivity (Rieusset *et al.*, 2002).

PPAR γ is required for development

Inactivation of both alleles of PPAR γ has been shown to be embryonic lethal. PPAR γ deficient CB6F1 mouse embryos die *in utero* at E9.5-E10 (Rosen *et al.*, 2002; Barak *et al.*, 1999). PPAR γ heterozygotes were able to survive, but were shown to have increased tumor susceptibility when treated with DMBA (7,12-dimethylbenz[a]anthracene), a chemical known to be able to induce tumor formation at various locations in normal animals. DMBA caused increased tumor formation at every time point between 2-16 weeks in PPAR γ heterozygotes compared to PPAR γ wild type animals (Nicol *et al.*, 2004).

The CRE/loxP system was used to determine the effects of a conditional disruption of PPAR γ (Akiyama *et al.*, 2002). The resulting effect was a nearly complete deletion of the targeted PPAR γ exon 2 which led to a loss of full-length PPAR γ mRNA

and protein. There was lower expression of genes encoding lipoprotein lipases as well as CD36 and LXR α in the PPAR γ null macrophages compared to the PPAR γ wild type macrophages (Akiyama *et al.*, 2002). The CRE/loxP system was also used to determine the effect of the loss of PPAR γ in mammary development in mice (Cui *et al.*, 2002). This loss neither affected mammary development, nor did it lead to increased spontaneous tumor formation in the mice (Cui *et al.*, 2002).

REGULATION OF PPAR γ

Transcriptional level

The human PPAR γ gene is comprised of nine exons and covers over 100 kilobases of genomic DNA (Fajas *et al.*, 1997). The PPAR γ promoter region contains a C/EBP site (Saladin *et al.*, 1999). Both C/EBP β and C/EBP δ have been shown to activate the transcription of PPAR γ (Saladin *et al.*, 1999; Wu *et al.*, 1995).

Another transcriptional regulator of PPAR γ is Adipocyte Differentiation and Determination factor 1, independently cloned also as Sterol Regulatory Element Binding Protein 1 (ADD-1/SREBP-1). SREBP-2 also has a binding site within the PPAR γ promoter (Fajas *et al.*, 1999). This family of SREBP transcription factors binds to two E-box sequence elements either within the PPAR γ promoter or 5' to the promoter sequence (Fajas *et al.*, 1999). It was shown that overexpression of this family of transcription factors in HepG2 cells significantly increased PPAR γ mRNA levels.

TGF β treatment of Human Aortic Smooth Muscle Cells (HASMC) was shown to stimulate PPAR γ mRNA expression at early time points (30 minutes – 1 hour). This

effect was shown to be mediated by the ERK/Egr-1 signaling pathway since both pharmacological inhibition of the MEK/ERK pathway, as well as overexpression of NAB2 (a selective repressor of Egr-1) resulted in the abrogation of early induction of PPAR γ mRNA expression upon TGF β treatment (Fu *et al.*, 2003). However, TGF β treatment was shown to have a biphasic effect on PPAR γ mRNA expression. After the initial early increase, at 6 hours – 12 hours, there was a marked inhibition of PPAR γ mRNA expression, and at 24 hours, expression was completely inhibited. This late-repression effect was shown to be mediated by AP1 and Smad3 (Fu *et al.*, 2003).

PPAR γ transcriptional inhibitors were discovered utilizing engineered activator- and repressor- zinc finger proteins (ZFPs). These are engineered from the C2H2 family of ZFPs to bind with high affinity and specificity to any number of DNA sequences (Desjarlais, J and Berg 1992; Greisman, H and Pabo 1997). By combining a functional transcription repressor regulatory element from KRAB with a customized DNA binding domain directed at the endogenous PPAR γ chromosomal loci, it was found that the engineered six-finger ZFP, ZFP55, was able to inhibit the expression of PPAR γ mRNA in the adipogenic mouse 3T3-L1 cell line (Ren *et al.*, 2002).

Post-translational Regulation

PPAR γ has been shown to be regulated at the protein level by several mechanisms including phosphorylation, ubiquitination, and nitration. PPAR γ activity can be down-regulated by phosphorylation of multiple serine residues including serine 82, serine 84, serine 110, and serine 112.

Serine 82 phosphorylation of PPAR γ by JNK was shown to negatively regulate PPAR γ activity *in vitro* in 293T cells (Camp *et al.*, 1999). When Ser82 was mutated to Ala, the MAPK-induced phosphorylation of PPAR γ was abolished in 293T cells (Camp *et al.*, 1999). EGF treatment, *in vivo*, resulted in phosphorylation at Ser82 leading to a reduction in PPAR γ transcriptional activity (Camp *et al.*, 1999). Serine 84 was shown to be phosphorylated by ERK2 and JNK leading to the repression of PPAR γ transcriptional activity in JEG-3 cells (Adams *et al.*, 1997). Serine 110 was shown to be phosphorylated by MAPK in adipocytes, again resulting in an inhibition of PPAR γ transcriptional activity (Hu *et al.*, 1996). Serine 112 is phosphorylated by ERK (Shao *et al.*, 1998). A constitutively active PPAR γ mutant was produced by mutating the Ser112 to Asp resulting in a decrease in ligand binding as well as coactivator recruitment (Shao *et al.*, 1998). Phosphorylation of Ser112 is thought to be important in regulating the conformation of the unliganded receptor, thus altering the ability of PPAR γ to bind ligand efficiently.

In addition to phosphorylation, PPAR γ has been shown to be modified at the post-translational level by ubiquitination which ultimately leads to its degradation via the proteasomal pathway (Hauser *et al.*, 2000). Ligand activation of PPAR γ was shown to enhance its ubiquitination (Hauser *et al.*, 2000).

Nitration is another post-translational modification of PPAR γ . Several tyrosine residues in PPAR γ were shown to be nitrated in response to TNF α , lipopolysaccharide or peroxynitrite treatment in RAW 264 macrophages (Shibuya *et al.*, 2002). This nitration was shown to inhibit the ligand-induced translocation of PPAR γ from the

cytosol to the nucleus, thus inhibiting its transactivation potential.

Corepressors and Coactivators

PPAR γ has been shown to interact with several coactivators and corepressors such as Nuclear Receptor CoRepressor (NCoR), CREB binding protein (CBP), p300, Steroid Receptor Coactivator-1 (SRC-1), and Fatty Acid Binding Protein (FABP).

NCoR is the major corepressor for PPAR γ transactivation (Lavinsky *et al.*, 1998). NCoR was shown to interact with the hinge region of PPAR γ (Zamir *et al.*, 1997). Along with NCoR, other corepressors interact with PPAR γ . The SRC-1 coactivator binds the LBD of PPAR γ in a ligand-dependent manner (Zhu *et al.*, 1996). The coactivator p300 interacts with the AF-2 region of PPAR γ in a ligand-dependent or -independent manner (Wang *et al.*, 2001). Antibodies directed at SRC-1 inhibited TZD-dependent PPRE reporter activation in Rat-1 cells (Westin *et al.*, 1998). Another coactivator for PPAR γ is FABP. Both liver FABP and adipose FABP directly interact with PPAR γ (Tan *et al.*, 2002).

Role of PPAR γ in Disease

PPAR γ is a key regulator of glucose and lipid homeostasis and its physiological function has mainly been explored in insulin sensitization, adipocyte differentiation, inflammation, and development of atherosclerosis. PPAR γ has also been implicated in a number of other conditions including cardiac hypertrophy and more recently, in carcinogenesis.

Cancer cells exhibit an inability to balance cell proliferation, apoptosis, and differentiation, which ultimately leads to tumor formation. PPAR γ has been suggested to play a crucial role in each of these aspects of cancer development. Activation of PPAR γ has been shown to either lead to apoptosis, terminal differentiation, or to the inhibition of cellular proliferation in several cancer cell lines (Wang *et al.*, 2006).

CDKs have been shown to be directly regulated by PPAR γ agonists in several cancer cell lines. Troglitazone treatment was shown to inhibit the growth of MCF-7 breast cancer cells (Yin *et al.*, 2001). The mechanism of action in these cells is thought to be interference with several proteins that are regulators of pRb phosphorylation such as cyclin D1. Re-introduction of cyclin D1 after troglitazone treatment partially rescued these cells from G1 phase cell cycle arrest.

PPAR γ also plays a role in regulating apoptosis. PPAR γ activation was shown to increase caspase-3 activity in human malignant astrocytoma cells (Chattopadhyay *et al.*, 2000). TNF-related apoptosis inducing ligand (TRAIL)-mediated apoptosis was triggered by treating multiple cell types, including SK-OV-3 and HUVEC cells with various PPAR γ ligands. Activation of PPAR γ was shown to reduce the levels of FLICE-Inhibitory Protein (FLIP), a negative regulator of TRAIL-induced apoptosis, by increasing its ubiquitination and subsequent degradation (Kim *et al.*, 2002).

Activation of PPAR γ induces differentiation of a number of cancer cell lines. In human primary and human metastatic breast adenocarcinomas, PPAR γ activation by TZD treatment resulted in changes in the cell's gene expression pattern to one closely resembling that of a more differentiated state (Mueller *et al.*, 1998). In T24 bladder

cancer cells, troglitazone was shown to increase the endogenous PPAR γ target gene A-FABP, Adipocyte – Type Fatty acid Binding Protein (A-FABP), a well known marker of differentiation in these cells (Guan *et al.*, 1999).

PPAR γ has been shown to play a role in angiogenesis. PPAR γ knockout mice die as embryos at ~ E10 in part due to deficient placental vascularization (Barak *et al.*, 1999). Rosiglitazone-induced PPAR γ activation has been shown to decrease vascular endothelial growth factor (VEGF), the major regulator of angiogenesis, production in LLC cells (Panigrahy *et al.*, 2002).

While the majority of reports suggest PPAR γ to be a tumor suppressor, there are a number of studies showing that it could have an opposite effect in some cancers. Multiple *in vivo* studies have shown that introducing TZDs into *mim* mice (mutation in the APC gene) led to a significant increase in both small and large colon adenocarcinomas (Saez *et al.*, 1998; Lefebvre *et al.*, 1998).

Transgenic mice expressing high levels of PPAR γ were mated with transgenic mice that expressed the mouse mammary tumor virus polyoma middle T and the offspring were shown to have an increased incidence of breast cancer formation (Saez *et al.*, 2004).

Role of PPAR γ in melanoma

Expression and effect of ligand activation of PPAR γ has been studied in human melanoma. Both WM35, an early stage melanoma, and A375, a metastatic melanoma cell line, have been reported to express PPAR γ mRNA and protein. While one study

concluded that the growth of A375 cells was inhibited by ciglitazone (Placha *et al.*, 2003), another showed that the proliferation of A375 cells was unaffected by this compound (Nunez *et al.*, 2006). Rosiglitazone has been shown to inhibit colony formation and induce apoptosis in A375 cells. This study also revealed that rosiglitazone induced differentiation in the A375 cells (Liu *et al.*, 2006).

PPAR α

PPAR α has a molecular weight of ~52 kD. The gene has six coding exons and is located on chromosome 22 in humans (Entrez Nucleotide Gene). Active PPAR α has been shown to increase lipid catabolism and decrease circulating lipid concentrations. PPAR α has also been shown to play some role in glucose metabolism (Knauf *et al.*, 2006).

Natural Ligands of PPAR α

PPAR α is known to be activated by fatty acids and their metabolites. It has been shown that long-chain fatty acids and eicosanoids are more potent ligands for PPAR α than even its strongest synthetic ligand, WY-14643 (Murakami *et al.*, 1999). This study showed that the fatty acids and eicosanoids were able to directly bind the LBD of PPAR α . Other studies have shown that mono- and polyunsaturated fatty acids at physiological concentrations can also directly bind PPAR α (Kliwer *et al.*, 1997).

Several arachidonic acid metabolites serve as ligands for PPAR α . Leukotriene B₄ (LTB₄) activates PPAR α and is thought to be the natural ligand for PPAR α (Gupta *et al.*, 2001). LTB₄ has been shown to bind to PPAR α with a K_d in the nanomolar range,

while 8-(S) HETE has also been reported to be a natural ligand for PPAR α (Lin *et al.*, 1999).

Synthetic ligands for PPAR α

The major class of synthetic ligands for PPAR α is the fibrate hypolipidemic drugs. Fibrates are amphipathic carboxylic acids. They are indicated for the treatment of several metabolic disorders such as high cholesterol. Some examples of fibrates are bezafibrate, ciprofibrate, gemfibrozil, fenofibrate, and clofibrates.

The major non-fibrate synthetic agonist for PPAR α is WY-14643. WY-14643 is a well known peroxisome proliferator having effects on DNA replication via PPAR α (Peters *et al.*, 1997). Results show that PPAR α null mice, when fed a diet containing 0.1% WY-14643 exhibited no hepatocarcinomas while 100% of PPAR α +/+ mice showed multiple lesions (Peters *et al.*, 1997).

GW7647 has been recently reported to be a very potent and selective PPAR α agonist. It was shown to have ~ 200-fold selectivity for PPAR α over both PPAR γ and PPAR δ (Brown *et al.*, 2001),

PPAR α Antagonists

The major antagonist for PPAR α is MK886. Upon treatment with WY-14643, MK886 treatment inhibited the activation of PPAR α by 80% in A549 cells (Kehrer *et al.*, 2001). MK886 had only minimal effects on PPAR δ or PPAR γ activity.

Other inhibitors for PPAR α include some acyl – CoA esters. Palmitoyl – CoA

was shown to bind PPAR α and compete with WY-14643 for binding to this receptor (Elholm *et al.*, 2001). Acyl-CoA esters were shown to directly induce PPAR α conformational change and are thought to be the endogenous regulators of PPAR α activity.

PPAR α Knockouts

Mice that lack expression of PPAR α exhibit no typical peroxisome proliferation in response to treatment with clofibrate or WY-14643 (Lee *et al.*, 1995). Also, PPAR α null mice challenged with a diet known to induce insulin resistance were protected from this effect. These mice, however, did show increased fat deposits (Guerre-Millo *et al.*, 2001).

Regulation of PPAR α

The promoter region of PPAR α has seven SP-1 binding sites (Gearing *et al.*, 1994). Coup – TFIID and HNF4 share a binding site within the PPAR α promoter (Pineda-Torra *et al.*, 2002). While overexpression of HNF4 increased PPAR α promoter activity, overexpression of Coup-TFIID decreased the activity of the PPAR α promoter.

Other negative regulators of PPAR α expression are some cytokines, such as TNF- α and IL-6, and some members of the STAT family of proteins, including STAT5 (Zhou *et al.*, 1999).

Post – translational PPAR α control

PPAR α undergoes phosphorylation and ubiquitination (Shalev *et al.*, 1996). The phosphorylation of PPAR α can be induced by several mechanisms/factors. Unlike

PPAR γ , where phosphorylation usually means a decrease in activity, phosphorylation can serve to activate PPAR α transcriptional activity.

PPAR α is phosphorylated by MAPK, resulting in transcriptional activation in insulin-treated HepG2 cells (Juge – Aubry *et al.*, 1999). This phosphorylation of serine12 and serine21 is thought to induce a conformational change which could bring about the dissociation of the corepressors, NCoR or SMRT, thus increasing transcriptional activation of PPAR α . This phosphorylation results in ligand independent activation of PPAR α . Regulation was further enhanced when fibrate ligand was added to the cells (Judge – Aubry *et al.*, 1999).

p38 MAPK can also phosphorylate PPAR α . This phosphorylation serves to increase the transcriptional activity of PPAR α through conformational change, allowing interactions with the coactivator PGC-1 (Barger *et al.*, 2001).

Stimulation of protein kinase A (PKA) activity has also been shown to activate PPAR α in the absence of ligand via phosphorylation. This activation was mainly dependent on an intact AF-2 domain. Phosphorylation by PKA was shown to increase the stability of the PPAR α :DNA interaction resulting in increased transcriptional activity (Lazennec *et al.*, 2000).

Recently, PKC α and PKC β II have been shown to phosphorylate PPAR α . Phosphorylation sites were mapped to serines 179 and 230. PKC phosphorylation acts as a switch that converts PPAR α from a transcriptional activator to a repressor (Blanquart *et al.*, 2004).

PPAR α is ubiquitinated and subsequently degraded by the proteasome. Ligand binding was shown to decrease the ubiquitination and extend the half life of PPAR α (Blanquart *et al.*, 2002).

Role of PPAR α in disease

PPAR α has been reported to play a major role in transcriptional regulation of the enzymes involved in the β -oxidation of fatty acids (Barger *et al.*, 2001). In cardiac metabolism, PPAR α has been shown to regulate fatty acid uptake and oxidation (Barger *et al.*, 2001). In contrast to PPAR γ , PPAR α can not differentiate fibroblasts into adipocytes (MacDougald OA and Lane 1995). PPAR α agonists such as fibrates have been shown to lower cholesterol levels by increasing lipoprotein lipase expression in liver and muscle (Schoonjans *et al.*, 1996). The metabolism of the reverse cholesterol transport vehicle, HDL, is highly dependent on PPAR α activity. Fibrate treatment results in HDL apolipoprotein gene activation leading ultimately to protection from atherosclerosis (Lefebvre *et al.*, 2006). Active PPAR α has been shown to play a role in inflammation, serving to decrease cytokine activity (Kleemann *et al.*, 2003). Active PPAR α plays a role in human breast cancer cell proliferation. PPAR α agonists WY-14643 and clofibrate increased the proliferation of both MCF-7 and MDA-MB-231 cells (Suchanek *et al.*, 2002). Primary rat liver cultures transiently transfected with human PPAR α were shown to have decreased nafenopin-induced apoptosis relative to control cells (Roberts *et al.*, 1998).

The role of PPAR α in human melanoma remains to be determined. One study showed that WY-14643 had no effect on the growth of A375 human metastatic

melanoma cells (Nunez *et al.*, 2005). Other investigators determined that fenofibrate was able to inhibit the migration of both B16F10 mouse melanoma cells and SK-Mel 28 human vertical growth phase melanoma cells. This inhibition of migration was restored when cells were treated with the PPAR α antagonist, MK886 (Grabacka *et al.*, 2006).

PPAR δ

PPAR δ is the least studied of the three PPAR subtypes. PPAR δ has a molecular weight of ~48kD. In humans, the gene coding for PPAR δ is located on chromosome 6. PPAR δ has been shown to have ubiquitous tissue distribution. It has been reported to be expressed in spleen, brain, macrophages, heart, adipose, muscle, placenta, lung, and intestine (Fredenrich and Grimaldi 2004). One of the proposed roles of PPAR δ is that it reportedly plays a role in the regulation of fatty acid oxidation (Fredenrich and Grimaldi 2004). The activation of PPAR δ was shown to reverse the main features of metabolic X syndrome in mice and monkeys. Some of these effects were a dose-dependent rise in serum high density lipoprotein cholesterol and lowering the levels of small-dense low density lipoprotein, fasting insulin and fasting triglycerides (Fredenrich and Grimaldi 2004).

Natural ligands of PPAR δ

PPAR δ can be activated by unsaturated or saturated long-chain fatty acids, some eicosanoids, prostacyclin, and retinoic acid (Amri *et al.*, 1995; Hertz *et al.*, 1996; Fredenrich and Grimaldi 2004). The triglyceride components of native very low-density lipoproteins (VLDLs) are also able to activate PPAR δ .

Synthetic ligands of PPAR δ

There are several synthetic ligands for PPAR γ and PPAR α ; however, there is very limited information on specific synthetic agonists for PPAR δ . The major synthetic agonist for PPAR δ is GW501516, a very high affinity ligand with a $K_i = 1.1 \pm 0.1$ nM. GW501516 was administered to a rhesus monkey model of metabolic X syndrome in which the lipid profile is representative of that seen in similarly afflicted humans. One hundred nM GW501516 treatment resulted in an increase of cholesterol efflux from cells. This effect was attributed to increased PPAR δ activity leading to increased transcription of ABCA1, a reverse cholesterol transporter (Oliver Jr. *et al.*, 2001). Similar treatment also resulted in a decrease in serum levels of small-dense low-density lipoprotein, fasting insulin, and fasting triglycerides. GW501516 produced a dose-dependent lowering of fasting triglycerides, with a 56% decrease at the 3.0 mg/kg dose (Oliver Jr. *et al.*, 2001).

Another high affinity ligand for PPAR δ is GW0742. This agonist has an EC₅₀ of 1.1 nM with a 1000 fold higher selectivity for PPAR δ over both PPAR α and PPAR γ (Sznajdman *et al.*, 2003). GW0742 stimulation of PPAR β/δ was found to selectively induce keratinocyte terminal differentiation and inhibit their proliferation *in vivo* (Kim *et al.*, 2006).

PPAR δ knockouts

The vast majority of PPAR δ *-/-* mouse embryos die at a very early stage due to a placental defect. The survivors showed a significant reduction in fat mass (Peters *et al.*,

2000; Barak *et al.*, 2002).

Regulation of PPAR δ

Transcriptional Regulation of PPAR δ

The PPAR δ promoter contains Tcf-4 binding sites and AP-1 elements (Entrez Gene). The AP-1 elements may allow regulation of PPAR δ transcription by TPA or TNF α . TPA induction of PPAR δ is mediated through the MAPK pathway (Bryan *et al.*, 2006).

Role of PPAR δ in disease

Due to the role of PPAR δ in regulating lipid metabolism, it is thought to play a role in atherosclerosis. Whether the role of PPAR δ in atherosclerosis is antiatherogenic or proatherogenic remains to be elucidated (Lee *et al.*, 2003). One study found that PPAR δ is a VLDL sensor in macrophages, suggesting it might be involved in the accumulation of atherosclerotic plaques (Lee *et al.*, 2003). Another report revealed that the effect on atherosclerosis may depend on whether or not ligand is bound to PPAR δ . The unliganded PPAR δ can sequester BCL-6 allowing progression of the inflammatory response. Liganded PPAR δ releases B-cell lymphoma gene 6 (BCL-6), possibly resulting in decreased atherosclerosis. (Lee *et al.*, 2003).

REVIEW OF THE LITERATURE

HIF-1

Oxygen is an essential component for cellular viability. O_2 is a critical player in mitochondrial respiration, ultimately resulting in the formation of ATP from glucose. O_2 is the final electron acceptor in the chain of metabolic reactions that result in the conversion of glucose to CO_2 and H_2O . This aerobic glycolysis generates 32 molecules of ATP per molecule of glucose, whereas anaerobic glycolysis only generates 2 molecules of ATP per molecule of glucose (Wiesener and Maxwell 2003).

Consistent with the wide range of physiological functions modulated by O_2 , the O_2 sensing system is equally necessary and widespread. This O_2 sensing system was uncovered with the discovery that red blood cell production is regulated by erythropoietin secretion (Bachman *et al.*, 1993). Under hypoxic conditions, erythropoietin expression was found to increase. It was also found that this increase was regulated by O_2 levels in hepatoma cells (Goldberg *et al.*, 1987). The promoter of the erythropoietin gene was found to have a hypoxia-responsive element (HRE) and this element was later shown to bind to a heterodimeric transcription factor, hypoxia-inducible factor 1 (HIF-1) (Wang and Semenza 1995). It is this transcription factor that is the master regulator of oxygen homeostasis.

HIF-1 is a heterodimeric protein complex consisting of a ~120kD HIF-1 α subunit and an ~86kD HIF-1 β subunit (Semenza G, 2002). HIF-1 is responsible for the regulation of >60 genes involved in a myriad of cellular functions and physiological

processes ranging from angiogenesis to glycolysis to cell proliferation and survival (Semenza G, 2002).

Structure of HIF-1

HIF-1 is the most important factor involved in the cells' adaptation to hypoxia (Mazure *et al.*, 2004). For cells to be able to respond to a range of O₂ concentrations, HIF-1 must be very tightly regulated. The structure of the HIF-1 subunits, especially HIF-1 α , is central to this regulation.

There are multiple isoforms of HIF-1 α . HIF-1 can be comprised of either HIF-1 α :HIF-1 β , HIF-2 α :HIF-1 β , or HIF-3 α :HIF-1 β . HIF-1 α is the full length isoform. HIF-2 α is structurally and functionally similar to HIF-1 α , however its tissue distribution is much more limited. HIF-3 α lacks the transactivation domain found in the HIF-1 α and HIF-2 α subunits. It is thought that the HIF-3 α isoform is a negative regulator of hypoxia-inducible gene expression by acting as a competitor for the dimerization of HIF-1 α /-2 α to HIF-1 β (Jang *et al.*, 2005).

Both the HIF-1 α and HIF-1 β subunits of HIF-1 are basic helix loop helix (bHLH) and Per Arnt Sim (PAS) domain proteins. bHLH domains are found in specific DNA-binding proteins that act as transcription factors and are usually 60-100 amino acids long. A DNA-binding basic region is followed by two alpha-helices separated by a variable loop region. bHLH regions form homo- and heterodimers (Entrez Conserved Domains <http://www.ncbi.nlm.nih.gov/Structure/cdd/cdd.shtml>). The PAS domain was named after three proteins that the domain occurs in: Per- period circadian protein,

Arnt- Ah receptor nuclear translocator protein, Sim- single-minded protein (Entrez Conserved Domains <http://www.ncbi.nlm.nih.gov/Structure/cdd/cdd.shtml>).

The HIF-1 α subunit is the “inducible” half of this heterodimer while HIF-1 β is considered to be constitutively expressed. The HIF-1 α subunit is O₂-labile which is stabilized by divalent cations, iron chelators, and hypoxia (Giaccia *et al.*, 2003). Currently, it is believed that the HIF-1A gene transcription is not a major point of regulation for HIF-1. It is thought that in most cell lines, under both hypoxic and normoxic conditions that the HIF-1A gene transcription is constitutive (Wenger *et al.*, 1997).

Regulation of HIF-1

Transcriptional regulation

The human HIF-1A gene, which encodes the HIF-1 α protein, consists of 15 exons. It is located on chromosome 14 in humans. There is a splice variant of the HIF-1A gene, HIF-1A2, which lacks an alternate segment in the 3' coding sequence, compared to variant 1, that results in a frame shift. The resulting protein, HIF-1 α isoform 2, is shorter and also has a distinct C-terminus, relative to isoform 1 (Entrez Gene <http://www.ncbi.nlm.nih.gov/entrez>). The HIF-1B gene encoding the HIF-1 β protein has 22 exons and is located on human chromosome 1. There are 2 additional splice variants for HIF-1B. HIF-1B2 lacks several alternate segments, relative to HIF-1B variant 1, which leads to a frame shift. The resulting protein, HIF-1 β isoform 2, is shorter and has a distinct C-terminus, compared to HIF-1B variant 1. HIF-1B3 is

missing an alternate in-frame exon in the 5' coding region, compared to HIF-1B variant 1. This exon deletion results in a protein, HIF-1 β isoform 3, that is shorter relative to HIF-1 β isoform 1 (Entrez Gene <http://www.ncbi.nlm.nih.gov/entrez>).

The promoter of HIF-1A belongs to the TATA-less promoter family and has a GC rich sequence with several Sp1 binding sites. There are also several HREs within the promoter of HIF-1A which act as HIF-1 *cis* elements (Iyer *et al.*, 1998). AP-1 and AP-2 elements are also present in the promoter of HIF-1A (Minet *et al.*, 1999). Downstream of the initiation site there are several putative transcription factor binding sites including c-Ets-1, NF-KB, and NF-1 indicating that the transcriptional control of HIF-1A may depend on *cis* acting elements located both upstream and downstream of the transcription start site (Minet *et al.*, 1999). Promoter sequence deletion experiments have shown that the core promoter sequence of HIF-1A is from +1bp to -200bp. The fragment between +1bp to -105 bp contains several necessary *cis* acting elements that control the increase in the transcription of the HIF-1A gene in response to hypoxia. An AP-1 binding site was found between -29bp to -23bp and could act as a stimulator of HIF-1A transcription since AP-1 is shown to be activated under hypoxic conditions (Rajpurohit *et al.*, 1996). Within the sequence spanning -105bp to -201bp there are several AP-2 *cis* acting elements. AP-2 may play some role in the repression of HIF-1A gene transcription in response to hypoxia since when this region of the promoter was present in the promoter-expression constructs, there was a decrease in HIF-1A gene expression down to normoxic levels upon treatment with CoCl₂, a hypoxia mimetic (Minet *et al.*, 1999).

Post translational regulation of HIF-1 α

It is widely held that HIF-1A gene transcription is not necessarily central to the regulation of HIF-1 activity. The post translational modifications, however, have been extensively covered and are considered the *de facto* method of control of HIF-1 transcriptional activation. The structure of the HIF-1 α protein contributes to this complex pattern of post translational regulation.

HIF-1 α consists of several regulatory domains (**Figure 3**). The N-terminal bHLH and PAS domains are required for both DNA binding and dimerization with HIF-1 β (Mazure *et al.*, 2004). The C-terminal region of HIF-1 α contains the domains that are required for transactivation and degradation. The oxygen-dependent degradation domain (ODDD) within HIF-1 α contains amino acids that are modified by several mechanisms including hydroxylation, sumoylation, and acetylation in response to O₂ tension (Jiang *et al.*, 1997). There are also two independent transcriptional activation domains within the C-terminal region termed N-TAD and C-TAD. Between the N-TAD and C-TAD domains there is an inhibitory domain (ID), which includes residues contributing to the negative regulation of the transactivation domains (Mazure NM 2004). Several residues within the C-terminal half of HIF-1 α are phosphorylated under normoxic and hypoxic conditions by p42/p44 MAPKs resulting in enhanced transcriptional activity of HIF-1 (Richard *et al.*, 1999). S-Nitrosation is another post-translational modification of HIF-1 α . The S-nitrosation of Cys800 was shown to increase HIF-1 transactivation by increasing the interaction of HIF-1 with p300 (Yasinska and Sumbayev 2003).

Some of these post-translational modifications are involved in regulating HIF-1 α protein stability; others are involved in controlling HIF-1 α activity directly. These methods of control will be discussed in further detail.

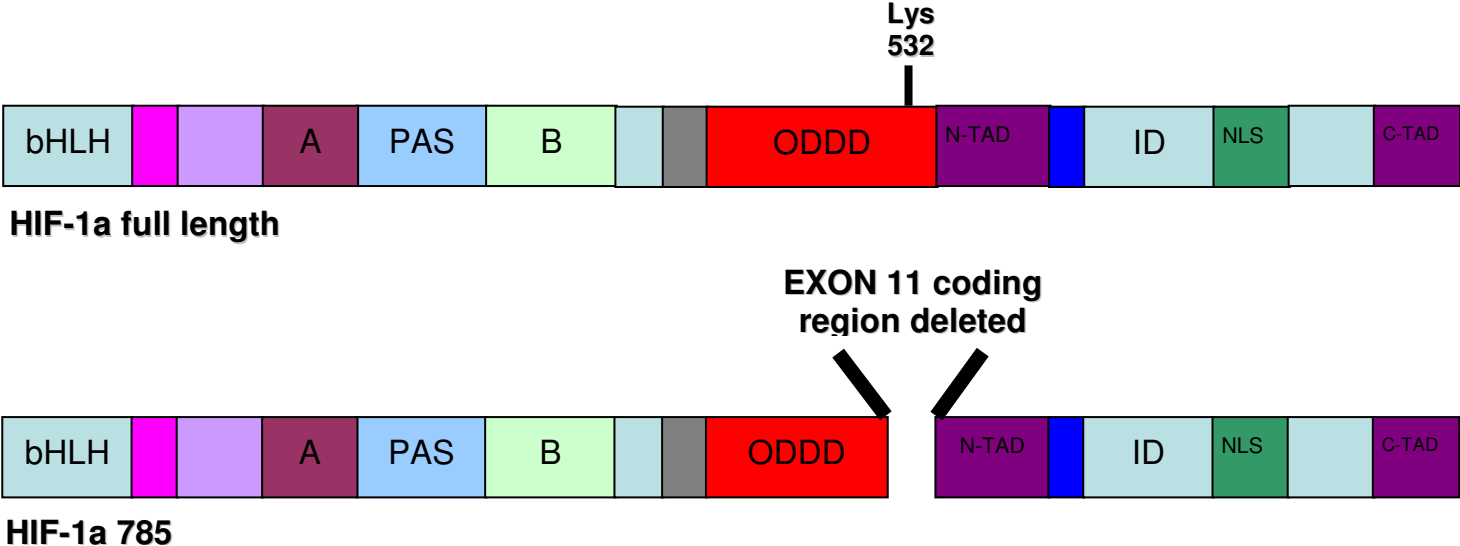
Control of HIF-1 α protein stability by hydroxylation

The conversion of proline into hydroxyproline requires the activity of iron-dependent enzymes in reactions requiring oxygen, 2-oxoglutarate, and ascorbate. Two prolines, Pro402 and Pro564, in HIF-1 α are hydroxylated by one of three prolyl hydroxylase enzymes: PHD1, PHD2, or PHD3. The activity of these enzymes is regulated by cellular O₂ concentration (Epstein *et al.*, 2001). Since these enzymes also require iron as a cofactor, iron-mimics such as CoCl₂ can act as hypoxia mimetics (Mazure *et al.*, 2004). The cellular localization of the PHD enzymes may play some role in their activity as well since PHD1 is nuclear, PHD2 is primarily cytoplasmic, and PHD3 can be located in either compartment (Metzen *et al.*, 2003). The hydroxylation of Pro402 and Pro564 serves to target HIF-1 α for interaction with the Von Hippel Lindau (VHL) tumor suppressor. VHL is the recognition component of an E3 ubiquitin ligase that brings about the polyubiquitination of HIF-1 α , ultimately resulting in the HIF-1 α degradation via the proteasome (Maxwell *et al.*, 1999).

In summary, when cellular O₂ concentration is normal (~21%) the PHD enzymes are active and can therefore hydroxylate HIF-1 α resulting in a decrease in HIF-1 α protein stability and an increase in its degradation. Under hypoxic conditions (~2% - 5% O₂ concentration) this chain of events should not occur, allowing HIF-1 α , *i.e.* the HIF-1 heterodimer, to turn on the transcription of its target genes.

Figure 3: Schematic representation of the functional domains of both HIF-1 α full length and HIF-1 α 785. Upon loss of exon 11 in HIF-1 α 785, part of the Oxygen Dependent Degradation Domain (ODDD) is deleted. This missing region contains the important lysine 532 residue which is acetylated by ARD1 leading to increased stabilization of HIF-1 α interaction with the von Hippel Lindau tumor suppressor. This interaction directs HIF-1 α to the ubiquitin-proteasome pathway for degradation under normoxic conditions.

Figure 3: Schematic representation of the functional domains of both HIF-1 α full length and HIF-1 α 785.



Control of HIF-1 α protein stability by acetylation

Lys532 within exon 11 of the ODDD of HIF-1 α , has been shown to be acetylated by the arrest-defective-1 (ARD1) protein (Jeong *et al.*, 2002). This acetylation of Lys532 results in a stabilization of the interaction between HIF-1 α and VHL. Thus, ARD1 acetylation of HIF-1 α results in the protein becoming less stable and ultimately increasing its degradation via the ubiquitin-proteasome pathway. Exon 11 is spliced out of HIF-1 α 785, leaving exons 10 and 12 to join in frame. This results in a variant of HIF-1 α that is thought to be more stable under normoxic conditions due to the ARD1 inability to acetylate this critical Lys532. No Lys532 acetylation leads to a less stable interaction between VHL and HIF-1 α , which is postulated to result in less degradation via the ubiquitin-proteasome pathway (Chun *et al.*, 2003).

Control of HIF-1 α activity by hydroxylation

In addition to proline hydroxylation, HIF-1 α has also been shown to undergo asparaginyl hydroxylation in response to O₂ tension. Under normoxic conditions, the factor inhibiting HIF-1 (FIH1) catalyzes this asparaginyl hydroxylation which serves to inhibit the interaction of HIF-1 α with p300/CBP. This results in decreased HIF-1 transcriptional activity under normoxic conditions (Lando *et al.*, 2002).

Control of HIF-1 α by growth factor stimulation

While the previous examples of control for HIF-1 α are O₂ dependent, there are O₂ independent mechanisms of HIF-1 control as well. An example of O₂ independent HIF-1 control is via growth factors. Hypoxia increases HIF-1 α protein expression in all

cell types. However, growth factors such as insulin, insulin-like growth factor, and epidermal growth factor, only stimulate HIF-1 α expression in a cell-type dependent manner. This expression is not dependent on the cellular oxygen concentrations. Growth factors activate PI3K or MAPK pathways, which in turn, increase HIF-1 α protein expression (Fukuda *et al.*, 2002).

Control of HIF-1 α activity by phosphorylation

The MAPK p42/p44 is capable of phosphorylating HIF-1 α (Richard *et al.*, 1999). It was shown that HIF-1 α is highly phosphorylated *in vivo* and that this phosphorylation results in a change in the electrophoretic migration pattern of HIF-1 α . HIF-1 α induced by hypoxia migrates at ~104kD to ~116kD. In HeLa cells, when HIF-1 α was immunoprecipitated and then incubated with lambda phosphatase, this resulted in a shift of 12kD below the control HIF-1 α (no lambda phosphatase treatment) resulting in a sharp band at ~104kD on the gel (Richard *et al.*, 1999). The p42/p44 phosphorylation of HIF-1 α resulted in an increase in HIF-1 transcriptional activity under normoxic conditions.

Control of HIF-1 α activity by sumoylation

HIF-1 α can be sumoylated by the sumo E3 ligase, RanBP2, *in vitro* (Mazure *et al.*, 2004). Sumoylation proceeds similarly to ubiquitination; however, it is not thought to target proteins for degradation. Sumoylation has been shown to regulate protein localization and in some instances activation of certain transcription factors (Mazure *et al.*, 2004). Sumoylation by SUMO-1 has been shown to increase the stability and

activity of HIF-1 α *in vitro* (Bae *et al.*, 2004).

Control of HIF-1 α activity by heterodimerization

The dimerization of HIF-1 α to HIF-1 β is required for HIF-1 transcriptional activity. This dimerization can be inhibited by competitive binding of inhibitory molecules. An inhibitory PAS (IPAS) molecule competes with HIF-1 β for heterodimerization with the HIF-1 α subunit under hypoxic conditions. This IPAS molecule is the third isoform of HIF-1 α , HIF3 α (Jang *et al.*, 2005). Ectopic expression of IPAS in Hepa 1c1c7 hepatoma cells was shown to selectively interfere with the induction of genes that are up-regulated by hypoxia, including VEGF (Makino *et al.*, 2001). Overexpression of IPAS also resulted in a decrease in tumor growth and tumor vascular density in mice (Makino *et al.*, 2001).

HIF-1 antagonists

TX-402, a potent hypoxia-selective cytotoxic agent, was shown to reduce the expression of VEGF and glucose transporter type 3 (GLUT-3) under hypoxic conditions. The mechanism of TX-402 action in the reduction of the VEGF and GLUT-3 genes appears to involve direct suppression of HIF-1 α mRNA and protein levels (Nagasawa *et al.*, 2003).

The National Cancer Institute Diversity Set of 2000 compounds was screened for potential HIF-1 α inhibitors. NSC-134754, a semisynthetic analogue of emetine (a natural alkaloid) and NSC-643735, a structural analog of actinomycin D aglycone, were both shown to have HIF-1 inhibitory effects. However, NSC-134754 inhibited hypoxia-

induced HIF-1 activity and HIF-1 α protein expression. Hypoxia-induced expression of Glut-1 was also significantly inhibited by NSC-134754. Both compounds were able to inhibit growth factor-induced HIF-1 α protein expression (Chau *et al.*, 2005).

A screen of 15,000 compounds revealed 3 hits for inhibitors of HIF-1 activity, DJ12, DJ15, and DJ30 (Jones and Harris 2006). None of the compounds were able to inhibit HIF-1 α protein expression; however they did inhibit hypoxia-induced HIF-1 α target gene expression. DJ12 was the only compound that could inhibit these target genes in multiple cancer cell lines including breast cancer cells, MDA-468 and ZR-75; melanoma cell line MDA-435; and pVHL mutant-renal cancer cell lines RCCR and 786-0 (Jones and Harris 2006). The DJ12 induced inhibition of HIF-1 α target genes was attributed to the inhibition of HIF-1 α DNA binding.

Physiological Roles of HIF-1

HIF-1 is operational in all mammalian cell types, while the HIF-1 – VHL – PHD system is fully conserved from *D. melanogaster* to *C. elegans* to *H. Sapiens* (Wiesener and Maxwell 2003). The importance of this system is also underscored by the multitude of physiological processes that HIF-1 can influence. These processes include erythropoiesis, iron metabolism, cellular glucose transport, glycolysis, angiogenesis, regulation of vascular tone, signal transduction, and cell survival (Wenger *et al.*, 2002). While there is *in vitro* data that suggests the possibility that HIF-1 is involved in several physiological and pathological processes, current data on the actual role HIF-1 plays *in vivo* is somewhat limited. *In vivo* data is limited to the role of HIF-1 in embryonic development, erythropoiesis, and cancer.

Role of HIF-1 in development

In a mouse model, either VHL, HIF-1 α , HIF-2 α , or HIF-1 β knockouts are embryonic lethal due to interference with vascular network development (Gnarra *et al.*, 1997; Ryan *et al.*, 1998; Peng *et al.*, 2000; Maltepe *et al.*, 1997). Reports of either partial knockout or tissue specific knockout of HIF-1 α are very few. One study showed that tissue specific knockout of HIF-1 α in chondrocytes resulted in failed growth plate development (Schipani *et al.*, 2001).

Role of HIF-1 in ischemia

While the actual role that HIF-1 plays in ischemia is difficult to predict, HIF-1 activation has been detected in certain ischemic conditions. In mice with oxygen-induced ischemic retinopathy, HIF-1 α levels were shown to be increased in the retina (Ozaki *et al.*, 1999). Brain ischemia also resulted in increased HIF-1 α activity. HIF-1 α and HIF-1 β protein levels were also significantly increased after intraperitoneal injection of CoCl₂ (Bergeron *et al.*, 2000). The kidney exhibits an increased potential for upregulation of HIF-1 transcriptional activity. Renal ischemia-induced upregulation of HIF-1 α has been reported, with the increase in HIF-1 α /2 α selective with respect to cell type and kidney zone, correlating with the known O₂ profiles in these areas (Rosenberger *et al.*, 2002). The functional role of this activation is still under investigation; however, since increased activation of HIF-1 leads to angiogenesis and hypoxia-induced metabolic adaptation, this adaptive response should prevent excessive death of kidney cells (Wiesener and Maxwell 2003).

Role of HIF-1 in cancer

By far, the most extensively studied area of HIF-1 function and regulation at both the *in vitro* and *in vivo* levels is in cancer biology. HIF-1 activation compensates for an inadequate O₂ supply. Solid tumors have regions of severe hypoxia, especially toward their core. Normal mammalian cells have evolved very sophisticated mechanisms of control for HIF-1 α . The need for survival under hypoxic conditions for malignant cells nearly always overpowers this tight control of HIF-1 activity. This survival is accommodated by increasing HIF-1 activity, which in turn, increases the transcription of genes involved in angiogenesis and metabolic adaptation. Overexpression of HIF-1 α and HIF-2 α has been shown to be poor prognostic indicators for several tumors (Harris *et al.*, 2002). Monoclonal antibody staining for HIF-1 α revealed overexpression in several cancers including breast, cervix, brain, ovary, oropharynx, and uterus (Semenza G., 2003). Other reports seemingly show contradictory results for non-small cell lung cancer and head and neck cancers, revealing that HIF-1 α overexpression correlated with decreased mortality (Beasley *et al.*, 2002; Volm and Koomagi 2000). However, these results could not be repeated (Giatromanolaki and Harris 2001; Koukourakis *et al.*, 2002). It seems that while the majority of studies link HIF-1 α overexpression and activity to enhanced tumor progression, the actual effect may be dependent on the type of cancer as well as the stage of the cancer progression (Semenza G., 2003).

Pancreatic cancer cells, PCI-10, which were overexpressing exogenous HIF-1 α showed a significant increase in the frequency of xenograft growth post injection (Akakura *et al.*, 2001). This study revealed that transfection of HIF-1 α into a series of

pancreatic cancer cells that were not expressing HIF-1 α at high levels made these cells more resistant to apoptosis and also resulted in increased tumorigenicity.

Hypoxia-induced or exogenous overexpression of HIF-1 α directly increased *in vitro* invasion by the human colon adenocarcinoma cells, HCT116 (Krishnamachary *et al.*, 2003). HIF-1 α overexpression in tumor xenografts of HCT116 cells resulted in increased growth and angiogenesis (Ravi *et al.*, 2000).

In addition to overexpression of HIF-1 α , the inhibition of this subunit has also revealed the relevance of HIF-1 to cancer pathology. Inhibition of HIF-1 α activity by overexpression of a dominant-negative form of HIF-1 α in pancreatic cancer cells, PCI-43, resulted in an increase in apoptotic cells and a decrease in their ability to form tumors in SCID mice (Chen *et al.*, 2003).

HIF-1 α $-/-$ mouse embryonic stem (ES) cells showed significantly impaired xenograft vascularization compared to HIF-1 α $+/+$ ES cells. HIF-1 α null ES cells were shown to form teratocarcinomas that were only $\frac{1}{4}$ the size of HIF-1 α $+/+$ ES cells (Ryan *et al.*, 1998). This study also showed that within the HIF-1 α $-/-$ tumors, there was a significant increase in apoptosis. Transformed fibroblasts derived from the HIF-1 α $-/-$ mouse embryos exhibited reduced tumor mass at 16 – 18 days post injection (Ryan *et al.*, 2000).

Inhibition of HIF-2 α by siRNA was recently shown to significantly decrease the growth of neuroblastoma tumor xenografts in athymic mice. HIF-2 α was shown to mediate the chronic response of the cells to hypoxia, while HIF-1 α was implicated in the

acute hypoxia response (Holmquist-Mengelbier *et al.*, 2006).

Role of HIF in melanoma

While there are over 1,000 articles relating to HIF-1 and cancer, there are relatively few articles discussing HIF-1 activity and its effect on human melanoma. This is an area of research that is critical, since it is well known that the skin is considered to have a hypoxic microenvironment. This hypoxic stress is thought to contribute to the Ras and Akt-induced transformation of normal human melanocytes (Michaylira and Nakagawa 2006). Akt was only able to transform normal human melanocytes in the presence of hypoxia (Bedogni *et al.*, 2005). This study also shows that inhibition of HIF-1 α using siRNA inhibits the Akt-hypoxia induced melanocyte transformation. Inhibition of HIF-1 α expression by rapamycin through mTOR also inhibited melanocyte transformation (Michaylira and Nakagawa 2006).

A recent study investigated the involvement of HIF-1 in uveal melanoma migration, invasion and adhesion. It was found that hypoxia increased migration, invasion and adhesion of Mum2B uveal melanoma cells *in vitro*. HIF-1 α silencing using RNAi resulted in a significant decrease in uveal melanoma cell migration, invasion and adhesion (Victor *et al.*, 2006).

EXPERIMENTAL OBJECTIVE

This project focused on the effect of transcription factors on the progression of human melanoma. One of the objectives was to elucidate the role of PPARs in cellular growth and differentiation in human melanoma cell lines SK-Mel 28, A375, and normal human melanocytes HEMn-LP. The hypothesis was that modulation of the PPARs activity and/or expression could lead to a less-tumorigenic phenotype in the human melanoma cells. The first part of this dissertation examined the effects of various PPAR agonists on these cell lines. Also, I determined the endogenous expression levels of the PPAR subtypes at both the RNA and protein levels in these cells. The first part of my dissertation work ends with determining the biological effects of PPAR α loss-of-function via siRNA knockdown.

The second part of this dissertation examines the function of HIF-1 in human melanoma progression. During the course of these experiments, I have found, for the first time, that the oxygen-labile subunit of HIF-1, HIF-1 α , is present under normoxic conditions in the human metastatic cell lines, A375 and WM9. The hypothesis was that an increase in expression of HIF1 α or HIF-1 α 785 in radial growth phase cells would render these cells more tumorigenic while a decrease in the expression of HIF-1 α in metastatic cells would lower their tumorigenicity. I have shown for the first time that there is regulation of HIF-1 α at the mRNA level in human melanoma. qPCR data shows that HIF-1 α mRNA increases as a function of malignant progression while remaining relatively undetectable in normal human melanocytes. Another objective of the second half of my dissertation was to determine the biological effects of siRNA-induced HIF-1 α

loss-of-function in the human metastatic melanoma cells WM9. The last part of my dissertation work concentrates on the biological effects of HIF-1 α gain-of-function in the radial growth phase human melanoma cell line, SbCl2.

CHAPTER I

Function of PPARs in human melanoma progression

INTRODUCTION

Activation of PPARs has been reported to decrease cell growth and stimulate differentiation in many cancer cell lines. However, there have been very few reports of the levels of their expression when comparing human melanoma cells to human melanocytes. The purpose of the following experiments in the first part of my dissertation was to characterize the expression and/or function of PPARs in human melanoma. I found that the levels of PPAR γ protein expression were ~50% lower in the human melanocytes compared to several human melanoma cell lines. PPAR α protein expression was between 80-90% lower in normal human melanocytes than in the melanoma cell lines, SK-Mel 28 and A375. I also examined the effect of PPAR agonists on proliferation of the human melanoma cells and normal human melanocytes. I found that there was a consistent dose dependent decrease in proliferation in the SK-Mel 28, A375, and the normal human melanocytes upon treatment for 48h with the PPAR γ agonists PGJ₂ and troglitazone. Quantigene® mRNA analysis of PPAR α revealed significantly higher levels in human melanoma compared to normal human melanocytes, correlating to the amount of PPAR α protein. PPAR α siRNA treatment consistently decreased PPAR α mRNA by ~80%, yet there was no significant change in morphology, or expression of a PPAR α target gene, MCAD. These data suggest that while PPAR α is overexpressed in human melanoma relative to normal human melanocytes, decreasing its expression has no significant influence on major biological properties of the melanoma cells.

MATERIALS AND METHODS

Cell and Culture Conditions

SK-Mel 28 human vertical growth phase melanoma cells were obtained from American Type Culture Collection (Manassas, VA). They were grown in a humidified atmosphere of 5% CO₂ and 95% air at 37°C in Dulbecco's Modified Eagle's Medium (DMEM). The DMEM contained 1g/L glucose and was supplemented with 10% bovine calf serum (Gibco, Carlsbad, CA), 50U/mL penicillin G and 50ug/mL streptomycin sulfate. A375 human metastatic amelanotic melanoma cells were also obtained from the ATCC. A375 cells were cultured similarly to the SK-Mel 28, with the exception that 10% fetal bovine serum was used as the supplement (Gibco, Carlsbad, CA). Normal human melanocytes, HEMn-LP (Cascade Biologics, Portland, OR) were grown in 5% CO₂ and 95% air at 37°C. They were grown in Media 254 supplemented with 50mL human melanocyte growth serum (HMGS) and 1mL penicillin/streptomycin mix (all from Cascade Biologics, Portland, OR).

PGJ₂, Ciglitazone, Troglitazone, WY-14643, and LTB₄

PGJ₂, ciglitazone, and WY-14643 were obtained from BioMol (Plymouth Meeting, PA) and were dissolved in DMSO to a stock concentration of 10mM. Fresh dilutions of each were prepared for each experiment by dilution of the 10mM stock solutions, which were stored at -20°C, with tissue culture media prior to cell treatment. Equal volumes of DMSO were used in the control treated cells. Troglitazone was obtained from Cayman Chemicals (Ann Arbor, MI) and prepared similarly to the aforementioned compounds.

LTB₄ was purchased from BioMol and was dissolved in 100% ethanol to a stock concentration of 10nM and stored under a layer of nitrogen gas. LTB₄ treatment was carried out under zero light conditions and the treated cells were protected from light until assays were performed. Fresh sample was prepared for each experiment and any remaining solution was discarded. Equal volumes of ethanol were used to treat the control cells. Forty eight hours after the cells were treated with either of these reagents they were assayed as described below.

Anchorage-Dependent Growth

All cells were seeded at 5.0×10^5 into 100mm culture dishes. After 72h, cells were treated with or without various PPAR agonists for 48h. Anchorage-dependent growth was determined by either hemacytometric analysis or by crystal violet staining. Hemacytometric analysis was carried out as follows: media was aspirated from the plates and they were then washed using PBS. After PBS aspiration, cells were trypsinized for 2 minutes, washed off the plate using the trypsin, pipetted into a 50mL centrifuge tube, and brought up in 15mL DMEM + 10% BCS. Cells were counted using a hemocytometer and corrected for control cell number. Results are expressed as % control in millions of cells. Experiments are representative of 3 or more independent assays. Crystal violet staining was performed as follows: Media was aspirated from the dishes and cells were fixed with 80% methanol for 1h. Next, cells were stained using 0.5% crystal violet for 1h with shaking. After staining, excess crystal violet was removed from the dishes by extensive washing with distilled H₂O. Once excess stain was removed, stain was eluted from each dish using 1mL of 10% acetic acid and 250 μ L

of the eluate was read on the spectrophotometer at 570nm. Results are expressed as % control. Experiments are representative of 3 or more independent assays.

Relative Melanin Content

Cells were seeded at 5.0×10^5 cells per 100mm dishes. After 72h of incubation, cells were treated with or without PPAR agonists. Cells were further incubated for 48h, washed with cold PBS, and dissolved in 1N KOH and incubated at 80°C for 1h. The lysate was subsequently centrifuged at 12,000 x g for 10 min and the relative melanin concentration of these supernatants was determined by spectrophotometric analysis at A_{462nm} and normalized to cell number.

RT-PCR

Total RNA was extracted using Tri-Reagent (Molecular Research Center Inc., Cincinnati, OH) as per the manufacturer's instructions. RNA integrity was determined using the Agilent Bioanalyzer®. Intact RNA was reverse transcribed to cDNA using the Advantage RT-for-PCR kit® (Clontech) as per the manufacturer's instructions. Five μ L of the resulting cDNA was used in the PCR amplification. PCR amplification was carried out as described by the manufacturer using the Advantage cDNA kit® (Clontech). PPAR γ 1 forward primer sequences were 5'-CCTCGAGGACACCGGAGAG-3'. PPAR γ 1 reverse primer sequences were 5'-CCCTTGCATCCTTCACAAGCATG-3'. PPAR γ 2 forward primer sequences were 5'-GGGTGAAACTCTGGGAGATTCTC-3'. PPAR γ 2 reverse primer sequences were 5'-CCCTTGCATCCTTCACAAGCATG-3'. PPAR δ forward primer sequences were 5'-

ATGGAGCAGCCACAGGAG-3'. PPAR δ reverse primer sequences were 5'-CCACCAGCTTCCTCTTCTCA-3'. All reactions were carried out for 25-30 pcr cycles. Typical reaction conditions were 1 min at 94 °C; 24-29 cycles at 94 °C for 30 sec and 68 °C for 4 min; then 5 min at 68 °C for the final extension of products. PCR products were separated by agarose gel electrophoresis using a 1% agarose gel and detected using ethidium bromide staining. Products were visualized by UV light. Photos were taken of the gels and visually analyzed for either the presence or absence of a band at the correct molecular weight.

Quantigene® assay

This method of mRNA analysis was developed by Genospectra, Inc. (now Panomics Inc.). This assay allows quantitation of mRNA from either whole cell lysate or extracted total RNA. This assay is based on branched DNA technology. The desired mRNA is hybridized to a gene specific probe set, here, PPAR α . The probe set consists of three types of probes: Capture Extender, Label Extender, and the Blocking probe, all designed to hybridize to the target mRNA. Manufacturer supplied protocol was followed throughout these experiments. Briefly, for the whole cell lysate method: Lysate from 20,000 cells was loaded in each well of a Quantigene® Capture Plate and hybridized to probes specific for PPAR α mRNA. The ratio of PPAR α expression corrected for β -actin relative to HEMn-LP was calculated. Extracted total RNA method: 2ug/10uL total RNA was loaded in each well of a Quantigene® Capture Plate and hybridized to probes specific for PPAR α mRNA. The fold change of PPAR α siRNA treated cells relative to control siRNA treated cells corrected for B-actin was calculated.

Western Blotting

Nuclear extract from SK-Mel 28, A375, and HEMn-LP was isolated from each cell line using the NePER kit® 72 hours after seeding when cells were at ~70% confluence (Pierce, Rockford, IL) according to the manufacturer's protocol. For MCAD western blot analysis, whole cell lysate was isolated from control and siRNA treated SK-Mel 28 cells at 48h or 96h post treatment. Protein concentration was determined using the BCA protein assay reagents from Pierce as per the manufacturer's instructions. 50ug protein was separated by SDS-PAGE and transferred to nitrocellulose membranes using the BioRAD MiniProtean3® system. Equal loading was also determined by Ponceau staining of the nitrocellulose membranes following transfer. Blots were blocked using ChemiBlocker reagent (Chemicon, Temecula, CA) and probed overnight at 4 °C with either anti-PPAR γ monoclonal (Cell Signaling, Danvers, MA) at 1:1000, anti-PPAR α monoclonal (Panomics, Inc., Fremont, CA) at 1:250, or anti-MCAD polyclonal at 1:2000 (Cayman Chemical, Ann Arbor, MI). Monoclonal mouse secondary IgG antibody (GE Healthcare, Piscataway, NJ) or polyclonal rabbit secondary IgG antibody (Cell Signaling, Danvers, MA) was applied after three 1x TBS + 0.05% Tween (TBS-T) washes. Blots were incubated with secondary antibody at 1:3,000 for 1h at room temperature and subsequently washed 3x with 1x TBS-T. A final 5 minute wash with TBS (no Tween) was performed just prior to incubating the blot with ECL reagent for chemiluminescence detection (GE Healthcare, Piscataway, NJ). Blots were then autoradiographed and densitometric analysis was performed. For PPAR blots, the ratio of GAPDH to PPAR α or PPAR γ is shown.

siRNA inhibition of PPAR α in SK-Mel 28 VGP melanoma cells

SK-Mel 28 cells seeded into 6 well plates at 5.0×10^4 were treated 24h after seeding with either 100nM PPAR α siRNA or 100nM control non-targeting siRNA (Dharmacon, Inc. Lafayette, CO) using the RNAifect $\text{\textcircled{R}}$ transfection reagent (Qiagen, Inc.) as per the manufacturers instructions. Briefly, siRNA oligos were diluted to a stock concentration of 10mM using 1x siRNA buffer (Dharmacon, Inc. Lafayette, CO). Final concentration of siRNA (100 nM) was obtained by diluting stock into the appropriate amount of RNAifect $\text{\textcircled{R}}$ transfection reagent as per product manual. PPAR α inhibition was confirmed by Quantigene $\text{\textcircled{R}}$ analysis at 48 and 96h post transfection. There was ~80% decrease in PPAR α mRNA relative to PPAR α mRNA levels in control siRNA treated SK-Mel 28 cells at each time point.

Statistical Analysis

Where applicable, data was analyzed by unpaired, two-tailed t tests. Statistical significance was defined as a *p* value of 0.05 or less. All error bars shown represent standard error.

RESULTS

Anchorage-Dependent growth in human melanoma and normal human melanocyte cell lines treated with PPAR agonists

The hypothesis that PPAR γ or PPAR α activation could lead to a less tumorigenic state in human melanoma was initially tested by determining the effects that various PPAR agonists had on each of the human melanoma and normal human melanocyte cell lines. To discern which PPAR subtypes might be involved in anchorage-dependent growth inhibition, I treated normal human melanocytes, SK-Mel 28 (VGP), and A375 (amelanotic metastatic) human melanoma cells with or without the PPAR γ agonists PGJ₂, ciglitazone, or troglitazone. The effects of PPAR α activation on anchorage-dependent growth were observed by treating these cells with or without the PPAR α agonists WY-14643 or LTB₄. Each cell line was treated for 48h and the growth rates were determined by either hemacytometer or crystal violet staining (**Figures 4-16**). Each treatment was performed in triplicate at least 3 times unless otherwise noted. Contrary to our original hypothesis, the SK-Mel 28 cells were not significantly growth inhibited by any of the PPAR γ or PPAR α agonists (**Figures 4, 6, 7 and 8**). In support of our hypothesis, however, I found that the A375 metastatic cells were significantly growth inhibited in response to the natural PPAR γ agonist, PGJ₂ at 10 μ M (**Figure 9**) and the synthetic PPAR γ agonist, troglitazone also at the 10 μ M concentration (**Figure 13**). Troglitazone treatment also resulted in significant anchorage-dependent growth inhibition in the normal human melanocytes at 10 μ M (**Figure 14**). Our hypothesis that PPAR α activation could lead to a significant decrease in anchorage-dependent growth

in these cells could not be supported by our data. No cell line tested was significantly affected by any PPAR α agonist used. In addition to anchorage-dependent growth, another marker of cellular differentiation in melanoma is an increase in melanin production. We hypothesized that treatment of the melanin producing cells with the PPAR agonists would increase their melanin production, thus indicating a more differentiated phenotype. However, SK-Mel 28 cells treated with PGJ₂ exhibited no reproducible significant change in melanin production (**Figure 5**). Normal human melanocytes had no significant reproducible change in melanin production when they were treated with the PPAR γ agonist troglitazone (**Figure 15**). A375 cells are amelanotic, therefore no melanin assay was performed. When treated with PGJ₂, the normal human melanocytes exhibited no significant reproducible change in anchorage dependent growth (**Figure 16**). In support of our hypothesis, I found that anchorage-dependent growth in the A375 human metastatic melanoma cells and the normal human melanocytes was significantly affected by PPAR γ agonists.

Expression of PPAR subtype mRNA

Since PPAR agonists elicited no significant reproducible effect on anchorage-dependent growth in SK-Mel 28 cells, and also in light of the fact that no PPAR α agonist had an effect on any cell line tested, I needed to determine whether or not there was expression of the PPAR subtypes in the cell lines. To determine the levels of PPAR γ 1, PPAR γ 2, and PPAR δ mRNA, RT-PCR was performed in the SK-Mel 28 and A375 cells. These results show that PPAR γ 1, PPAR γ 2, and PPAR δ are all expressed in these cell lines (**Figure 17**). To determine the relative levels of PPAR α in the normal human

melanocytes, SK-Mel 28, and A375 cells, the Quantigene® assay was used. I found that PPAR α mRNA levels were ~2 fold higher in the SK-Mel 28 cells relative to the normal human melanocytes (**Figure 18**). A375 levels of PPAR α mRNA were only ~0.14 fold higher than the levels found in the normal human melanocytes (**Figure 18**). To summarize, both SK-Mel 28 and A375 cells were positive for PPAR γ 1, PPAR γ 2, PPAR δ , and PPAR α mRNA expression. The normal human melanocytes were only tested for PPAR α and were positive for this PPAR subtype mRNA.

Figure 4: Anchorage-dependent growth study in SK-Mel 28 treated with PGJ₂.

SK-Mel 28 cells (5.0×10^5) were seeded into each 100mm dish. At 72h post seeding, cells were treated with or without agonist. The PPAR_γ agonist, PGJ₂, or DMSO vehicle (**Control**) was used to treat SK-Mel 28 cells. After 48h treatment, cellular growth was determined by crystal violet staining as described in materials and methods. Results are expressed as fraction of control. Experiments were performed in triplicate and figure is representative of 3 or more independent assays. Error bars represent standard error.

Figure 4: Anchorage-dependent growth study in SK-Mel 28 treated with PGJ₂

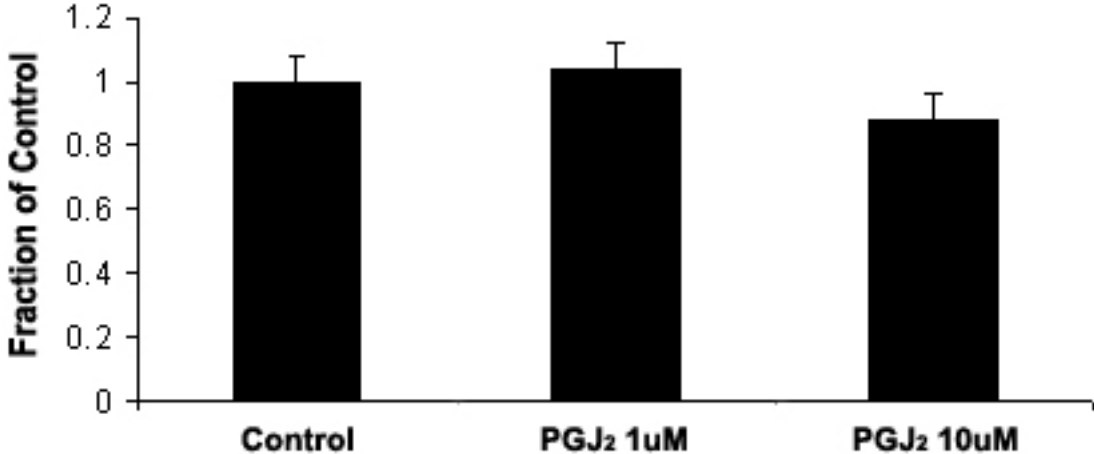


Figure 5: Melanin production in SK-Mel 28 treated with PGJ₂. SK-Mel 28 cells were seeded at 5.0×10^5 into 100mm dishes. Seventy two hours later, cells were treated with PGJ₂ or DMSO vehicle (**Control**) for 48h. Cells were subsequently lysed with 1N KOH and the lysate was placed in 80°C water bath. One hundred μ L of cellular lysate was loaded into the wells of a 96-well plate and the amount of melanin determined by measuring the absorbance at 462 nm. Results are corrected for cell number and shown as fraction of control.

Figure 5: Melanin production in SK-Mel 28 treated with PGJ₂

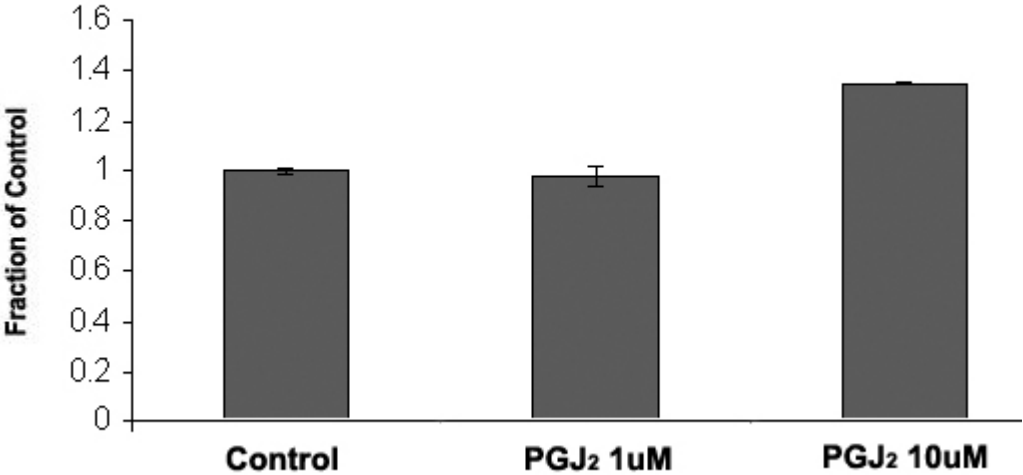


Figure 6: Anchorage-dependent growth study in SK-Mel 28 treated with ciglitazone. SK-Mel 28 cells were seeded at 5.0×10^5 cells per 100mm dish. At 72h post seeding the PPAR γ agonist, ciglitazone (**Cig**) or DMSO vehicle (**Control**) was used to treat the cells. After 48h of troglitazone treatment, cellular growth was determined by hemocytometric analysis. Cells were counted and corrected for control cell number. Results are expressed as fraction of the control. Experiments were performed in triplicate and figure is representative of 3 or more independent assays. Error bars represent standard error.

Figure 6: Anchorage-dependent growth study in SK-Mel 28 treated with ciglitazone

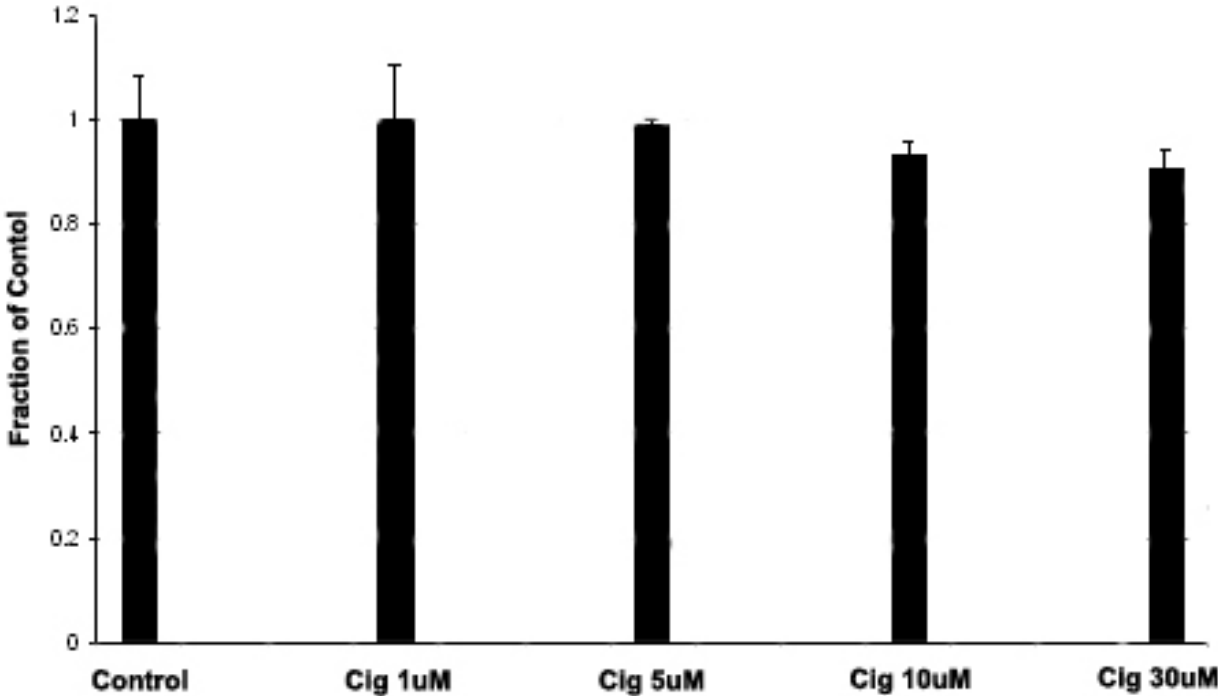


Figure 7: Anchorage-dependent growth study in SK-Mel 28 treated with WY-14643. SK-Mel 28 cells were seeded at 5.0×10^5 cells per 100mm dish. At 72h post seeding the PPAR α agonist, WY-14643 (**WY**) or DMSO vehicle (Control) was used to treat the cells. After 48h of WY-14643 treatment, cellular growth was determined by hemocytometric analysis. Cells were counted and corrected for cell number. Results are expressed as fraction of control. Experiments were performed in triplicate and figure is representative of 3 or more independent assays. Error bars represent standard error.

Figure 7: Anchorage-dependent growth study in SK-Mel 28 treated with WY-14643

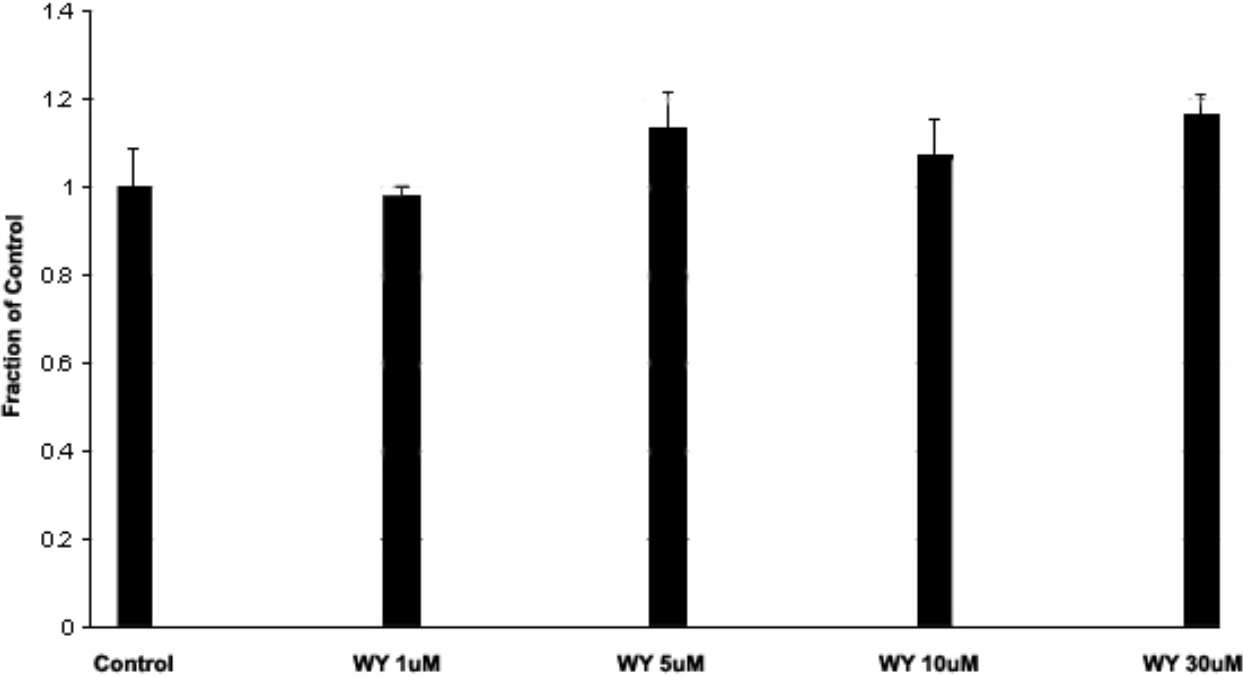


Figure 8: Anchorage-dependent growth study in SK-Mel 28 treated with troglitazone. SK-Mel 28 cells were seeded 5.0×10^5 cells per 100mm dish. At 72h post seeding the PPAR γ agonist, troglitazone (**Trog**), or DMSO vehicle (**Control**) was used to treat the cells. After 48h of troglitazone treatment, cellular growth was determined by crystal violet staining as described in materials and methods. Results are expressed as fraction of control. Experiments were performed in triplicate and figure is representative of 3 or more independent assays. Error bars represent standard error.

Figure 8: Anchorage-dependent growth study in SK-Mel 28 treated with troglitazone

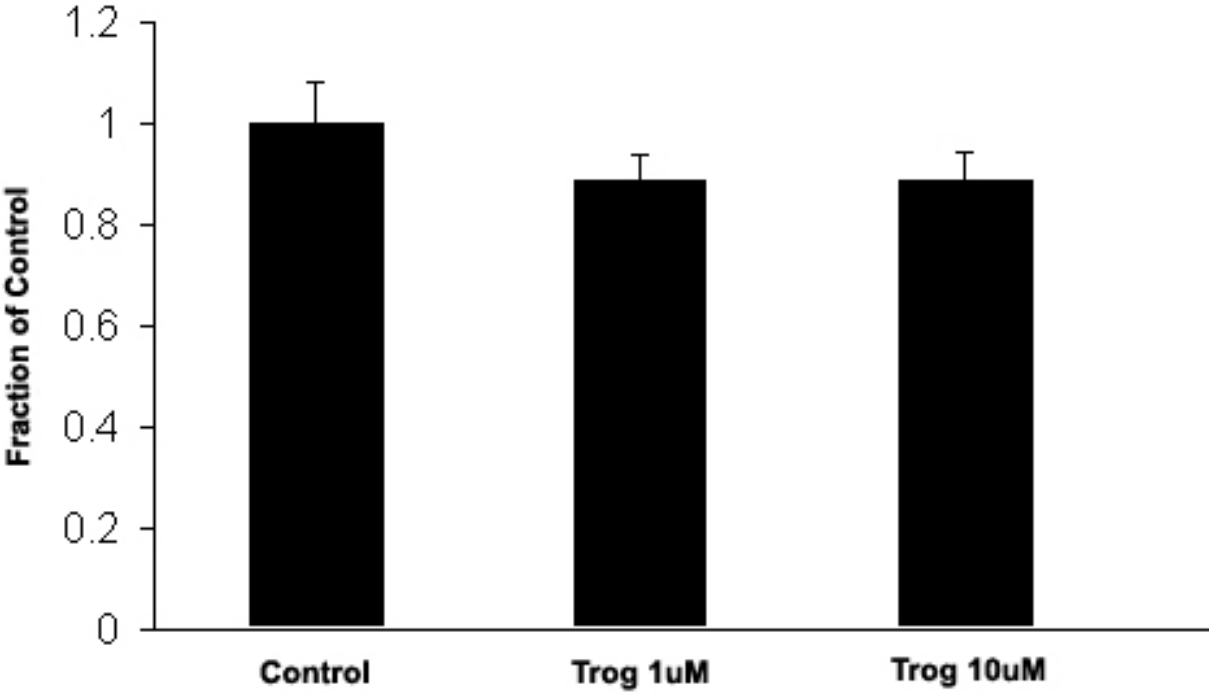


Figure 9: Anchorage-dependent growth study in A375 treated with PGJ₂. A375 cells were seeded at 5.0×10^5 cells per 100mm dish. At 72h post seeding, the PPAR γ agonist, PGJ₂, or DMSO vehicle (**Control**) was used to treat the cells. After 48h of PGJ₂ treatment, cellular growth was determined by crystal violet staining as described in materials and methods. Results are expressed as fraction of control. Experiments were performed in triplicate and figure is representative of 3 or more independent assays. Error bars represent standard error. * denotes $p < 0.006$

Figure 9: Anchorage-dependent growth study in A375 treated with PGJ₂

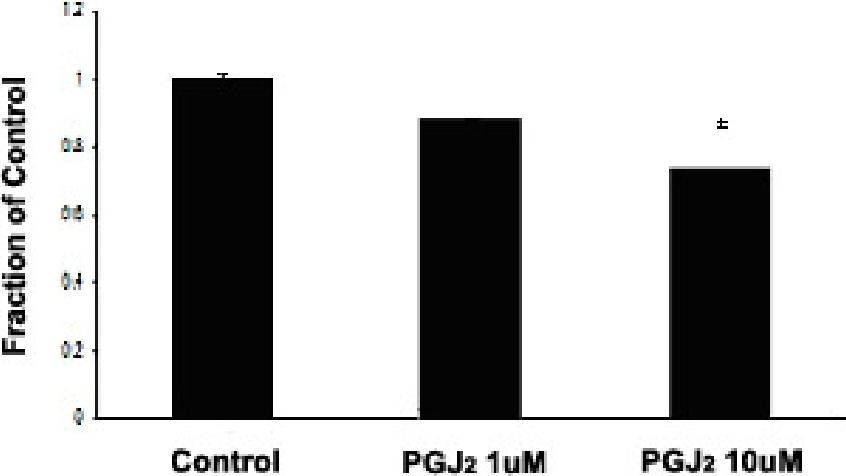


Figure 10: Anchorage-dependent growth study in A375 treated with ciglitazone.

A375 cells were seeded at 5.0×10^5 cells per 100mm dish. At 72h post seeding the PPAR γ agonist, ciglitazone (**Cig**), or DMSO vehicle (**Control**) was used to treat the cells. After 48h of ciglitazone treatment, cellular growth was determined by hemacytometric analysis. Cells were counted and corrected for DMSO treated (control) cell number. Results are expressed as fraction of control. Experiments were performed in triplicate and figure is representative of 3 or more independent assays. Error bars represent standard error.

Figure 10: Anchorage-dependent growth study in A375 treated with ciglitazone

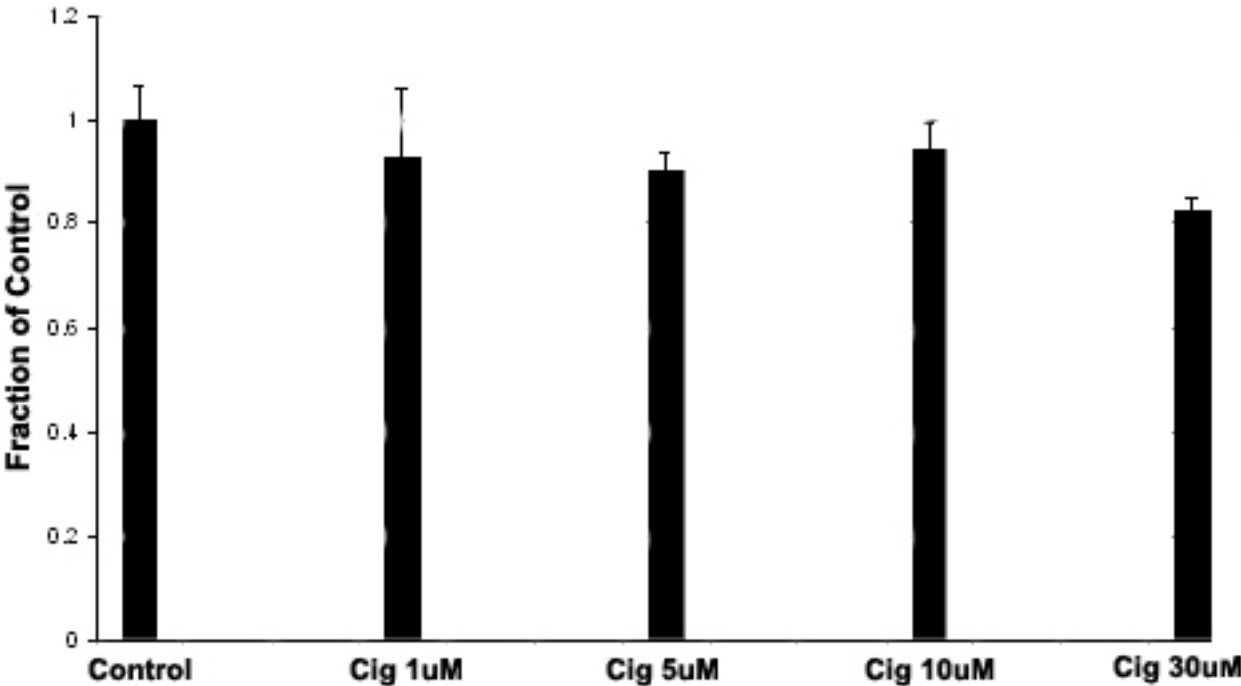


Figure 11: Anchorage-dependent growth study in A375 treated with WY-14643.

A375 cells were seeded at 5.0×10^5 cells per 100mm dish. At 72h post seeding the PPAR α agonist, WY-14643 (**WY**), or DMSO vehicle (**Control**) was used to treat the cells. After 48h of WY-14643 treatment, cellular growth was determined by hemacytometric analysis. Cells were counted and corrected for DMSO treated control cell number. Results are expressed as fraction of control. Experiments were performed in triplicate and figure is representative of 3 or more independent assays. Error bars represent standard error.

Figure 11: Anchorage-dependent growth study in A375 treated with WY-14643

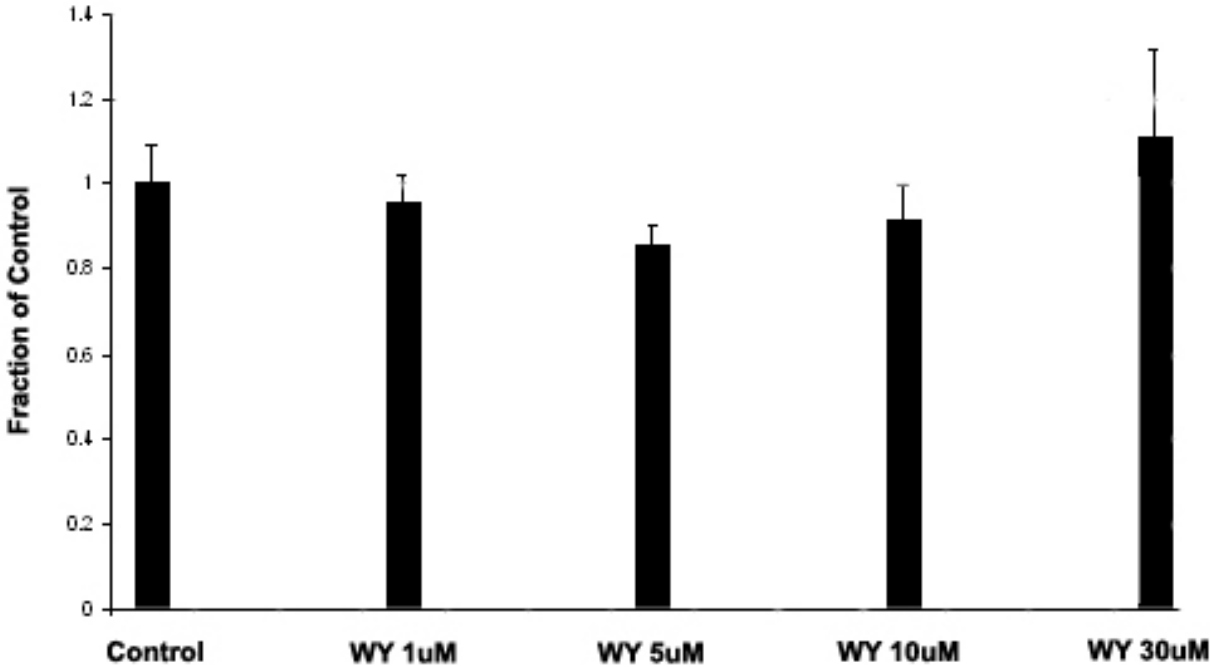


Figure 12: Anchorage-dependent growth study in A375 treated with LTB₄. A375 cells were seeded at 5.0×10^5 cells per 100mm dish. At 72h post seeding the PPAR α agonist, LTB₄, or ethanol vehicle (**Control**) was used to treat the cells. After 48h of LTB₄ treatment, cellular growth was determined by hemacytometric analysis. Cells were counted and corrected for DMSO treated control cell number. Results are expressed as fraction of control. Experiments were performed in triplicate and figure is representative of 3 or more independent assays. Error bars represent standard error.

Figure 12: Anchorage-dependent growth study in A375 treated with LTB₄.

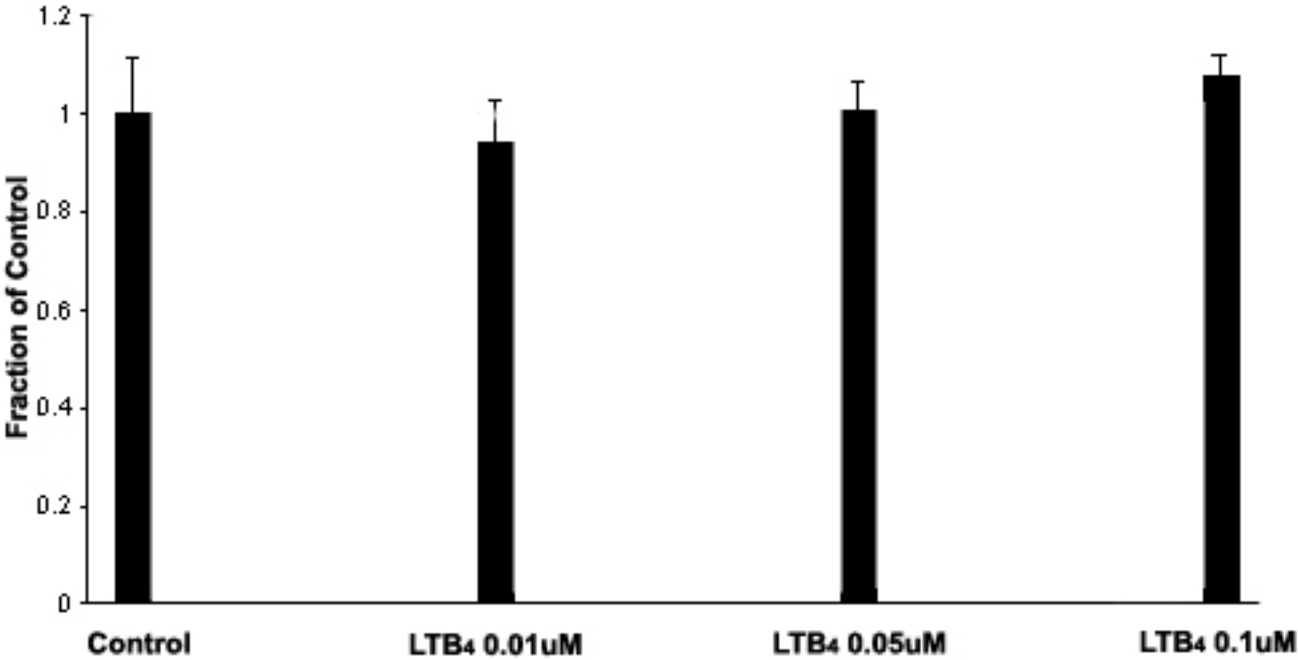


Figure 13: Anchorage-dependent growth study in A375 treated with troglitazone.

A375 cells were seeded at 5.0×10^5 cells per 100mm dish. At 72h post seeding the PPAR γ agonist, troglitazone (**Trog**), or DMSO vehicle (**Control**) was used to treat the cells. After 48h of troglitazone treatment, cellular growth was determined by crystal violet staining as described in materials and methods. Results are expressed as fraction of control. Experiments were performed in triplicate and figure is representative of 3 or more independent assays. Error bars represent standard error. * denotes $p < 0.003$

Figure 13: Anchorage-dependent growth study in A375 treated with troglitazone

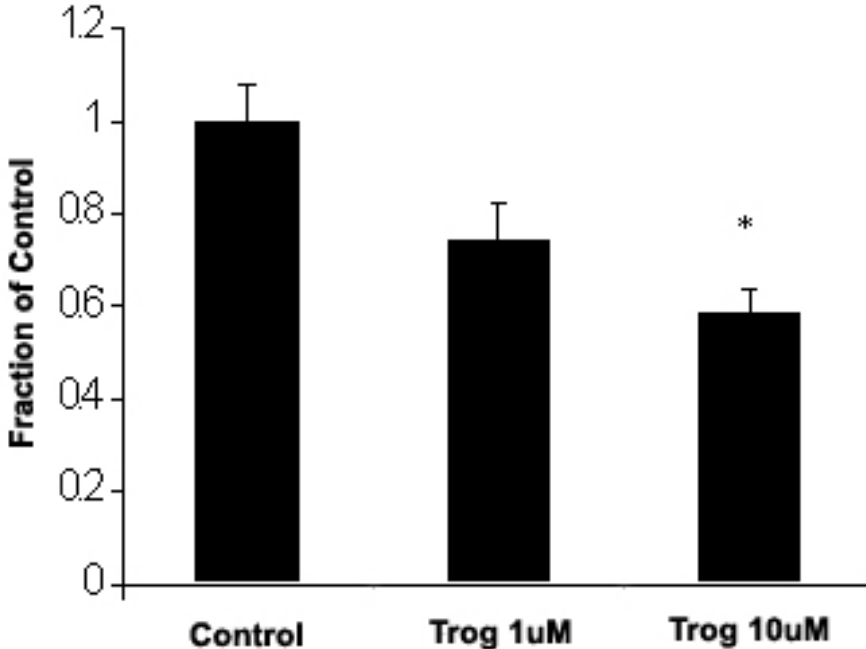


Figure 14: Anchorage-dependent growth study in HEMn-LP treated with troglitazone. HEMn-LP cells were seeded at 5.0×10^5 cells per 100mm dish. At 72h post seeding the PPAR γ agonist, troglitazone (**Trog**), or DMSO vehicle (**Control**) was used to treat the cells. After 48h of troglitazone treatment, cellular growth was determined by crystal violet staining as described in materials and methods. Results are expressed as fraction of control. Experiments were performed in triplicate and figure is representative of 3 or more independent assays. Error bars represent standard error. * denotes $p < 0.002$

Figure 14: Anchorage-dependent growth study in HEMn-LP treated with troglitazone

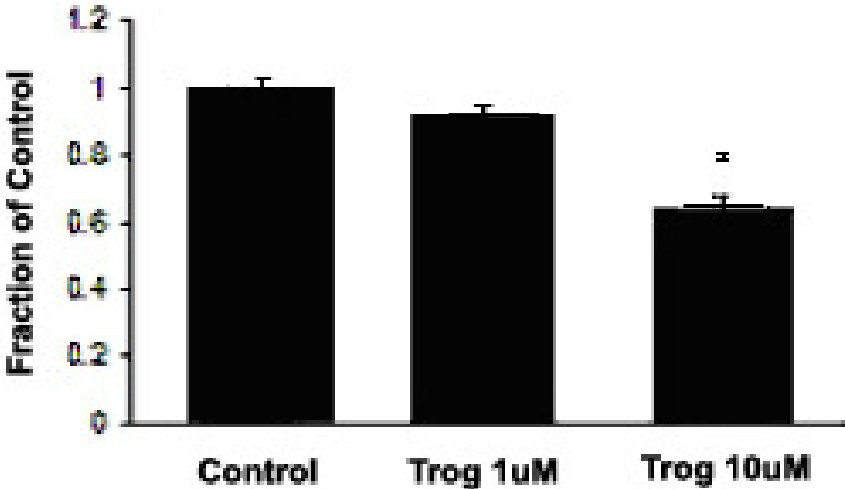


Figure 15: Melanin production in HEMn-LP treated with troglitazone. HEMn-LP cells were seeded at 5.0×10^5 into 100mm dishes. At 72h post-seeding cells were treated with troglitazone (**Trog**) or DMSO vehicle (**Control**) for 48h. Subsequently, cells were lysed and melanin assay was performed as described in materials and methods. Results are corrected for cell number and shown as fraction of control. Experiments were performed in triplicate and figure is representative of 3 or more independent assays. Error bars represent standard error.

Figure 15: Melanin production in HEMn-LP treated with troglitazone

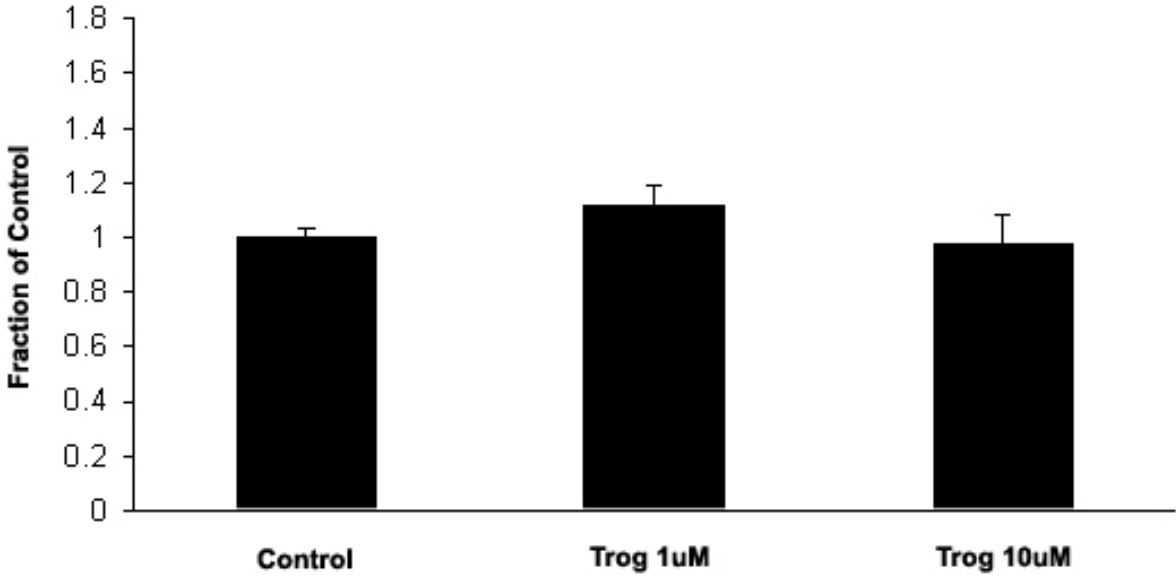


Figure 16: Anchorage-dependent growth study in HEMn-LP treated with PGJ₂.

HEMn-LP cells were seeded at 5.0×10^5 cells per 100mm dish. At 72h post-seeding, the PPAR γ agonist, PGJ₂, was used to treat the cells. After 48h of PGJ₂ or vehicle (DMSO) treatment, cellular growth was determined by crystal violet staining as described in materials and methods. Results are expressed as fraction of DMSO treated (control) cells. Experiments were performed in triplicate and figure is representative of 3 or more independent assays. Error bars represent standard error.

Figure 16: Anchorage-dependent growth study in HEMn-LP treated with PGJ₂

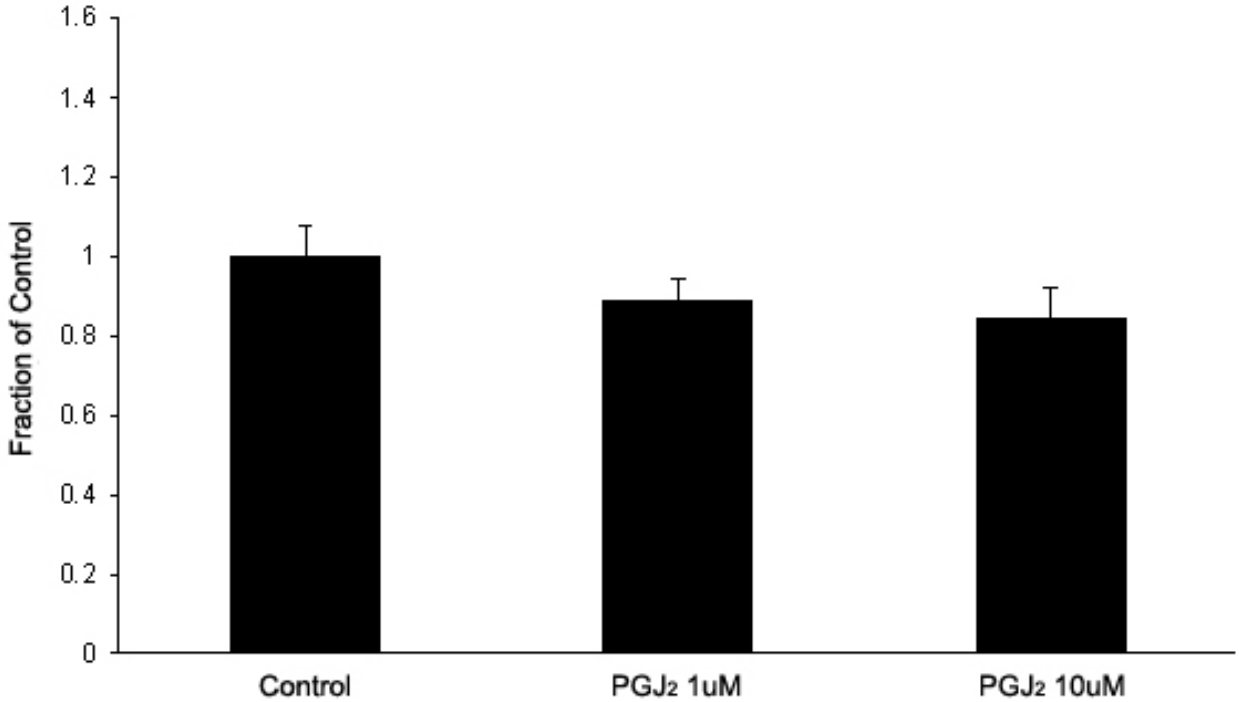


Figure 17: RT-PCR for PPARs in human melanoma cells. Total RNA was extracted from SK-Mel 28 vertical growth phase cells and A375 metastatic melanoma cells at 72 hours post-seeding when cells were at ~70% confluence. RNA integrity was determined using the Agilent Bioanalyzer®. RNA was reverse transcribed using the Advantage RT-for PCR kit®. 5uL of the resulting cDNA was used in the PCR reaction as described in the Advantage cDNA kit® manual using primers specific for either PPAR γ 1, PPAR γ 2, or PPAR δ .

Figure 17: RT-PCR for PPARs in human melanoma cells

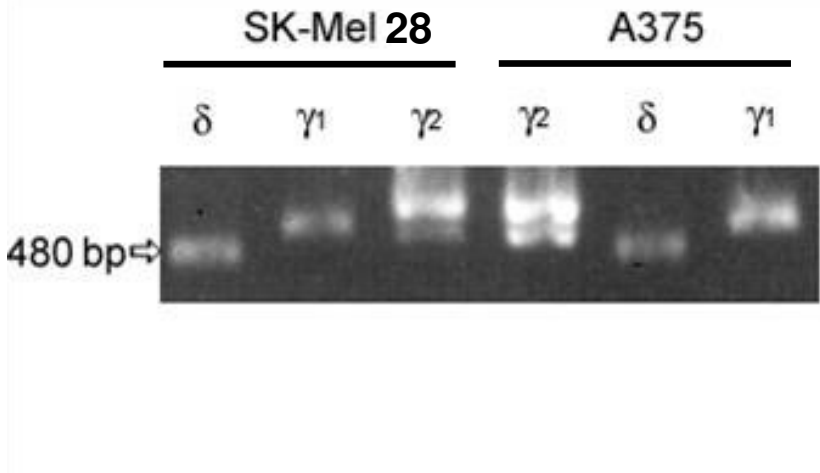
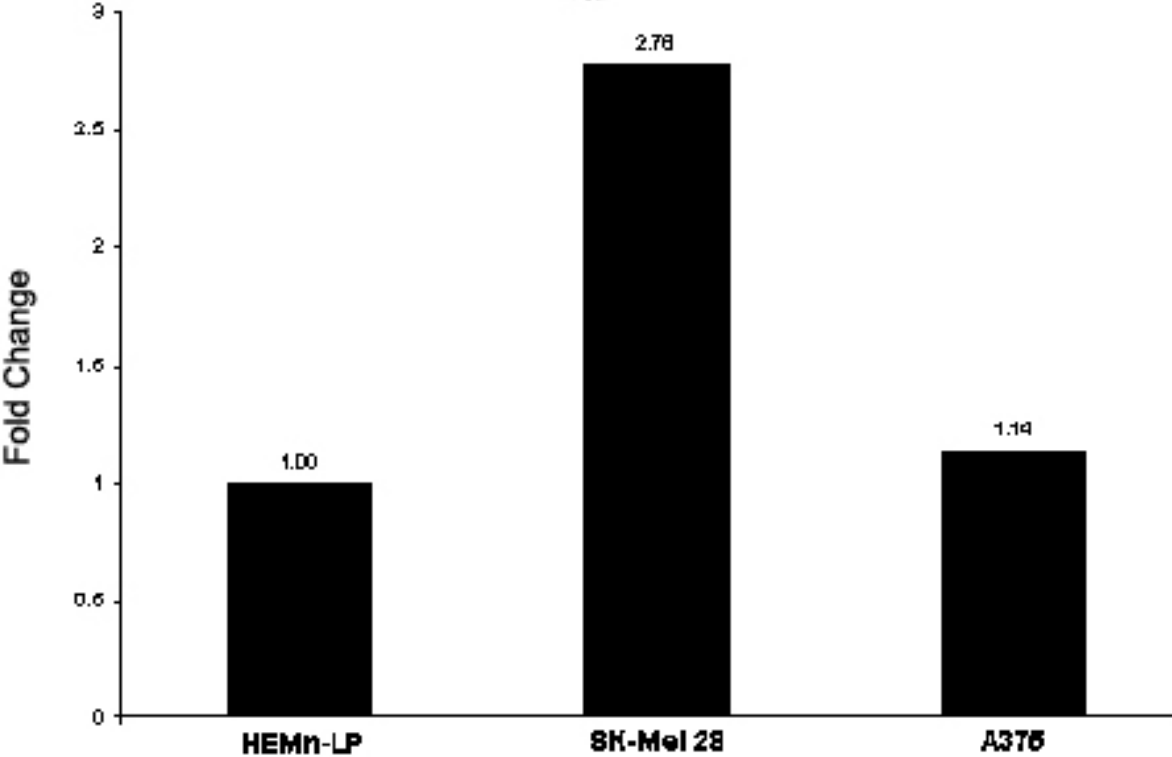


Figure 18: Quantigene® analysis to determine relative expression of PPAR α mRNA. The Quantigene® assay system was used to determine the relative levels of PPAR α mRNA in HEMn-LP, SK-Mel 28, and A375 human melanoma cells. This assay allows quantitation of mRNA species directly from cell lysates without the need to isolate total RNA. Cells were harvested at ~70% confluence. Total cell extract from 20,000 cells was loaded in each well of a Quantigene® Capture Plate and hybridized to probes specific for PPAR α mRNA. The data is expressed as the fold increase of PPAR α expression corrected for β -actin expression (internal control) relative to the amount of HEMn-LP PPAR α expression (also corrected for β -actin expression).

Figure 18: Quantigene® analysis to determine relative expression of PPARα mRNA



Expression of PPAR subtype protein

While PPAR subtype mRNA was shown to be present in each cell line tested, the protein levels had yet to be determined. Relative protein expression levels of PPAR α (**Figure 19**) and PPAR γ (**Figure 20**) subtypes were determined by western blot analysis. Either whole cell lysates or nuclear extracts from normal human melanocytes, SK-Mel 28, or A375 cells were subjected to SDS-PAGE and the resulting blots were visualized and density of the immunoreactive PPAR protein signals analyzed using the BioRad Chemi-Doc®. All blots were re-probed with GAPDH antibody and the density of the PPAR reactive protein signal divided by the density of the GAPDH signal. I found that PPAR α protein levels were highest in the A375 cells (**Figure 19**). PPAR γ protein was ~50% higher in both SK-Mel 28 and A375 melanoma cells relative to the normal human melanocytes (**Figure 20**). SK-Mel 28 PPAR α protein was ~20% less than that of A375 cells while the normal human melanocytes had ~70% less than the A375 cells (**Figure 19**).

Decrease in SK-Mel 28 cell PPAR α by siRNA knockdown

Since the mRNA levels of PPAR α were highest in the SK-Mel 28 cells, siRNA targeting PPAR α was used to determine the effects of PPAR α knockdown on the physiology of these human melanoma cells. Even though consistent 80% PPAR α mRNA knockdown was achieved (**Figure 21**), as determined by the Quantigene® assay, no major biological effect was seen in these cells. There was no change in morphology in these cells treated with PPAR α siRNA compared to control siRNA-treated cells (**Figure 23 A and B**). The expression of MCAD is a direct indicator of

PPAR α transcriptional activity. The expression of MCAD should decrease when the PPAR α level/activity decreases. This was not the case as shown in **Figure 22**.

Figures 19: PPAR α protein expression in human melanoma and normal melanocytes. Fifty μ g nuclear extract from SK-Mel 28, A375, and HEMn-LP was separated by SDS-PAGE. The resulting blot was probed with PPAR α antibody (Panomics, Inc.) at a titer of 1:250 and bands were visualized by chemiluminescence. Densitometry was performed and the ratio of PPAR α to GAPDH relative to SK-Mel 28 was calculated. Data is shown as fraction of control (**SK-Mel 28**). **M** = molecular weight marker.

Figure 19: PPAR α protein expression in human melanoma and normal melanocyte

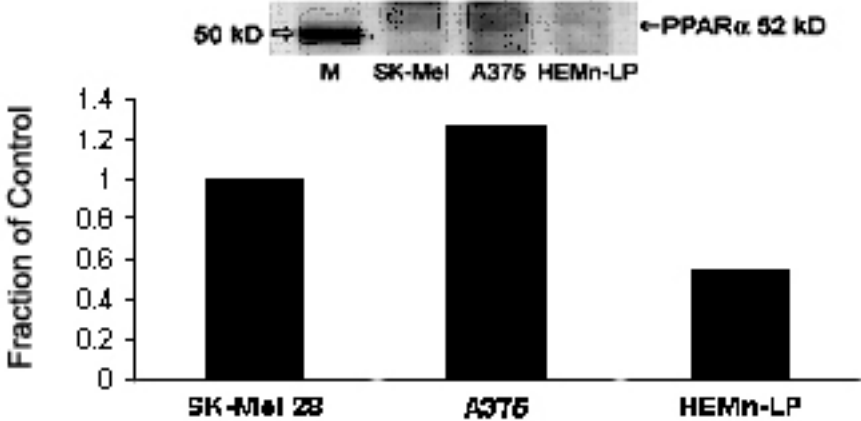


Figure 20: PPAR γ protein expression in human melanoma and HEMn-LP. Fifty μ g whole cell lysate was extracted from SK-Mel 28, A375, and HEMn-LP and subsequently separated by SDS-PAGE. The resulting blot was probed using Anti-PPAR γ (Cell Signaling, Inc.) at 1:1000. Bands were visualized using chemiluminescence detection. Densitometric analysis was performed and the ratio of PPAR γ to GAPDH relative to SK-Mel 28 was calculated. Data is presented as fraction of control (**SK-Mel 28**). Data is presented fold change.

Figure 20: PPAR γ protein expression in human melanoma and HEMn-LP

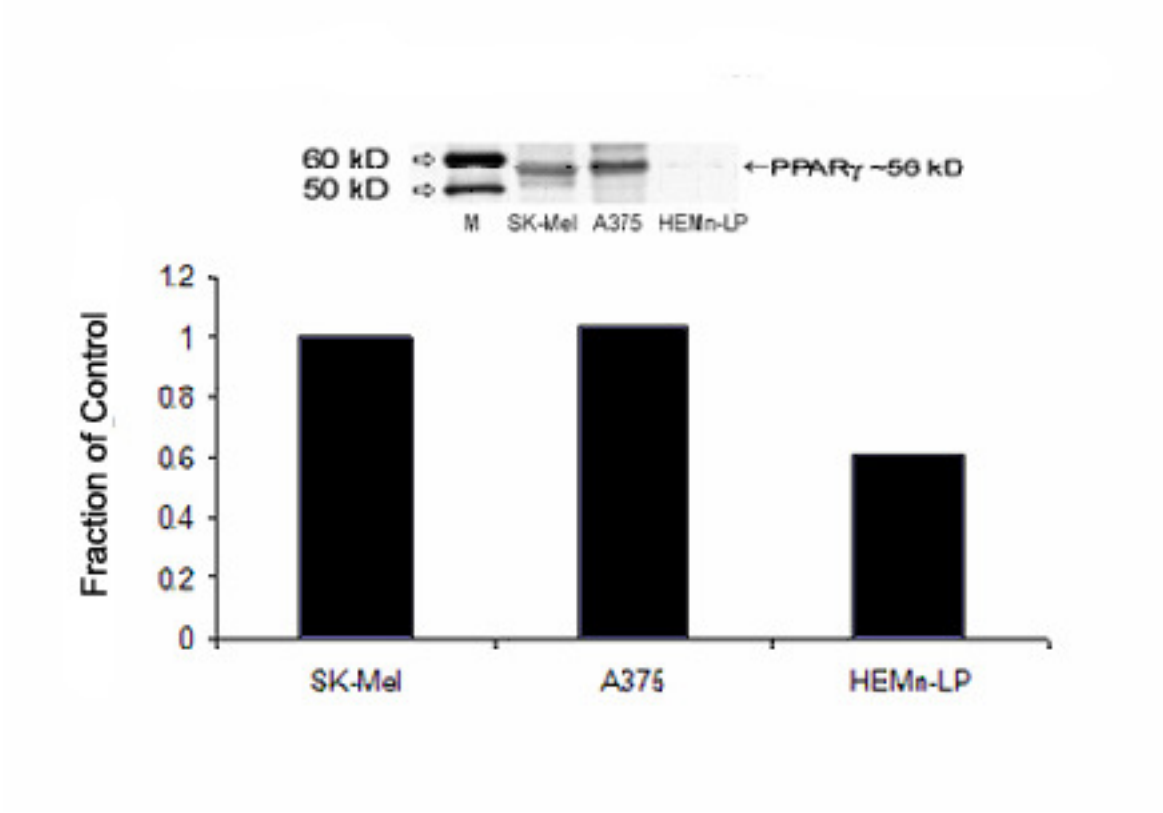


Figure 21: Quantigene® analysis to determine siRNA knockdown of PPAR α . SK-Mel 28 cells were seeded at 1.5×10^5 cells/well into a 6-well plate. At 24 hours post-seeding, cells were treated with 100nM PPAR α siRNA using the RNAifect® kit (Qiagen, Inc). Total cellular RNA was isolated 48h or 96h later, using Tri Reagent® (Molecular Research Corp. Cincinnati, OH). RNA integrity was determined using the Agilent Bioanalyzer®. The Quantigene® assay system was used to determine % knockdown of the PPAR α mRNA. The Quantigene® assay is based on branched DNA technology that allows quantitation of mRNA species from total RNA. The desired mRNA is hybridized to a gene specific probe set, here, PPAR α . The probe set consists of three types of probes: Capture Extender, Label Extender, and the Blocking probe, all designed to hybridize to the target mRNA. Total RNA (2 μ g/10 μ L) was loaded in each well of a Quantigene® Capture Plate and hybridized to probes specific for PPAR α mRNA. The ratio of PPAR α to β -actin (internal control) was calculated. The data is presented as a fraction of control siRNA-derived PPAR α mRNA levels.

Figure 21: Quantigene® analysis to determine siRNA knockdown of PPARα

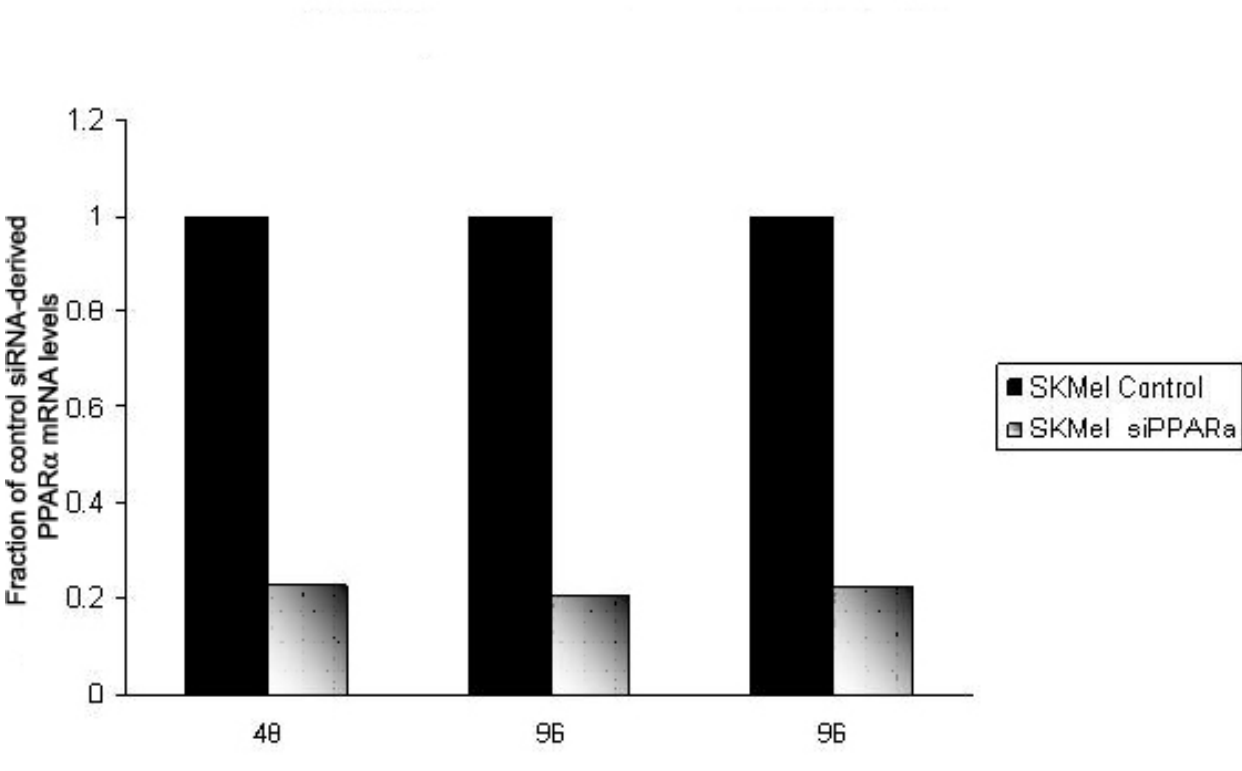


Figure 22: MCAD protein expression in SK-Mel 28 cells. Fifty μg whole cell lysate was extracted from control and PPAR α siRNA treated SK-Mel 28 cells at ~70% confluence and subsequently separated by SDS-PAGE. The resulting blot was probed using anti-MCAD (Cayman Chemical, Ann Arbor, MI) at 1:2000. Bands were visualized using chemiluminescence detection. Equal loading was determined by Ponceau staining.

Figure 22: MCAD protein expression in SK-Mel 28 cells

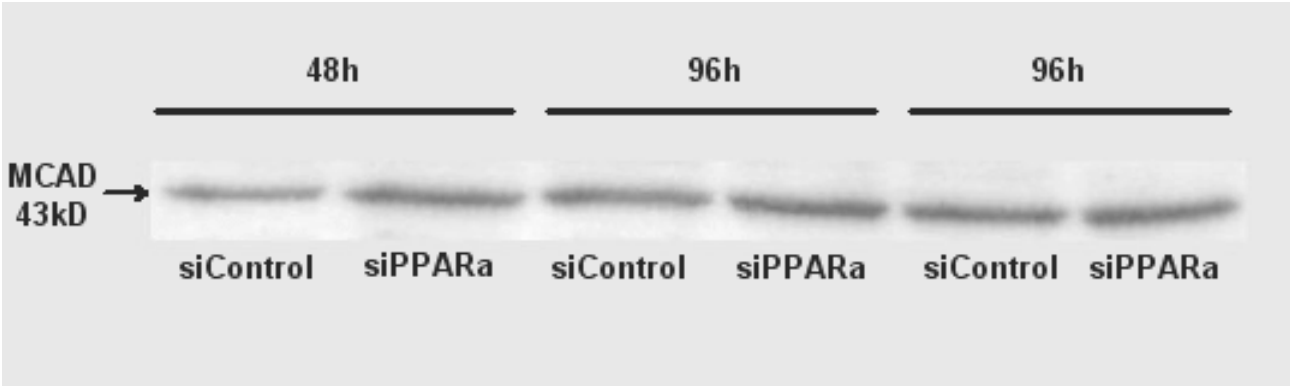
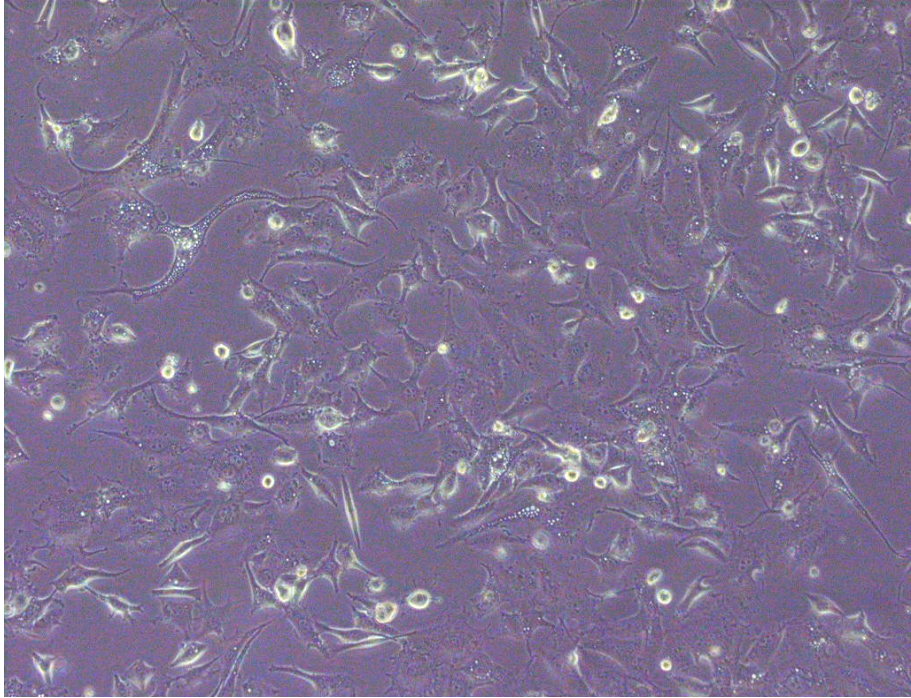


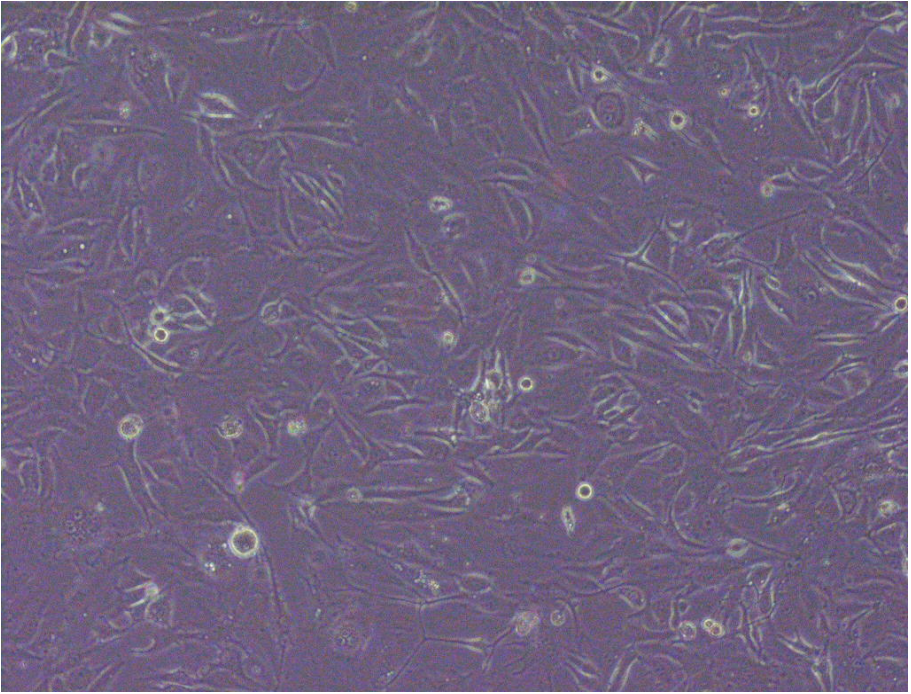
Figure 23 A and B: Images of SK-Mel 28 cells treated with control siRNA (A) or PPAR α siRNA (B). Ninety-six hour control siRNA (A) or PPAR α siRNA(B) treatment. Cell morphology was analyzed by visual analysis using images acquired by Olympus® DX-184 microscope. Images are also representative of 48h siRNA experiment.

Figure 23 A and B: Images of SK-Mel 28 cells treated with control siRNA (A) or PPAR α siRNA (B)

A



B



DISCUSSION – Part I

PPARs have been implicated in a diverse range of biological processes. They have been shown to activate many target genes that regulate a myriad of cellular functions including cell cycle progression, differentiation, and apoptosis - all of which are important to tumorigenesis. The first part of my dissertation tests the hypothesis that the PPARs play a role in the development and/or progression of human melanoma.

Initially, I treated either normal human melanocytes, SK-Mel 28, or A375, vertical growth phase and metastatic human melanoma cells respectively, with various PPAR α or PPAR γ agonists to determine whether or not these could affect cellular growth, and melanin production (**Figures 4-16**). I found that no PPAR α agonist had any significant effect on these human melanocytes and melanoma cells. Other studies have reported similar results in human melanoma, concluding that the PPAR α agonist WY-14643 had no effect on the growth of A375 human metastatic melanoma cells (Nunez NP, Liu H 2005). My western blotting experiments show that PPAR α is expressed in these cells. However, it has been reported that PPAR α may need to be phosphorylated to be fully active in some cell lines (Juge – Aubry *et al.*, 1999; Lazennec *et al.*, 2000). It could be that one of the kinases responsible for this phosphorylation is not fully active, or is not present at sufficient levels in these cells. Another possibility is that a phosphatase is overly targeting the activated PPAR α resulting in a dephosphorylation, and thus deactivation of this receptor in some sort of negative feedback scenario. Also, it is possible that there are sufficient levels of active PPAR α but it is saturated with an endogenous ligand. Since the PPAR α agonist also did not inhibit the growth of the

normal human melanocytes, it is likely that PPAR α activation does not lead to inhibition of growth in melanocytes/melanoma cells.

Unlike PPAR α , some PPAR γ agonists were shown to have a significant effect on cellular growth in the metastatic melanoma cells and the normal human melanocytes. Expression and effect of ligand activation of PPAR γ has been studied in human melanoma. Both WM35, an early stage melanoma, and A375, a metastatic melanoma cell line, have been reported to express PPAR γ mRNA and protein. While one study concluded that the growth of A375 cells was inhibited by ciglitazone (Placha *et al.*, 2003), another showed that the proliferation of A375 cells was unaffected by this compound (Nunez *et al.*, 2006). Ciglitazone had no effect on either SK-Mel 28 or A375 in these studies (**Figures 6** and **10** respectively). PGJ₂, a natural PPAR γ agonist, significantly inhibited A375 metastatic melanoma cell growth ~30% at 10 μ M compared to DMSO treated cells (**Figure 9**). PGJ₂ had no reproducible significant impact on anchorage dependent growth or melanin production in the SK-Mel 28 vertical growth phase (**Figures 4** and **5** respectively) cells. PGJ₂ had no reproducible significant effect on the anchorage dependent growth in normal human melanocytes either (**Figure 16**). Troglitazone, a potent synthetic PPAR γ agonist, had a significant impact on cellular growth in both the A375 cells (**Figure 13**) and the normal human melanocytes (**Figure 14**). At 10 μ M, TZD inhibited A375 cellular growth by ~55% compared to DMSO treated cells. Normal human melanocytes showed a clear dose dependent response to TZD with the 10 μ M treatment significantly inhibiting cellular growth by ~40% compared to DMSO controls.

Troglitazone had no reproducible significant impact on the SK-Mel 28 vertical growth phase cells. Expression and effect of ligand activation of PPAR γ has been studied in human melanoma by others as well. While one study concluded that the growth of A375 cells was inhibited by ciglitazone (Placha *et al.*, 2003), another showed that the proliferation of A375 cells was unaffected by this PPAR γ agonist (Nunez *et al.*, 2006). It has been reported by others that PPAR γ protein is expressed in WM35, an early stage melanoma, and A375, the metastatic melanoma cell line (Placha *et al.*, 2003). My western blot analysis (**Figure 20**) shows that PPAR γ is overexpressed in the SK-Mel 28 cells relative to the normal human melanocytes, however it seems to not be active in these cells. Neither PGJ₂, TZD, nor ciglitazone had any significant affect on these vertical growth phase cells. In contrast to PPAR α , PPAR γ phosphorylation results in an inhibition of transcriptional activation of this receptor (Camp *et al.*, 1999; Adams *et al.*, 1997). It is possible that there is a mutation in the PPAR γ amino acid sequence at either of the serines that are candidates for phosphorylation (Ser 82, 84, 110, or 112) which results in a constitutively-inactive pseudophosphorylated conformation in these cells. Another possible explanation is that the kinases responsible for the phosphorylation of PPAR γ are overexpressed or overly active in these cells resulting in a hyperphosphorylated (thus inactive) PPAR γ protein. Conversely, a phosphatase that could be responsible for removing the phosphorylation from PPAR γ could be inactivated in these cells. Any of these changes, together with increased expression relative to normal human melanocytes would result in a dominant-negative PPAR γ in SK-mel 28 cells.

Next, I determined whether the human melanoma cells expressed the various

PPAR subtype mRNAs. PPAR δ and PPAR γ 1 and PPAR γ 2 are expressed in both SK-Mel 28 and A375 cells according to RT-PCR results (**Figure 17**). PPAR α mRNA was measured quantitatively using the Quantigene[®] assay system. Quantigene analysis of the relative amounts of these PPAR subtypes was not performed, since no PPAR γ probes were available at the time of these experiments. PPAR α mRNA was ~2 fold higher in the SK-Mel 28 cells relative to both the normal human melanocytes and the A375 metastatic cells (**Figure 18**). The PPAR α mRNA level in the A375 was only a negligible 0.14 fold higher than in the normal human melanocytes. This was not consistent with the protein levels of PPAR α , in these cells (discussed below). I determined whether the various subtypes of PPARs are expressed at the protein level in these cell lines. After numerous attempts, I found that both PPAR α and PPAR γ are expressed in normal human melanocytes, vertical growth phase melanoma SK-Mel 28 cells, and metastatic melanoma A375 cells (**Figures 19 and 20**). PPAR α protein was highest in the A375 cells, being ~30% higher in these cells than in the SK-Mel 28 cells. Normal human melanocytes, HEMn-LP, expressed the least amount of PPAR α at ~60% less than SK-Mel 28 and ~80% less than the A375 cells. This does not correlate with the mRNA data from the same cell lines, where SK-Mel 28 cells had the highest levels of PPAR α mRNA, while A375 and HEMn-LP cells were nearly equal. This inconsistency could be attributed to the fact that PPAR α can be degraded via the ubiquitin-proteasome pathway (Blanquart *et al.*, 2002). It is possible that even though the mRNA levels of PPAR α are highest in the SK-Mel 28 cells, the PPAR α protein in these cells could be ubiquitinated at a higher rate relative to the A375 metastatic cells. This would result in lower overall PPAR α protein levels in the SK-Mel 28 cells compared

to the A375 cells. PPAR γ protein levels were consistently ~50% higher in the human melanoma cells, SK-Mel 28 and A375, relative to the normal human melanocytes.

Lastly, I explored PPAR α loss of function in the SK-Mel 28 vertical growth phase cells. Since the mRNA levels of PPAR α were highest in the SK-Mel 28 cells, I decided to silence the expression of this gene using siRNA to determine how loss of PPAR α expression in these cells might affect their function. siRNA treatment from 48h up to 96h showed consistent knockdown of PPAR α mRNA by ~80% in the SK-Mel 28 vertical growth phase cells (**Figure 21**). Even though the knockdown was significant and persistent, there was no observable biological effect in terms of morphology (**Figures 23 A and B**), nor was there any decrease in the expression of a PPAR α target gene MCAD (medium chain acyl-CoA dehydrogenase) (**Figure 22**). This lack of biological effects could be due to the fact that there is redundancy of PPAR function between the subtypes. In cells where PPAR α is decreased the other PPARs, namely PPAR γ , could compensate for this loss. Another explanation is that 80% knockdown is not enough to completely abolish PPAR α function in these cells. However, the 80% knockdown of PPAR α results in an RNA level considerably below that found in normal human melanocytes and therefore a reasonable conclusion is that the increased expression of PPAR α in SK-Mel28 melanoma cells is not contributing to its *in vitro* transformed phenotypes.

INTRODUCTION TO DISSERTATION PART II

The incidence of melanoma is increasing more rapidly than any other tumor type. Melanoma accounts for 4% of all skin cancers, but for 79% of all skin cancer-related deaths in the United States (Melanoma Research Foundation). It is notoriously resistant to both chemo- and radiotherapy (Soengas and Lowe 2003). Melanoma cells derive from the skin's natural defense system to UV light, the melanocyte. Melanocytes absorb UV light and in response, produce the pigment, melanin. To defeat the stresses of this unique function, the melanocytes are inherently and naturally resistant to apoptosis (Soengas and Lowe 2003). Understanding the molecular changes involved in the progression of melanoma as well as the basis of its resistance to current therapies is imperative to devising new strategies for its treatment.

One of the potential regulators of melanoma progression is the heterodimeric transcriptional complex, HIF-1, also known as the master regulator of O₂ homeostasis in cells (Semenza G., 2003). HIF-1 controls over 60 genes involved in many aspects of oncogenesis, including tumorigenesis (Kondo *et al.*, 2005; Zhang *et al.*, 2004). Several markers of tumorigenesis have been shown to be altered by either the overexpression or inhibition of HIF-1. Hypoxia-induced or exogenous overexpression of HIF-1 α directly increased *in vitro* invasion by the human colon adenocarcinoma cells, HCT116 (Krishnamachary *et al.*, 2003). Pancreatic cancer cells, PCI-10, which were overexpressing exogenous HIF-1 α showed a significant increase in the frequency of xenograft growth post injection (Akakura *et al.*, 2001). Inhibition of HIF-1 α activity by

overexpression of a dominant-negative form of HIF-1 α in pancreatic cancer cells, PCI-43, resulted in an increase in apoptotic cells and a decrease in their ability to form tumors in SCID mice (Chen *et al.*, 2003). Other genes controlled by HIF-1 include those involved in apoptosis (Zhang *et al.*, 2004; Greijer, A. 2004) and genetic instability (Koshiji *et al.*, 2005). HIF-1 has also been implicated in the progression of several cancers including mammary gland, prostate, brain, and lung (Goda *et al.*, 2003). HIF-1 α is the regulatory subunit of HIF-1. It is regulated at the protein level by both oxygen-dependent and independent pathways (Semenza G., 2002). Overexpression of HIF-1 α has been shown to increase the tumorigenic potency of renal cell carcinoma and bladder cancer cells (Kondo *et al.*, 2005). HIF-1 α inhibition by siRNA in HCT116 (human colon cancer) cells resulted in no tumor growth compared to control cells when introduced into nude mice (Zhang *et al.*, 2004).

HIF-1 α 785 is a novel splice variant of HIF-1 α that is characterized by excision of exon 11 and splicing of exons 10 and 12 (Chun *et al.*, 2003). While this splice variant retains the remainder of the functional domains of HIF-1 α , it loses lysine 532 in exon 11 that is usually acetylated by the acetyltransferase, ADP-ribosylation factor domain protein 1 (ARD-1) (Jeong *et al.*, 2002). This acetylation on lys 532 of HIF-1 α is critical for enhanced HIF-1 α binding to the von Hippel Lindau (VHL) tumor suppressor protein, which acts as an E3 ubiquitin ligase. VHL binding to HIF-1 α brings about degradation of HIF-1 α by the proteasome. Since binding to VHL is a critical component of HIF-1 α degradation, HIF-1 α 785 is rendered more stable by lacking this lysine 532.

In addition to the stability, there are other characteristics that set the splice

variant apart from full length HIF-1 α . HIF-1 α 785 has been shown to be regulated by different stimuli and pathways in comparison to HIF-1 α . HIF-1 α 785 does not require hypoxic conditions to be stabilized. Instead, HIF-1 α 785 can be stabilized by the phorbol ester, PMA (Lim *et al.*, 2004). HIF-1 α 785 has also been shown to be upregulated in response to hyperthermia (42°C) as well as by the Ras/Raf/MEK/ERK pathway (Lim *et al.*, 2004). In an *in vivo* nude mouse model, this splice variant was shown to render a faster growing, larger, and more hypervascular tumor than HIF-1 α (Chun *et al.*, 2003). Expression and role of HIF-1 α 785 in melanoma has yet to be elucidated.

The hypothesis was that inhibition of HIF-1 α or HIF-1 α 785 would decrease tumorigenicity in the human metastatic melanoma cells while overexpression of HIF-1 α or HIF-1 α 785 in radial growth phase cells would increase their tumorigenicity. In this part of my thesis I found that this splice variant is expressed in human melanoma cell lines while it is significantly lower in the normal human melanocytes. qPCR data shows an increase in HIF-1 α and especially HIF-1 α 785 mRNA as a function of malignant progression, while remaining nearly undetectable in normal human melanocytes. Overexpression of HIF-1 α and HIF-1 α 785 resulted in increased anchorage independent growth in the radial growth phase SbCl₂ human melanoma cells, with HIF-1 α 785 having a greater effect. Knockdown of HIF-1 α by siRNA in the human metastatic melanoma cell line, WM9, resulted in a ~50% decrease in matrigel invasion. Suppression of HIF-1 α also led to a ~50% - 60% decrease in anchorage independent growth in the WM9 cells. The gain of function data in SbCl₂ radial growth phase human melanoma cells indicates that the putative tumor promoter, HIF-1 α 785, is a potent effector of tumorigenicity in these cells. These data show that the full length HIF-1 α is able to

increase soft agar colony formation, while the HIF-1 α 785 variant has an even greater effect. The loss-of-function data for HIF-1 α induced by siRNA, suggest that inhibition of this transcription factor in metastatic human melanoma cells has a negative effect on tumorigenicity.

CHAPTER II

Function of HIF-1 in human melanoma progression

MATERIALS AND METHODS

Cell lines and cell culture conditions

SbCl₂ (RGP), WM1366 (VGP), and WM9 (Metastatic melanoma) cells were a generous gift from Meenhard Herlyn's lab at the Wistar Institute (University of Pennsylvania). All cells were incubated in a humidified incubator with 5% CO₂ and 95% air at 37 °C. The SbCl₂ cells were cultured in MCDB153 media (Invitrogen, Carlsbad CA), a powder brought up in autoclaved ddH₂O. Sodium bicarbonate (1.2g/L) was added and the pH was adjusted to ~7.4 using NaOH. Approximately 400mL of the resulting liquid MCDB153 media was supplemented with 10 mL fetal bovine serum, 800uL CaCl₂, 250uL insulin (Sigma Chemical, St. Louis, MO), and 5mL penicillin/streptomycin solution at 10,000 U/L (Invitrogen Corp., Carlsbad CA). WM1366 and WM9 cells were cultured in RPMI medium (Invitrogen Corp., Carlsbad CA). RPMI (500 mL) was supplemented with 10% fetal bovine serum and 5 mL penicillin streptomycin solution. Normal human melanocyte (HEMn-LP) cell culture conditions were as described previously.

Western Blot analysis of HIF-1 α

Nuclear extracts from each cell line were isolated using the NePER kit® (Pierce, Rockford, IL) according to the manufacturer's protocol when cells were no more than ~70% confluent. Protein concentration was determined using the BCA protein assay reagents from Pierce as per the manufacturer's instructions. Proteins were separated by SDS-PAGE and transferred to nitrocellulose membranes using the BioRAD MiniProtean3® system. Equal loading was also determined by Ponceau staining of the

nitrocellulose membranes. Blots were blocked using ChemiBlocker® reagent (Chemicon, Temecula, CA) and probed overnight at 4°C with anti-HIF-1 α monoclonal antibody at 1 μ g/mL (R&D Systems, Minneapolis, MN). Monoclonal mouse secondary IgG antibody (GE Healthcare, Piscataway, NJ) was applied after three 100 mL 1x TBS + 0.05% Tween (TBS-T) washes. Blots were incubated with secondary antibody at 1:3,000 for 1h at room temperature and subsequently washed 3x with 100mL 1x TBS-T. A final 5 minute wash with 100mL TBS (no Tween) was performed just prior to incubating the blot with ECL reagent (GE Healthcare, Piscataway, NJ). Blots were then autoradiographed.

RT-PCR for HIF-1 α and HIF-1 α 785

RT-PCR was carried out as described previously. Primers were designed to either amplify only HIF-1 α or HIF-1 α 785 exclusively. HIF-1 α primers would exclude HIF-1 α 785 by targeting exon 11, which is absent in HIF-1 α 785. HIF-1 α 785 primers were designed to exclude HIF-1 α by targeting the exon 10:12 boundary only present in HIF-1 α 785. The sequence of HIF-1 α forward primer is 5'-AAAGTTCACCTGAGCCTAAT-3', and the sequence of the reverse primer is 5'-TAAGAAAAAGCTCAGTTAAC-3'. The sequence of HIF-1 α 785 forward primers is 5'-AAAGTTCACCTGAGGACAC-3'. The sequence of the HIF-1 α 785 reverse primer is 5'-TAAGAAAAAGCTCAGTTAAC-3'.

Quantitative PCR for HIF-1 α and HIF-1 α 785

Total RNA was extracted from HEMn-LP, SbCl₂, WM1366, and WM9 cells at

both 24h (~40% confluent) and 72h (~70% confluent) after seeding using TRIZOL® reagent according to the manufacturer's protocol. RNA was then converted to cDNA using the High Capacity cDNA Archive Kit (Applied Biosystems Inc. (ABI), Foster City, CA). qPCR analysis was performed using TaqMan probes for HIF-1 α (ABI Catalog number Hs00936366) or HIF-1 α 785 (ABI Custom Primer Order) as well as β -actin (ABI Catalog number 4326315E). The reactions were performed under conditions specified in the ABI TaqMan Gene Quantitation assay protocol. Data was corrected for efficiency and loading using the Pfaffl method (Pfaffl M., 2001). Data are representative of at least 3 separate experiments.

Overexpression of HIF-1 α or HIF-1 α 785 in SbCl₂ cells

The pLenti-V5-D-TOPO vector was used in gain of function experiments in the SbCl₂ radial growth phase human melanoma cells. I cloned either HIF-1 α or HIF-1 α 785 into this vector by amplifying these genes by primers specific for both the 5' and 3' ends of HIF-1 α . The linearized pLenti-V5-D-TOPO Vector contains a GTGG overhang at one end while the insert is Taq Amplified to contain a 5'-CACC overhang at one end. Following amplification, 20 μ L of the 50 μ L PCR amplification reactions were separated on a 1% agarose gel stained with ethidium bromide to ensure the correct size amplicon was present. HIF-1 α and HIF-1 α 785 amplicons were purified from the remainder of the PCR reaction using the Zymo DNA Clean & Concentrate Kit® (Zymo Research Inc., Orange, CA). After ligation, plasmids were transformed into a premade OneShot® vial of Stbl3® competent cells (Invitrogen Corp., Carlsbad, CA) and plated onto agar plates containing 100ug/mL ampicillin. Plates were incubated at 37°C overnight and then

colonies were screened for intact insert in the correct orientation. Plasmids were isolated from positive colonies and analyzed by DNA sequencing to ensure the correct plasmid expression construct. Control plasmid, pLenti-V5-LacZ, was supplied in the ViraPower kit® (Invitrogen Corp., Carlsbad, CA).

siRNA inhibition of HIF-1 α in WM9 human metastatic cells

WM9 cells seeded into 6 well plates at 5.0×10^4 cells per well were treated 24h after seeding with either 100nM HIF-1 α siRNA or 100nM control non-targeting siRNA (Dharmacon, Inc. Lafayette, CO) using the RNAiFect® transfection reagent (Qiagen, Inc.) as per the manufacturer's instructions. Briefly, siRNA oligos were diluted to a stock concentration of 10mM using 1x siRNA buffer (Dharmacon, Inc. Lafayette, CO). Final concentration of siRNA (100 nM) was obtained by diluting stock into the appropriate amount of RNAiFect® transfection reagent as per product manual. HIF-1 α down-regulation was confirmed by western blot at 48, 72, 96, and 120h after transfection. There was ~60% - 70% decrease in HIF-1 α protein relative to control siRNA treated WM9 cells at each time point.

Matrigel invasion assay

WM9 cells treated with either 100nM HIF-1 α siRNA or 100nM control non-targeting siRNA (Dharmacon, Inc.) for 24h were seeded into 6-well matrigel (+) chambers, and, as a control, 6-well matrigel (-) chambers (BD Biosciences) at 7.0×10^4 cells per well. At 24 hours post-seeding, the matrigel was removed from the chambers using a cotton-tipped applicator. After all the matrigel on the inner part of the chambers

was removed, invading cells were fixed with 80% methanol for 5 minutes and then stained with 0.5% crystal violet for 5 minutes. After staining, the cells/chambers were extensively washed in dH₂O. Once excess stain was removed, cells were manually counted using a grid system covering the entire lower surface of the chamber. Results are expressed as % HIF-1 α siRNA treated-WM9 invasion relative to control siRNA treated-WM9 invasion, both corrected for the invasion of similarly treated cells seeded in matrigel (-) chambers.

Anchorage-independent growth assay

CytoSelect 96 well Cell Transformation Assay® (Cell Biolabs, Inc.) was used to determine anchorage-independent growth of SbCl₂ cells overexpressing either HIF-1 α , HIF-1 α 785, or LacZ. SbCl₂ cells were transfected at ~80% confluence with either pLenti-LacZ, pLenti-V5-D-TOPO-HIF-1 α , or pLenti-V5-D-TOPO-HIF-1 α 785 using FuGene 6 transfection reagent as per manufacturer's protocol (Roche, Palo Alto, CA). The next day 1.0×10^4 cells from each of the control (non-transfected), LacZ, HIF-1 α FL, or HIF-1 α 785 cells were seeded into a 0.4% agar layer poured over a 0.6% agar layer in wells of a 96 well plate. Wells lacking cells served as a fluorescent blank control. Agar layers were solubilized using a multichannel pipette, cells were lysed, and nucleic acid content stained with 15 μ L CyQuant dye. The amount of Cyquant dye in each well was determined using a fluorescent plate detector at 485/520 nm.

RESULTS

Expression of HIF-1 α in human melanoma cells

Here, we show for the first time in human melanoma, the oxygen-labile HIF-1 α protein is expressed endogenously with no external stimuli under normoxic conditions in both metastatic cell lines A375 and WM9. Normoxic expression of HIF-1 α is usually inhibited due to the activity of the PHD and ARD1 proteins. These proteins target the HIF-1 α subunit for degradation via the ubiquitin-proteasome pathway. HIF-1 α was detected as a band ranging from ~114kD – 120kD in nuclear extracts from the metastatic human melanoma cells. **Figures 24 A and B** show that HIF-1 α is clearly overexpressed in the A375 and WM9 cells relative to normal human melanocyte (HEMn-LP), radial growth phase (SbCl₂), and vertical growth phase cells (WM1366).

Expression of HIF-1 α mRNA

Regulation of HIF-1 α at the RNA level, while very rarely mentioned in the literature, could be significant in the progression of human melanoma. I determined HIF-1 α and HIF-1 α 785 mRNA levels initially by RT-PCR (**Figure 25**) and subsequently by qPCR (**Figure 26 A and B**). Both **Figures 25 and 26** show that in the cell lines examined, the relative amounts of HIF-1 α and HIF-1 α 785 mRNA increase as a function of malignant progression, while remaining nearly undetectable in normal human melanocytes. Primers were designed so that full length HIF-1 α would exclude HIF-1 α 785 by targeting exon 11, which is absent in HIF-1 α 785. Primers for HIF-1 α 785 excluded HIF-1 α by targeting the exon 10:12 boundary only present in HIF-1 α 785. At

24h there is an increase of ~9 fold for the HIF-1 α full length mRNA over the HEMn-LP levels while the HIF-1 α 785 mRNA levels rise ~8 fold over the HEMn-LP levels. At 72h post seeding, the HIF-1 α full length exhibited ~21 fold increase over the HEMn-LP levels. HIF-1 α 785 mRNA levels showed ~78 fold increase in expression over the HEMn-LP.

HIF-1 α and HIF-1 α 785 gain of function in radial growth phase SbCl2 cells

The relative levels of HIF-1 α protein are nearly undetectable in the early stage radial growth phase SbCl2 cells. To test the hypothesis that overexpression of HIF-1 α in a cell line that initially had very low levels could increase their tumorigenicity I used these SbCl2 cells as a model for this overexpression. I wanted to determine the effects that HIF-1 α or HIF-1 α 785 overexpression would have on the malignant properties of these cells. HIF-1 α or HIF-1 α 785 was cloned into the pLenti-V5-D-TOPO vector, represented in **Figure 27**. While cloning of the HIF-1 α gene was very routine, the successful cloning of the HIF-1 α 785 fragment with no rearrangements/mutations was extremely difficult. Cloning into lentiviral vectors proves arduous since the long terminal repeat sequences in the vectors are prime targets for *e. coli*-derived rearrangements. After numerous attempts, a positive clone was identified. To be sure that there were no rearrangements or mutations, DNA sequencing was performed in the Marshall University DNA core facility and an experiment to determine whether or not the V5 epitope was cloned in frame was performed. **Figure 28** shows that the HIF-1 α 785 variant was successfully cloned in frame and tagged with the V5 epitope. **Figure 29** shows overexpression of HIF-1 α or HIF-1 α 785 in SbCl2 cells leads to increased

anchorage-independent growth, with HIF-1 α 785 having the greater impact. These results do support the hypothesis that in a cell line initially void of HIF-1 α or HIF-1 α 785 expression can exhibit increased tumorigenicity when these genes, especially the HIF-1 α 785 are introduced.

HIF-1 α loss-of-function in human metastatic melanoma WM9 cells

I have shown that HIF-1 α protein is stabilized under normoxic conditions in both human metastatic melanoma cell lines. HIF-1 α could be affording these cells certain survival advantages, therefore, the effects of HIF-1 α inhibition was determined. To test the hypothesis that lowering the levels of HIF-1 α in a cell line could lessen the cells tumorigenicity, WM9 cells were treated with siRNA targeting HIF-1 α . The siRNA treatment decreased the expression of HIF-1 α by ~75-85% consistently. In the human metastatic cell line, WM9, knock down of HIF-1 α significantly inhibits both matrigel invasion and anchorage-independent growth. Matrigel invasion was decreased in HIF-1 α -siRNA treated WM9 cells by 53% compared to control siRNA treated WM9 cells (**Figure 30**). Anchorage-independent growth at day 4 was inhibited by 40% relative to control siRNA-treated WM9 cells (**Figure 31**). Anchorage-independent growth was inhibited by 70% at day 5 compared to control siRNA-treated WM9 cells (**Figure 32**). These results support the suggestion that lowering availability of the HIF-1 α in the WM9 cells decreases their tumorigenicity.

Figure 24 A and B: HIF-1 α protein expression in A375 and HEMn-LP (A) and HEMn-LP, SbCl₂, WM1366, and WM9 (B). **A.** Sixty μ g of cytoplasmic and nuclear extracts from ~70% confluent A375 and normal human melanocytes were separated via SDS-PAGE and probed with monoclonal anti-HIF-1 α (1 μ g/mL) at 1:10,000. Equal loading was determined by Ponceau staining. This blot is representative of at least 4 separate experiments. **B.** Sixty μ g of nuclear extracts from HEMn-LP (normal human melanocytes), SbCl₂ (radial growth phase melanoma), WM1366 (vertical growth phase melanoma), and WM9 (metastatic melanoma) were separated via SDS-PAGE and probed with monoclonal anti-HIF-1 α (1 μ g/mL) at 1:10,000. Equal loading was determined by Ponceau staining. This blot is representative of at least 4 separate experiments. **M** = molecular weight marker.

Figure 24: HIF-1 α protein expression in A375 and HEMn-LP (A) and HEMn-LP, SbCl₂, WM1366, and WM9 (B)

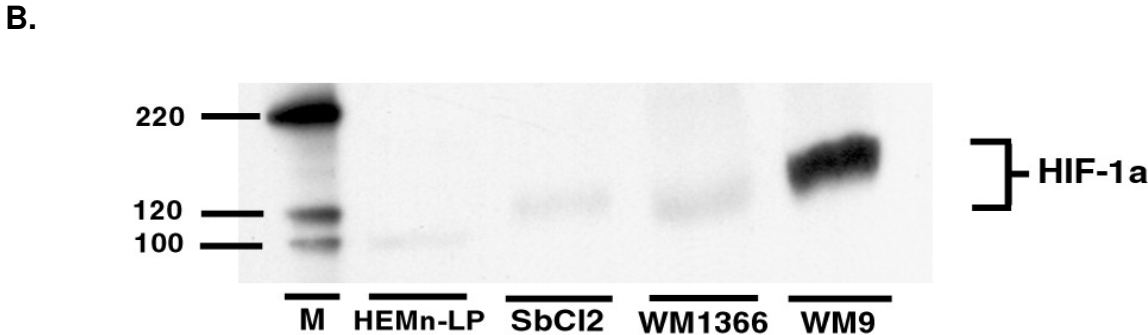
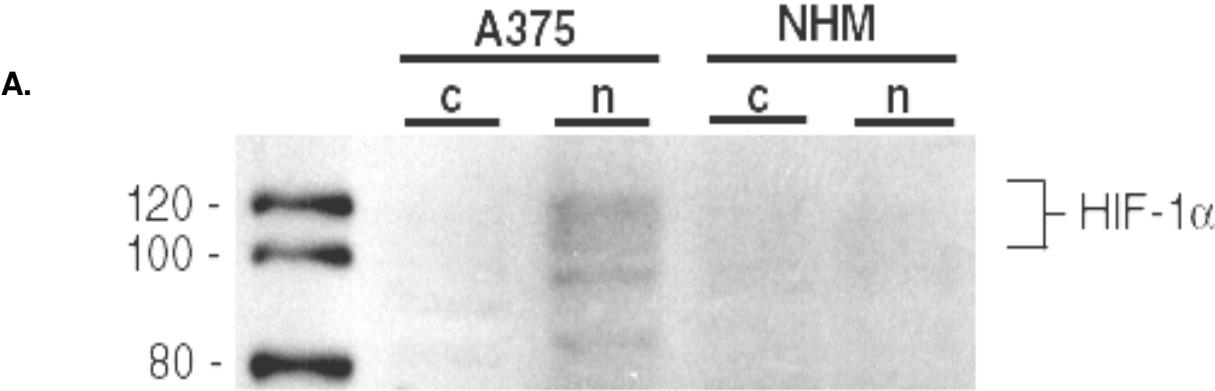


Figure 25: RT-PCR for HIF-1 α and HIF-1 α 785 in HEMn-LP, SbCl₂, WM1366, and WM9. Total RNA was extracted from normal human melanocytes (HEMn-LP), radial growth phase (SbCl₂), vertical growth phase (WM1366), and metastatic melanoma cells (WM9). RNA integrity was determined using the Agilent Bioanalyzer®. RNA was reverse transcribed using the Advantage RT-for PCR kit®. 5 μ L of the resulting cDNA was used in the PCR reaction as described in the Advantage cDNA kit® manual. Primers for HIF-1 α and HIF-1 α 785 were designed to specifically amplify each variant with no cross-amplification. Primers for the housekeeping gene control GAPDH were included in the Advantage cDNA kit®. Control primers amplifying a fragment of the control plasmid included in the Advantage cDNA kit® were used to ensure optimal PCR conditions. **M** = molecular weight marker.

Figure 25: RT-PCR for HIF-1 α and HIF-1 α 785 in HEMn-LP, SbCl₂, WM1366, and WM9

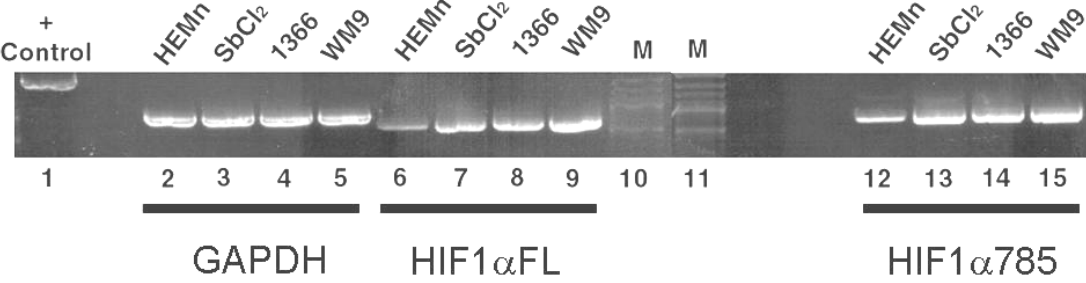


Figure 26 A and B: qPCR for HIF-1 α and HIF-1 α 785 in HEMn-LP, SbCl₂, WM1366, and WM9 at 24h (A) or 72h (B). Total RNA was extracted from HEMn-LP, SbCl₂, WM1366, and WM9 cells at both 24 (A) and 72h (B). RNA was then converted to cDNA using the High Capacity cDNA Archive Kit (ABI). qPCR analysis was performed using TaqMan probes directed at HIF-1 α or HIF-1 α 785 as well as β -actin. The reactions were performed under conditions specified in the ABI TaqMan Gene Quantitation assay protocol. Data was corrected for efficiency and loading using the Pfaffl method. Data is presented as fold change corrected for β -actin relative to HEMn-LP. Data is representative of at least 3 separate experiments.

Figure 26 A and B: qPCR for HIF-1 α and HIF-1 α 785 in HEMn-LP, SbCl₂, WM1366, and WM9 at 24h (A) or 72h (B)

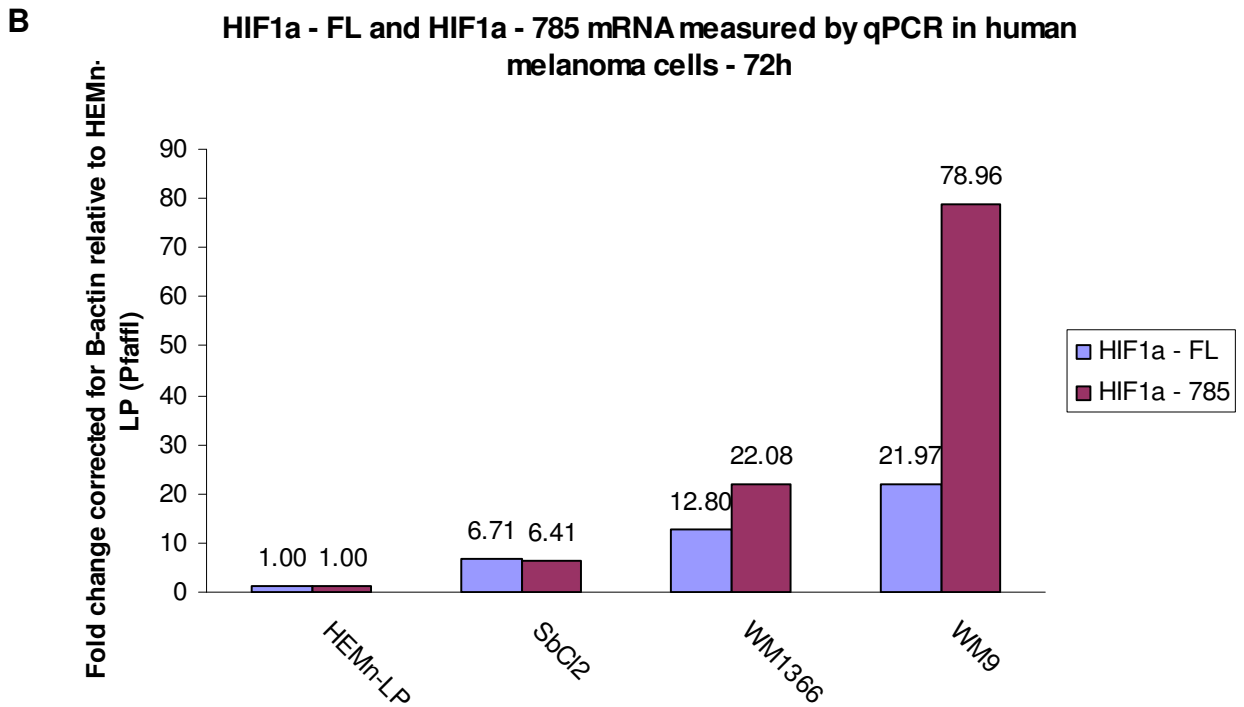
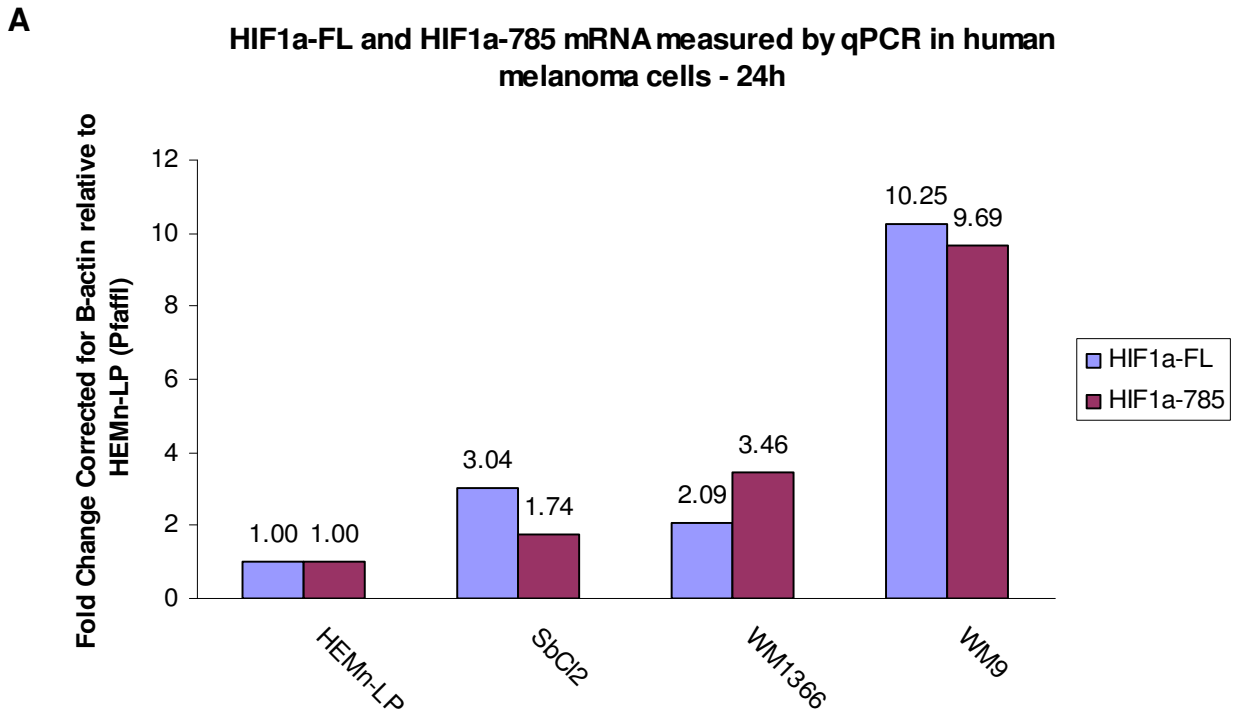


Figure 27: Representation of the pLenti-V5-D-TOPO vector. Representation of the pLenti-V5-D-TOPO vector (taken from Invitrogen Corp.) used in gain of function experiments in the SbCl₂ radial growth phase human melanoma cells. Both full length genes for HIF-1 α and HIF-1 α ⁷⁸⁵ were amplified by primers specific for HIF-1 α . A linearized D-TOPO Vector contains a GTGG overhang at one end while the insert is Taq Amplified containing a 5' -CACC overhang at one end. Expression results in the protein of interest tagged with the V5 epitope. The V5 epitope tag is derived from a small epitope (Pk) present on the P and V proteins of the paramyxovirus of simian virus 5. It usually consists of either all 14 amino acids (GKPIPPLLGLDST) or sometimes a shorter version consisting of only 9 amino acids (IPNPLLGLD).

Figure 27: Representation of the pLenti-V5-D-TOPO vector taken from Invitrogen Corp.

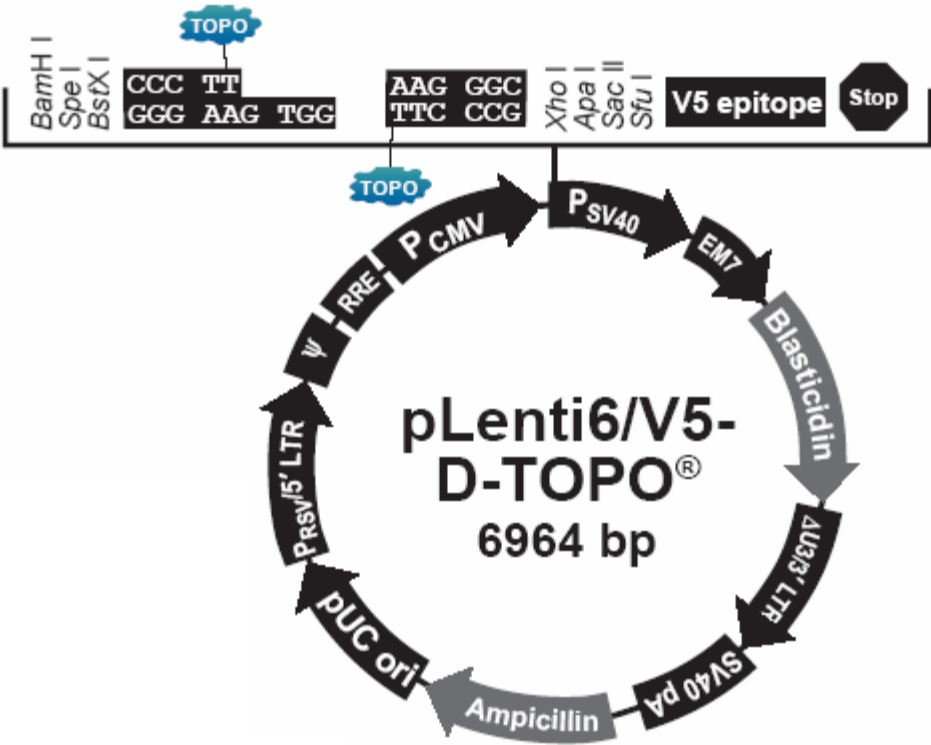


Figure 28: Expression of HIF-1 α 785 tagged with the V5 epitope in SbCl₂ cells.

SbCl₂ cells were transiently transfected with pLenti-D-TOPO-HIF-1 α 785. At 48h post transfection, cells were lysed and whole cell lysate was extracted and separated by SDS-PAGE. After transfer and blocking with Chemi-Blocker®, HRP-conjugated Anti-V5 antibody was incubated with the membrane for 1h. After extensive washing and a 5 minute incubation with ECL® reagent, bands were visualized using autoradiography. Molecular weight marker, MagicMark XP® (**M**), was used to confirm correct kD size for the expected expression product (~87kD).

Figure 28: Expression of HIF-1 α 785 tagged with the V5 epitope in SbCl₂ cells.

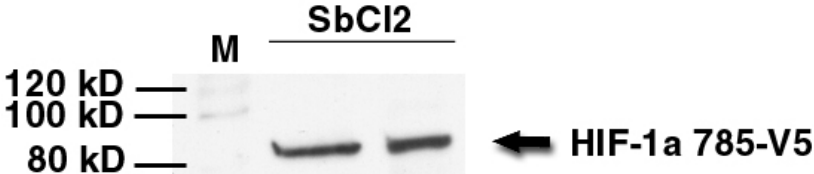


Figure 29: Anchorage-independent growth of SbCl₂ cells expressing HIF-1 α or HIF-1 α 785. CytoSelect 96 well Cell Transformation Assay® (Cell Biolabs, Inc.): SbCl₂ cells were transfected at 80% confluence with either pLenti-LacZ, pLenti-V5-D-TOPO-HIF-1 α FL, or pLenti-V5-D-TOPO-HIF-1 α 785 using FuGene 6 transfection reagent. The next day 1.0x10⁴ of each of the control (non-transfected), LacZ, HIF-1 α FL, or HIF-1 α -785 cells were seeded into a 0.4% agar layer poured over a 0.6% agar layer in wells of a 96 well plate. Wells lacking cells served as a blank control. Agar layers were solubilized, cells were lysed, and nucleic acid stained with CyQuant dye. The intensity of fluorescence in the well was determined by a fluorescent plate reader at 485/520 nm. Data is shown as relative light units of CyQuant® fluorescence. Figure is representative of at least 3 experiments.

Figure 29: Anchorage-independent growth of SbCl₂ cells expressing HIF-1 α or HIF-1 α 785

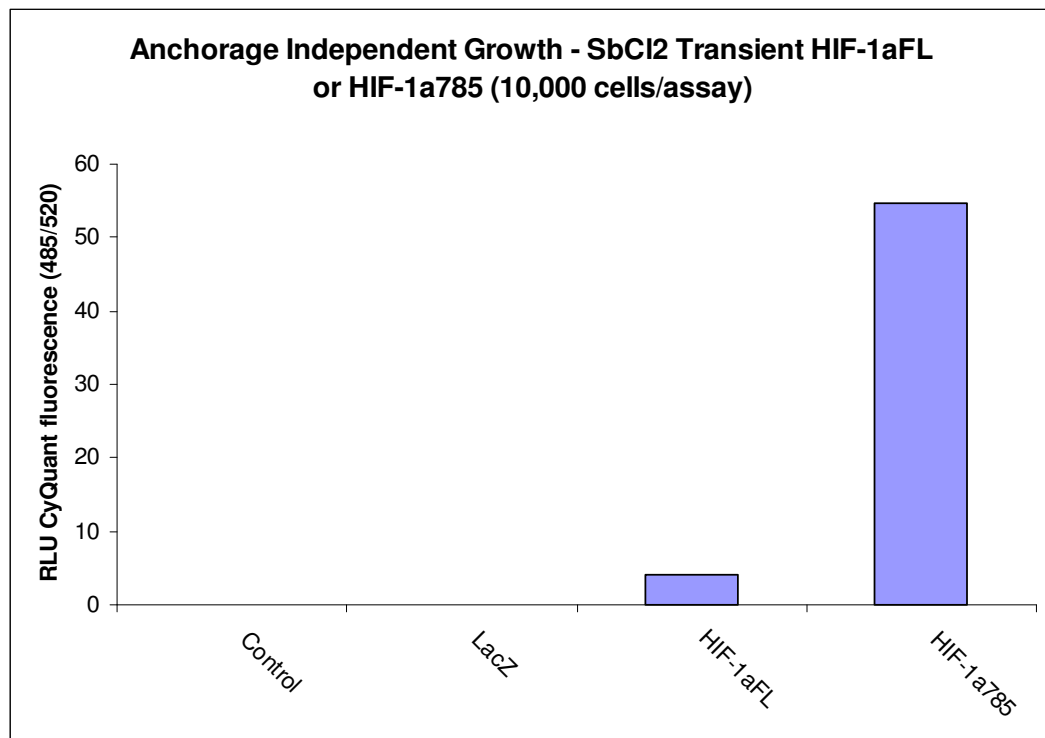


Figure 30: Matrigel invasion assay in WM9 cells treated with HIF-1 α siRNA. WM9 cells were treated with either 100nM HIF-1 α siRNA or 100nM control #1 non-targeting siRNA (Dharmacon, Inc.) using the RNAifect[®] transfection reagent (Qiagen, Inc.). At 24h post transfection, the cells were seeded into 6-well matrigel (+) chambers, and as a control, 6-well matrigel (-) chambers (BD Biosciences) at 7.0×10^4 cells per well. At 24 hours after seeding, the matrigel was removed from the matrigel (+) chambers using a cotton-tipped applicator. After all matrigel on the inner part of the chambers was removed, invading cells were fixed with 80% methanol for 5 minutes and then stained with 0.5% crystal violet for 5 minutes. After staining, the cells/chambers were extensively washed in enough dH₂O to remove excess stain. Once excess stain was removed, cells were manually counted using a grid system covering the entire lower surface of the chamber. The number of invaded cells treated with HIF-1 α siRNA relative to the number of invaded cells treated with control siRNA was determined. Both were corrected for the number of similarly-treated invading cells seeded in matrigel (-) chambers. Results are expressed as cell number as % control. Experiment was done in triplicate and repeated at least 3 times. Error bars represent standard error. * denotes $p = 0.0022$.

Figure 30: Matrigel invasion assay in WM9 cells treated with HIF-1α siRNA

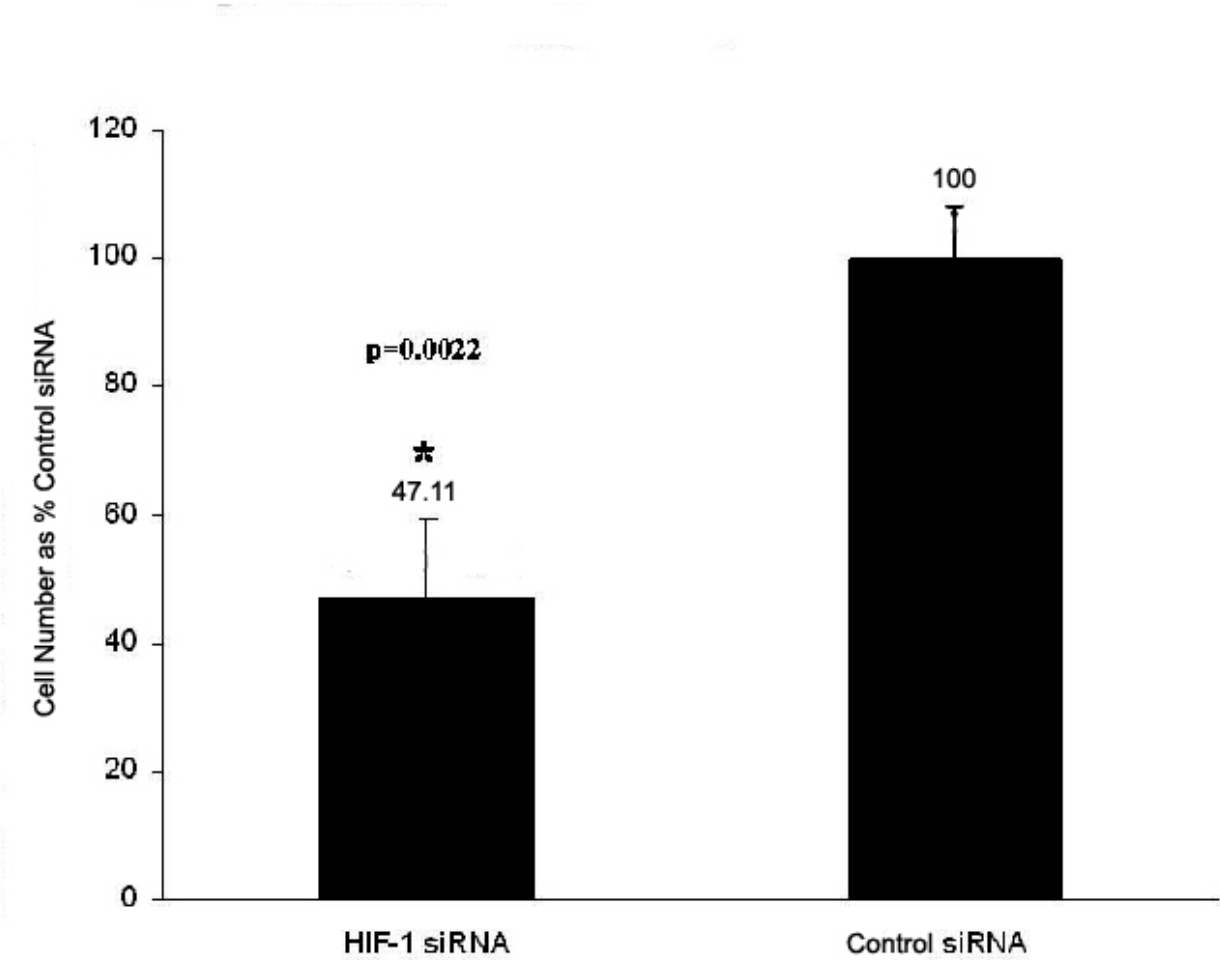


Figure 31: Anchorage independent growth of WM9 cells treated with HIF-1 α

siRNA – Day 4. WM9 cells were treated with either 100nM HIF-1 α siRNA or 100nM

control #1 non-targeting siRNA (Dharmacon, Inc.) using the RNAifect® transfection

reagent (Qiagen, Inc.). At 24h post transfection, anchorage independent growth was

analyzed using the CytoSelect 96 well Cell Transformation Assay® (Cell Biolabs, Inc.).

Briefly, the cells were seeded at 8.0×10^3 cells/well into a 0.4% agar layer poured over a

0.6% agar layer in wells of 96 well plate. Wells lacking cells served as a blank control.

On day 4 after seeding, agar layers were solubilized, cells were lysed, and nucleic acid

stained with CyQuant® dye. Intensity of the fluorescence in each well was determined

by a fluorescent plate reader at 485/520 nm. Results are expressed in Relative

Fluorescent Units. Experiment was done in triplicate and repeated at least 3 times.

Error bars represent standard error. * denotes $p = 0.032$

Figure 31: Anchorage independent growth of WM9 cells treated with HIF-1 α siRNA – Day 4

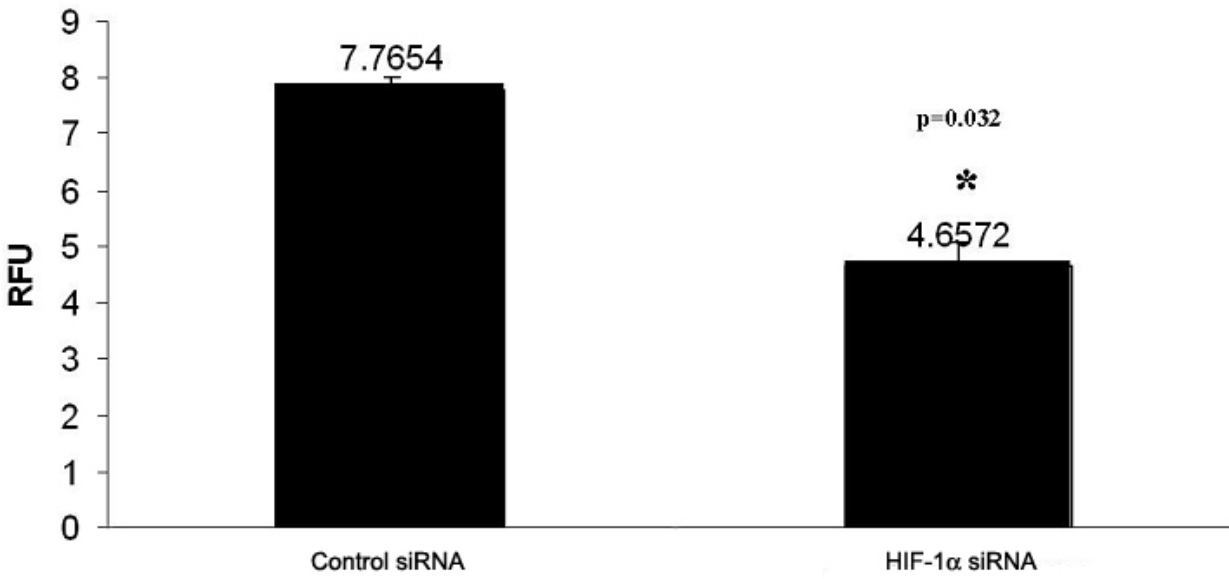
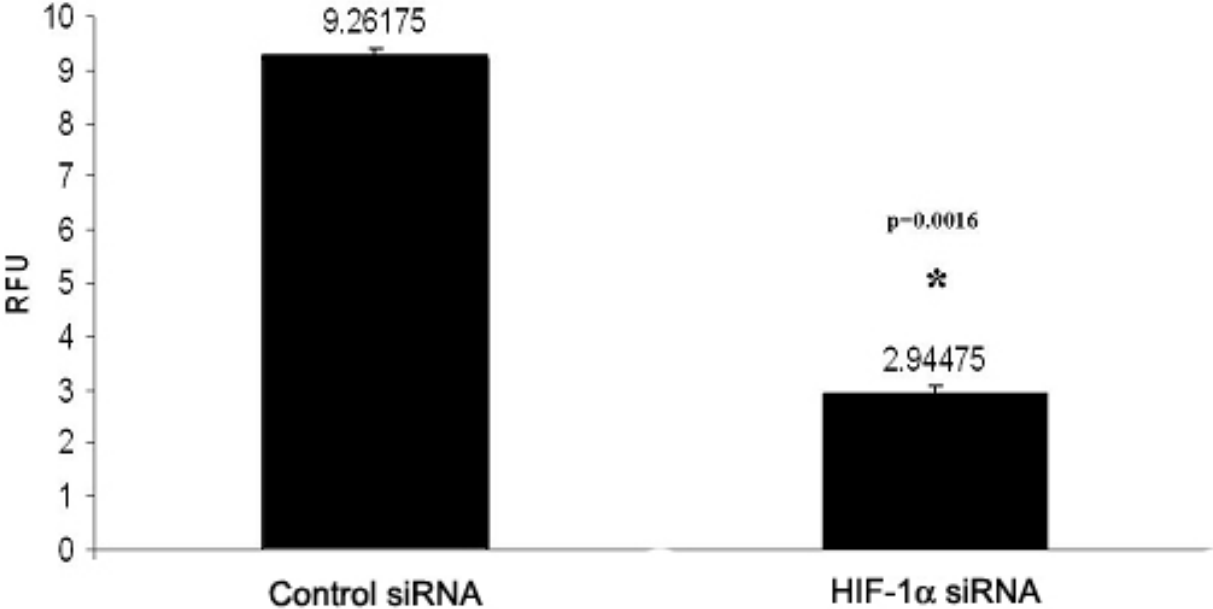


Figure 32: Anchorage independent growth of WM9 cells treated with HIF-1 α

siRNA – Day 5. WM9 cells were treated with either 100nM HIF-1 α siRNA or 100nM control #1 non-targeting siRNA (Dharmacon, Inc.) using the RNAifect® transfection reagent (Qiagen, Inc.). At 24h post transfection, anchorage independent growth was analyzed using the CytoSelect 96 well Cell Transformation Assay® (Cell Biolabs, Inc.). Briefly, the cells were seeded at 8.0×10^3 cells/well into a 0.4% agar layer poured over a 0.6% agar layer in wells of a 96 well plate. Wells lacking cells served as a blank control. On day 5 after seeding, agar layers were solubilized, cells were lysed, and nucleic acid stained with CyQuant® dye. Fluorescence intensity in each well was determined by a plate reader at 485/520 nm. Results are expressed in Relative Fluorescent Units. Figure is representative of at least 3 independent assays each done in triplicate. Error bars represent standard error. * denotes $p = 0.0016$

Figure 32: Anchorage independent growth of WM9 cells treated with HIF-1 α siRNA – Day 5



DISCUSSION – Part II

For the second half of my dissertation work, I wanted to determine the role of the hypoxia inducible factor -1 α (HIF-1 α) and its splice variant, HIF-1 α 785 in human melanoma progression. These results indicate that HIF-1 α and its variant likely play important roles in the progression of this disease.

Melanocytes, the cells responsible for producing the skin-coloring pigment, melanin, are the point of origin for melanoma. Melanoma, if diagnosed and treated early, has a very high cure rate. If the melanoma progresses, it can metastasize (becoming metastatic melanoma) to the lymph nodes, lungs, and the brain. Metastatic melanoma is very difficult to treat and has a much higher mortality rate than primary melanoma. Several studies have confirmed that HIF-1 α is very often a survival factor in various cancers, however this has not been shown in human melanoma.

I found that HIF-1 α protein is expressed under normoxic conditions at higher levels in human metastatic melanoma cells (A375 and WM9) than in the normal human melanocytes (HEMn-LP), radial growth phase melanoma (SbCl₂), and vertical growth phase melanoma (WM1366) cells (**Figure 24 A and B**). The fact that it is detectible in the metastatic cells is novel, since it is very quickly degraded under normoxic conditions in the majority of all cell lines tested to date.

More importantly, I have shown that both the full length HIF-1 α as well as its splice variant, HIF-1 α 785, show increasing levels of mRNA expression as a function of malignant progression (**Figure 26 A and B**). Once corrected for both a housekeeping

gene and for primer/probe binding efficiency, the metastatic melanoma cells, WM9, showed ~10 fold increase in both HIF-1 α and HIF-1 α 785 mRNA levels relative to the normal human melanocytes at 24h after seeding and ~21 fold increase over normal human melanocytes at 72h after seeding in the HIF-1 α . There was nearly a 78 fold increase in the expression of HIF-1 α 785 in the metastatic melanoma cells over the normal human melanocytes at the 72h time point. These time points are significant since in the literature there are hints that “crowding” of the cells in culture dishes can influence HIF-1 α protein levels. At 24h after seeding there was around 30% confluence, while at 72h there was ~70% confluence. All protein isolations were done at 48h post-seeding, therefore it can reasonably be concluded that this “crowding” effect should not have been a confounding variable in my western blot data. While there is some chance that these results could be due to the cells being exposed to different culture conditions, there is currently no way to correct for this situation. However, it does seem reasonable that if the normal human melanocytes need a certain microenvironment to flourish *in vivo* and the RGPs need an even more altered microenvironment *in vivo*, and so on for the other phases of human melanoma represented here, that these different culture conditions *in vitro* are valid for comparison.

There is very little information from any cell line on regulation of HIF-1 α or its variant at the RNA level. Thus my findings are significant since they indicate a novel control point for HIF-1 activity in human melanoma, as well as in other cell lines. This RNA regulation could be due to transcription factors responsible for HIF-1 α /HIF-1 α 785 gene expression becoming overexpressed or over-active as a function of melanoma progression. However, since I have not shown that the increase in HIF-1 α mRNA is due

to increased transcription, there remains the formal possibility that post-transcriptional regulation, such as increased mRNA stability could contribute to the increase I observed in the melanoma cells. This overexpression of HIF-1 α and thus availability of the active HIF-1 heterodimer, would give these cells a survival advantage. One survival advantage that HIF-1 overexpression could lend to the metastatic cells is their ability to invade and metastasize since HIF-1 is a transcriptional regulator of many genes involved in these processes, such as matrix metalloproteinases (MMPs).

The SbCl2 radial growth phase melanoma cells showed negligible levels of HIF-1 α protein expression and were therefore chosen to determine the effects of HIF-1 gain of function. I have shown that the human melanoma radial growth phase cell line, SbCl2, which has very limited anchorage independent growth capabilities, has an increased ability to grow in soft agar when overexpressing full length HIF-1 α . Overexpression of the HIF-1 α 785 splice variant resulted in the greatest increase in soft agar colony formation relative to control cells (**Figure 29**). One possibility for the increased anchorage independent growth exhibited in the splice variant HIF-1 α 785-overexpressing cell line is the splice variant protein having a longer half-life compared to the full length HIF-1 α . The longer half life for HIF-1 α 785 is presumed since it is missing a critical Lys532 that is acetylated by ARD1. This acetylation enhances HIF-1 α interaction with the von Hippel Lindau tumor suppressor protein which acts as an E3 ubiquitin ligase. Without this acetylation, HIF-1 α could have a less favorable interaction with this protein, therefore increasing the chances it will not be degraded by the ubiquitin-proteosomal system. HIF-1 α 785 has the same function as HIF-1 α ; therefore longer half life could ultimately lead to more active heterodimeric HIF-1 available for

cellular processes. Future studies need to be done to determine the relative half-life of both the full length and splice variant using traditional methods.

HIF-1 α loss of function experiments were carried out in the WM9 metastatic melanoma cell line. This cell line was chosen due to its high levels of HIF-1 α expression. Silencing of HIF-1 α by siRNA treatment resulted in a significant decrease (52%) in matrigel invasion compared to WM9 cells treated with control siRNA (**Figure 30**). One possibility of these results is that HIF-1 has been shown to control the expression of several genes involved in invasion such as matrix metalloproteinase 2 (MMP2), urokinase plasminogen activator receptor (uPAR), and cathepsin D (Krishnamachary *et. al.*, 2003; Luo *et. al.*, 2006).

HIF-1 α loss of function also resulted in a significant decrease in anchorage-independent growth in the metastatic melanoma cells. Silencing of WM9 cell HIF-1 α by siRNA resulted in ~40% decrease in their ability to form colonies in soft agar at 4 days of treatment (**Figure 31**). After 5 days of treatment, there was ~68% decrease in anchorage-independent growth in the HIF-1 α silenced WM9 cells relative to the control siRNA treated cells (**Figure 32**). Anchorage-independent growth is a hallmark of cancer cells. The WM9 cells were shown to have a marked increase in the endogenous amount of HIF-1 α protein according to western blotting (**Figure 24 A and B**).

Anchorage-independent growth could be decreased in the WM9 cells treated with HIF-1 α siRNA due to PI3K/Akt and HIF-1 pathway interactions. The PI3K/Akt pathway is one of the most critical pathways involved in anchorage-independent growth (Wang L., 2004). Anoikis, or cellular death due to loss of interaction with the extracellular matrix

and subsequent initiation of caspase-mediated apoptosis, is increased in these cells when HIF-1 α levels are depleted by the siRNA treatment. PI3K/Akt has been shown to control HIF-1 activity by increasing the translation of the HIF-1 α protein (Treins *et. al.*, 2002). If PI3K/Akt regulates anchorage-independent growth through this increased HIF-1 activity, the silencing of HIF-1 α could lead to a decrease in anchorage-independent growth.

The normoxic regulation of HIF-1 has only recently been explored. Studies are needed to determine the role that elevated HIF-1 α levels under normoxic conditions may play in the progression of cancers. One future goal of our laboratory is to determine whether or not there are different gene sets activated by normoxic HIF-1 relative to hypoxic HIF-1. Other future studies could include using the recombinant lentiviral particles that I have generated to introduce both full length and the splice variant of HIF-1 α into normal human melanocytes to determine their effects on malignant transformation.

SUMMARY AND CONCLUSIONS

The first part of my dissertation work dealt with the expression and possible function that PPARs play in human melanocytes compared to human melanoma cells. These studies revealed that none of the human melanoma cells tested were significantly or reproducibly affected by PPAR α agonists, but the normal human melanocytes and metastatic melanoma cells, A375 were significantly growth inhibited by PPAR γ agonists. While PPAR α and PPAR γ protein levels are overexpressed relative to the normal human melanocytes, only the SK-Mel 28 cells exhibited a significant increase in PPAR α mRNA levels. When PPAR α expression was silenced in SK-Mel 28 cells utilizing siRNA, no observable biological effect was seen in these cells compared to cells treated with control siRNA. A reasonable conclusion is that the increased expression of PPAR α in SK-Mel 28 cells is not contributing to its *in vitro* transformed phenotype.

The second part of my dissertation work focuses on the expression and role HIF-1 α , under normoxic conditions in human melanoma progression. These results revealed, for the first time, that HIF-1 α is overexpressed in the metastatic melanoma cells. Also, I have shown, for the first time, that there is regulation of HIF-1 α at the transcriptional level in human melanoma. The expression of both HIF-1 α and HIF-1 α 785 increases as a function of melanoma progression. Gain-of-function studies in the HIF-1 α -negative SbCl2 cells reveal that introduction of exogenous HIF-1 α , or its splice variant, can significantly increase their anchorage-independent growth. Loss-of-function studies in the HIF-1 α positive WM9 metastatic melanoma cells show that there is a

significant decrease in matrigel invasion compared to control siRNA treated cells. The loss of HIF-1 α in these cells also significantly diminished their ability to form colonies in soft agar. These results suggest that development of new therapeutic agents that inhibit HIF-1 function may be of use in the treatment of human melanoma.

REFERENCES

- Adams M, Reginato MJ, Shao D, Lazar MA, Chatterjee VK. Transcriptional activation by peroxisome proliferator-activated receptor gamma is inhibited by phosphorylation at a consensus mitogen-activated protein kinase site. *J Biol Chem.* 1997 Feb 21;272(8):5128-32.
- Akakura N, Kobayashi M, Horiuchi I, Suzuki A, Wang J, Chen J, Niizeki H, Kawamura Ki, Hosokawa M, Asaka M. Constitutive expression of hypoxia-inducible factor-1alpha renders pancreatic cancer cells resistant to apoptosis induced by hypoxia and nutrient deprivation. *Cancer Res.* 2001 Sep 1;61(17):6548-54.
- Akiyama TE, Sakai S, Lambert G, Nicol CJ, Matsusue K, Pimprale S, Lee YH, Ricote M, Glass CK, Brewer HB Jr, Gonzalez FJ. Conditional disruption of the peroxisome proliferator-activated receptor gamma gene in mice results in lowered expression of ABCA1, ABCG1, and apoE in macrophages and reduced cholesterol efflux. *Mol Cell Biol.* 2002 Apr;22(8):2607-19.
- Amri EZ, Bonino F, Ailhaud G, Abumrad NA, Grimaldi PA. Cloning of a protein that mediates transcriptional effects of fatty acids in preadipocytes. Homology to peroxisome proliferator-activated receptors. *J Biol Chem.* 1995 Feb 3;270(5):2367-71.
- Avis I, Martinez A, Tauler J, Zudaire E, Mayburd A, Abu-Ghazaleh R, Ondrey F, Mulshine JL. Inhibitors of the arachidonic acid pathway and peroxisome proliferator-activated receptor ligands have superadditive effects on lung cancer growth inhibition. *Cancer Res.* 2005 May 15;65(10):4181-90.
- Bachmann S, Le Hir M, Eckardt KU. Co-localization of erythropoietin mRNA and ecto-5'-nucleotidase immunoreactivity in peritubular cells of rat renal cortex indicates that fibroblasts produce erythropoietin. *J Histochem Cytochem.* 1993 Mar;41(3):335-41.
- Bae SH, Jeong JW, Park JA, Kim SH, Bae MK, Choi SJ, Kim KW. Sumoylation increases HIF-1alpha stability and its transcriptional activity. *Biochem Biophys Res Commun.* 2004 Nov 5;324(1):394-400.
- Barak Y, Liao D, He W, Ong ES, Nelson MC, Olefsky JM, Boland R, Evans RM. Effects of

peroxisome proliferator-activated receptor delta on placentation, adiposity, and colorectal cancer. *Proc Natl Acad Sci U S A*. 2002 Jan 8;99(1):303-8. Epub 2001 Dec 26.

Barak Y, Nelson MC, Ong ES, Jones YZ, Ruiz-Lozano P, Chien KR, Koder A, Evans RM. PPAR gamma is required for placental, cardiac, and adipose tissue development. *Mol Cell*. 1999 Oct;4(4):585-95.

Barger PM, Browning AC, Garner AN, Kelly DP p38 mitogen-activated protein kinase activates peroxisome proliferator-activated receptor alpha: a potential role in the cardiac metabolic stress response. *J Biol Chem*. 2001 Nov 30;276(48):44495-501.

Beasley NJ, Leek R, Alam M, Turley H, Cox GJ, Gatter K, Millard P, Fuggle S, Harris AL. Hypoxia-inducible factors HIF-1alpha and HIF-2alpha in head and neck cancer: relationship to tumor biology and treatment outcome in surgically resected patients. *Cancer Res*. 2002 May 1;62(9):2493-7

Bedogni B, Welford SM, Cassarino DS, Nickoloff BJ, Giaccia AJ, Powell MB. The hypoxic microenvironment of the skin contributes to Akt-mediated melanocyte transformation. *Cancer Cell*. 2005 Dec;8(6):443-54.

Bergeron M, Gidday JM, Yu AY, Semenza GL, Ferriero DM, Sharp FR. Role of hypoxia-inducible factor-1 in hypoxia-induced ischemic tolerance in neonatal rat brain. *Ann Neurol*. 2000 Sep;48(3):285-96

Blanquart C, Mansouri R, Paumelle R, Fruchart JC, Staels B, Glineur C. The protein kinase C signaling pathway regulates a molecular switch between transactivation and transrepression activity of the peroxisome proliferator-activated receptor alpha. *Mol Endocrinol*. 2004 Aug;18(8):1906-18.

Blanquart C, Barbier O, Fruchart JC, Staels B, Glineur C. Peroxisome proliferator-activated receptor alpha (PPARalpha) turnover by the ubiquitin-proteasome system controls the ligand-induced expression level of its target genes. *J Biol Chem*. 2002 Oct 4;277(40):37254-9.

Brown PJ, Stuart LW, Hurley KP, Lewis MC, Winegar DA, Wilson JG, Wilkison WO, Itoop

OR, Willson TM. Identification of a subtype selective human PPARalpha agonist through parallel-array synthesis. *Bioorg Med Chem Lett*. 2001 May 7;11(9):1225-7

Bryan BA, Dyson OF, Akula SM. Identifying cellular genes crucial for the reactivation of Kaposi's sarcoma-associated herpesvirus latency. *J Gen Virol*. 2006 Mar;87(Pt 3):519-29.

Camp HS, Chaudhry A, Leff T. A novel potent antagonist of peroxisome proliferator-activated receptor gamma blocks adipocyte differentiation but does not revert the phenotype of terminally differentiated adipocytes. *Endocrinology*. 2001 Jul;142(7):3207-13.

Camp HS, Tafuri SR, Leff T. c-Jun N-terminal kinase phosphorylates peroxisome proliferator-activated receptor-gamma1 and negatively regulates its transcriptional activity. *Endocrinology*. 1999 Jan;140(1):392-7.

Chattopadhyay N, Singh DP, Heese O, Godbole MM, Sinohara T, Black PM, Brown EM. Expression of peroxisome proliferator-activated receptors (PPARS) in human astrocytic cells: PPARgamma agonists as inducers of apoptosis. *J Neurosci Res*. 2000 Jul 1;61(1):67-74.

Chau NM, Rogers P, Aherne W, Carroll V, Collins I, McDonald E, Workman P, Ashcroft M. Identification of novel small molecule inhibitors of hypoxia-inducible factor-1 that differentially block hypoxia-inducible factor-1 activity and hypoxia-inducible factor-1alpha induction in response to hypoxic stress and growth factors. *Cancer Res*. 2005 Jun 1;65(11):4918-28.

Chen J, Zhao S, Nakada K, Kuge Y, Tamaki N, Okada F, Wang J, Shindo M, Higashino F, Takeda K, Asaka M, Katoh H, Sugiyama T, Hosokawa M, Kobayashi M. Dominant-negative hypoxia-inducible factor-1 alpha reduces tumorigenicity of pancreatic cancer cells through the suppression of glucose metabolism. *Am J Pathol*. 2003 Apr;162(4):1283-91.

Chun YS, Lee KH, Choi E, Bae SY, Yeo EJ, Huang LE, Kim MS, Park JW. Phorbol ester stimulates the nonhypoxic induction of a novel hypoxia-inducible factor alpha isoform: implications for tumor promotion. *Cancer Res*. 2003 Dec 15;63(24):8700-7.

Cui Y, Miyoshi K, Claudio E, Siebenlist UK, Gonzalez FJ, Flaws J, Wagner KU, Hennighausen L. Loss of the peroxisome proliferation-activated receptor gamma (PPARgamma) does not affect mammary development and propensity for tumor formation but leads to reduced fertility. *J Biol Chem*. 2002 May 17;277(20):17830-5.

Desjarlais JR, Berg JM. Redesigning the DNA-binding specificity of a zinc finger protein: a data base-guided approach. *Proteins*. 1992 Feb;12(2):101-4. Erratum in: *Proteins*. 1992 Jul;13(3):272.

Elholm M, Dam I, Jorgensen C, Krogsdam AM, Holst D, Kratchmarova I, Gottlicher M, Gustafsson JA, Berge R, Flatmark T, Knudsen J, Mandrup S, Kristiansen K. Acyl-CoA esters antagonize the effects of ligands on peroxisome proliferator-activated receptor alpha conformation, DNA binding, and interaction with Co-factors. *J Biol Chem*. 2001 Jun 15;276(24):21410-6.

Entrez Conserved Domains <http://www.ncbi.nlm.nih.gov/Structure/cdd/cdd.shtml>

Epstein AC, Gleadle JM, McNeill LA, Hewitson KS, O'Rourke J, Mole DR, Mukherji M, Metzen E, Wilson MI, Dhanda A, Tian YM, Masson N, Hamilton DL, Jaakkola P, Barstead R, Hodgkin J, Maxwell PH, Pugh CW, Schofield CJ, Ratcliffe PJ. *C. elegans* EGL-9 and mammalian homologs define a family of dioxygenases that regulate HIF by prolyl hydroxylation. *Cell*. 2001 Oct 5;107(1):43-54.

Fajas L, Schoonjans K, Gelman L, Kim JB, Najib J, Martin G, Fruchart JC, Briggs M, Spiegelman BM, Auwerx J. Regulation of peroxisome proliferator-activated receptor gamma expression by adipocyte differentiation and determination factor 1/sterol regulatory element binding protein 1: implications for adipocyte differentiation and metabolism. *Mol Cell Biol*. 1999 Aug;19(8):5495-503.

Fajas L, Auboeuf D, Raspe E, Schoonjans K, Lefebvre AM, Saladin R, Najib J, Laville M, Fruchart JC, Deeb S, Vidal-Puig A, Flier J, Briggs MR, Staels B, Vidal H, Auwerx J. The organization, promoter analysis, and expression of the human PPARgamma gene. *J Biol Chem*. 1997 Jul 25;272(30):18779-89.

Forman BM, Tontonoz P, Chen J, Brun RP, Spiegelman BM, Evans RM. 15-Deoxy- delta 12, 14-prostaglandin J2 is a ligand for the adipocyte determination factor PPAR gamma. *Cell*. 1995 Dec 1;83(5):803-12.

- Fredenrich A, Grimaldi PA. Roles of peroxisome proliferator-activated receptor delta in skeletal muscle function and adaptation *Curr Opin Clin Nutr Metab Care*. 2004 Jul;7(4):377-81.
- Friedmann PS, Cooper HL, Healy E. Peroxisome proliferator-activated receptors and their relevance to dermatology. *Acta Derm Venereol*. 2005;85(3):194-202.
- Fu M, Zhang J, Lin Y, Zhu X, Zhao L, Ahmad M, Ehrenguber MU, Chen YE. Early stimulation and late inhibition of peroxisome proliferator-activated receptor gamma (PPAR gamma) gene expression by transforming growth factor beta in human aortic smooth muscle cells: role of early growth-response factor-1 (Egr-1), activator protein 1 (AP1) and Smads. *Biochem J*. 2003 Mar 15;370(Pt 3):1019-25.
- Fukuda R, Hirota K, Fan F, Jung YD, Ellis LM, Semenza GL. Insulin-like growth factor 1 induces hypoxia-inducible factor 1-mediated vascular endothelial growth factor expression, which is dependent on MAP kinase and phosphatidylinositol 3-kinase signaling in colon cancer cells. *J Biol Chem*. 2002 Oct 11;277(41):38205-11.
- Gearing KL, Crickmore A, Gustafsson JA. Structure of the mouse peroxisome proliferator activated receptor alpha gene. *Biochem Biophys Res Commun*. 1994 Feb 28;199(1):255-63.
- Giaccia A, Siim BG, Johnson RS. HIF-1 as a target for drug development. *Nat Rev Drug Discov*. 2003 Oct;2(10):803-11.
- Giatromanolaki A, Harris AL. Tumour hypoxia, hypoxia signaling pathways and hypoxia inducible factor expression in human cancer. *Anticancer Res*. 2001 Nov-Dec;21(6B):4317-24.
- Gnarra JR, Ward JM, Porter FD, Wagner JR, Devor DE, Grinberg A, Emmert-Buck MR, Westphal H, Klausner RD, Linehan WM. Defective placental vasculogenesis causes embryonic lethality in VHL-deficient mice. *Proc Natl Acad Sci U S A*. 1997 Aug 19;94(17):9102-7.
- Goda N, Dozier SJ, Johnson RS. HIF-1 in cell cycle regulation, apoptosis, and tumor progression. *Antioxid Redox Signal*. 2003 Aug;5(4):467-73.

- Goldberg MA, Glass GA, Cunningham JM, Bunn HF. The regulated expression of erythropoietin by two human hepatoma cell lines. *Proc Natl Acad Sci U S A*. 1987 Nov;84(22):7972-6.
- Grabacka M, Plonka PM, Urbanska K, Reiss K. Peroxisome proliferator-activated receptor alpha activation decreases metastatic potential of melanoma cells in vitro via down-regulation of Akt. *Clin Cancer Res*. 2006 May 15;12(10):3028-36.
- Greijer AE, van der Wall E. The role of hypoxia inducible factor 1 (HIF-1) in hypoxia induced apoptosis. *J Clin Pathol*. 2004 Oct;57(10):1009-14.
- Greisman HA, Pabo CO. A general strategy for selecting high-affinity zinc finger proteins for diverse DNA target sites. *Science*. 1997 Jan 31;275(5300):657-61.
- Guan YF, Zhang YH, Breyer RM, Davis L, Breyer MD. Expression of peroxisome proliferator-activated receptor gamma (PPARgamma) in human transitional bladder cancer and its role in inducing cell death. *Neoplasia*. 1999 Oct;1(4):330-9.
- Guerre-Millo M, Rouault C, Poulain P, Andre J, Poitout V, Peters JM, Gonzalez FJ, Fruchart JC, Reach G, Staels B. PPAR-alpha-null mice are protected from high-fat diet-induced insulin resistance. *Diabetes*. 2001 Dec;50(12):2809-14.
- Gupta RA, Brockman JA, Sarraf P, Willson TM, DuBois RN. Target genes of peroxisome proliferator-activated receptor gamma in colorectal cancer cells. *J Biol Chem*. 2001 Aug 10;276(32):29681-7. Epub 2001 Jun 7.
- Harris AL. Hypoxia--a key regulatory factor in tumour growth. *Nat Rev Cancer*. 2002 Jan;2(1):38-47.
- Hauser S, Adelmant G, Sarraf P, Wright HM, Mueller E, Spiegelman BM. Degradation of the peroxisome proliferator-activated receptor gamma is linked to ligand-dependent activation. *J Biol Chem*. 2000 Jun 16;275(24):18527-33.

- Hertz R, Berman I, Keppler D, Bar-Tana J. Activation of gene transcription by prostacyclin analogues is mediated by the peroxisome-proliferators-activated receptor (PPAR). *Eur J Biochem.* 1996 Jan 15;235(1-2):242-7.
- Holmquist-Mengelbier L, Fredlund E, Lofstedt T, Noguera R, Navarro S, Nilsson H, Pietras A, Vallon-Christersson J, Borg A, Gradin K, Poellinger L, Pahlman S. Recruitment of HIF-1alpha and HIF-2alpha to common target genes is differentially regulated in neuroblastoma: HIF-2alpha promotes an aggressive phenotype. *Cancer Cell.* 2006 Nov;10(5):413-23.
- Houseknecht KL, Cole BM, Steele PJ. Peroxisome proliferator-activated receptor gamma (PPARgamma) and its ligands: a review. *Domest Anim Endocrinol.* 2002 Mar;22(1):1-23.
- Hu E, Kim JB, Sarraf P, Spiegelman BM. Inhibition of adipogenesis through MAP kinase-mediated phosphorylation of PPARgamma. *Science.* 1996 Dec 20;274(5295):2100-3.
- Hu X, Feng Y, Shen Y, Zhao XF, Yu JH, Yang YS, Leng Y. Antidiabetic effect of a novel non-thiazolidinedione PPAR gamma/alpha agonist on ob/ob mice. *Acta Pharmacol Sin.* 2006 Oct;27(10):1346-52.
- Hussein MR. Melanocytic dysplastic naevi occupy the middle ground between benign melanocytic naevi and cutaneous malignant melanomas: emerging clues. *J Clin Pathol.* 2005 May;58(5):453-6.
- Issemann I, Green S. Activation of a member of the steroid hormone receptor superfamily by peroxisome proliferators. *Nature.* 1990 Oct 18;347(6294):645-50.
- Iyer NV, Leung SW, Semenza GL. The human hypoxia-inducible factor 1alpha gene: IF1A structure and evolutionary conservation. *Genomics.* 1998 Sep 1;52(2):159-65.
- Jang MS, Park JE, Lee JA, Park SG, Myung PK, Lee DH, Park BC, Cho S. Binding and regulation of hypoxia-inducible factor-1 by the inhibitory PAS proteins. *Biochem Biophys Res Commun.* 2005 Nov 11;337(1):209-15.

- Jeong JW, Bae MK, Ahn MY, Kim SH, Sohn TK, Bae MH, Yoo MA, Song EJ, Lee KJ, Kim KW. Regulation and destabilization of HIF-1alpha by ARD1-mediated acetylation. *Cell*. 2002 Nov 27;111(5):709-20.
- Jiang BH, Zheng JZ, Leung SW, Roe R, Semenza GL. Transactivation and inhibitory domains of hypoxia-inducible factor 1alpha. Modulation of transcriptional activity by oxygen tension. *J Biol Chem*. 1997 Aug 1;272(31):19253-60.
- Jones DC, Ding X, Daynes RA. Nuclear receptor peroxisome proliferator-activated receptor alpha (PPARalpha) is expressed in resting murine lymphocytes. The PPARalpha in T and B lymphocytes is both transactivation and transrepression competent. *J Biol Chem*. 2002 Mar 1;277(9):6838-45.
- Jones DC, Manning BM, Daynes RA. A role for the peroxisome proliferator-activated receptor alpha in T-cell physiology and ageing immunobiology. *Proc Nutr Soc*. 2002 Aug;61(3):363-9.
- Jones DT, Harris AL. Identification of novel small-molecule inhibitors of hypoxia-inducible factor-1 transactivation and DNA binding. *Mol Cancer Ther*. 2006 Sep;5(9):2193-202.
- Juge-Aubry CE, Hammar E, Siegrist-Kaiser C, Pernin A, Takeshita A, Chin WW, Burger AG, Meier CA. Regulation of the transcriptional activity of the peroxisome proliferator-activated receptor alpha by phosphorylation of a ligand-independent trans-activating domain. *J Biol Chem*. 1999 Apr 9;274(15):10505-10.
- Kehrer JP, Biswal SS, La E, Thuillier P, Datta K, Fischer SM, Vanden Heuvel JP
Inhibition of peroxisome-proliferator-activated receptor (PPAR)alpha by MK886
Biochem J. 2001 Jun 15;356(Pt 3):899-906.
- Kim DJ, Bility MT, Billin AN, Willson TM, Gonzalez FJ, Peters JM. PPARbeta/delta selectively induces differentiation and inhibits cell proliferation. *Cell Death Differ*. 2006 Jan;13(1):53-60.
- Kim Y, Suh N, Sporn M, Reed JC. An inducible pathway for degradation of FLIP protein sensitizes tumor cells to TRAIL-induced apoptosis. *J Biol Chem*. 2002 Jun 21;277(25):22320-9.

- Kleemann R, Gervois PP, Verschuren L, Staels B, Princen HM, Kooistra T. Fibrates down-regulate IL-1-stimulated C-reactive protein gene expression in hepatocytes by reducing nuclear p50-NFkappa B-C/EBP-beta complex formation. *Blood*. 2003 Jan 15;101(2):545-51. Epub 2002 Aug 29.
- Kliwer SA, Lenhard JM, Willson TM, Patel I, Morris DC, Lehmann JM. A prostaglandin J2 metabolite binds peroxisome proliferator-activated receptor gamma and promotes adipocyte differentiation. *Cell*. 1995 Dec 1;83(5):813-9.
- Kliwer SA, Sundseth SS, Jones SA, Brown PJ, Wisely GB, Koble CS, Devchand P, Wahli W, Willson TM, Lenhard JM, Lehmann JM. Fatty acids and eicosanoids regulate gene expression through direct interactions with peroxisome proliferator-activated receptors alpha and gamma. *Proc Natl Acad Sci U S A*. 1997 Apr 29;94(9):4318-23.
- Kliwer SA, Umesono K, Mangelsdorf DJ, Evans RM. Retinoid X receptor interacts with nuclear receptors in retinoic acid, thyroid hormone and vitamin D3 signalling. *Nature*. 1992 Jan 30;355(6359):446-9.
- Knauf C, Rieusset J, Foretz M, Cani PD, Uldry M, Hosokawa M, Martinez E, Bringart M, Waget A, Kersten S, Desvergne B, Gremlich S, Wahli W, Seydoux J, Delzenne NM, Thorens B, Burcelin R. Peroxisome proliferator-activated receptor-alpha-null mice have increased white adipose tissue glucose utilization, GLUT4, and fat mass: Role in liver and brain. *Endocrinology*. 2006 Sep;147(9):4067-78. Epub 2006 Jun 15.
- Kondo Y, Hamada J, Kobayashi C, Nakamura R, Suzuki Y, Kimata R, Nishimura T, Kitagawa T, Kunimoto M, Imura N, Hara S. Over expression of hypoxia-inducible factor-1alpha in renal and bladder cancer cells increases tumorigenic potency. *J Urol*. 2005 May;173(5):1762-6.
- Koshiji M, To KK, Hammer S, Kumamoto K, Harris AL, Modrich P, Huang LE. HIF-1alpha induces genetic instability by transcriptionally downregulating MutSalpha expression. *Mol Cell*. 2005 Mar 18;17(6):793-803.
- Koukourakis MI, Giatromanolaki A, Sivridis E, Simopoulos C, Turley H, Talks K, Gatter KC, Harris AL. Hypoxia-inducible factor (HIF-1A and HIF-2A), angiogenesis, and chemoradiotherapy outcome of squamous cell head-and-neck cancer. *Int J Radiat*

Oncol Biol Phys. 2002 Aug 1;53(5):1192-202.

Krishnamachary B, Berg-Dixon S, Kelly B, Agani F, Feldser D, Ferreira G, Iyer N, LaRusch J, Pak B, Taghavi P, Semenza GL. Regulation of colon carcinoma cell invasion by hypoxia-inducible factor 1. *Cancer Res.* 2003 Mar 1;63(5):1138-43.

Lando D, Peet DJ, Whelan DA, Gorman JJ, Whitelaw ML. Asparagine hydroxylation of the HIF transactivation domain a hypoxic switch. *Science.* 2002 Feb 1;295(5556):858-61.

Latruffe N, Vamecq J. Evolutionary aspects of peroxisomes as cell organelles, and of genes encoding peroxisomal proteins. *Biol Cell.* 2000 Sep;92(6):389-95.

Lavinsky RM, Jepsen K, Heinzl T, Torchia J, Mullen TM, Schiff R, Del-Rio AL, Ricote M, Ngo S, Gemsch J, Hilsenbeck SG, Osborne CK, Glass CK, Rosenfeld MG, Rose DW. Diverse signaling pathways modulate nuclear receptor recruitment of N-CoR and SMRT complexes. *Proc Natl Acad Sci U S A.* 1998 Mar 17;95(6):2920-5.

Lazennec G, Canaple L, Saugy D, Wahli W. Activation of peroxisome proliferator-activated receptors (PPARs) by their ligands and protein kinase A activators. *Mol Endocrinol.* 2000 Dec;14(12):1962-75.

Lee CH, Chawla A, Urbiztondo N, Liao D, Boisvert WA, Evans RM, Curtiss LK. Transcriptional repression of atherogenic inflammation: modulation by PPARdelta. *Science.* 2003 Oct 17;302(5644):453-7. Epub 2003 Sep 11. Erratum in: *Science.* 2003 Nov 14;302(5648):1153.

Lee SS, Pineau T, Drago J, Lee EJ, Owens JW, Kroetz DL, Fernandez-Salguero PM, Westphal H, Gonzalez FJ. Targeted disruption of the alpha isoform of the peroxisome proliferator-activated receptor gene in mice results in abolishment of the pleiotropic effects of peroxisome proliferators. *Mol Cell Biol.* 1995 Jun;15(6):3012-22.

Leesnitzer LM, Parks DJ, Bledsoe RK, Cobb JE, Collins JL, Conslor TG, Davis RG, Hull-Ryde EA, Lenhard JM, Patel L, Plunket KD, Shenk JL, Stimmel JB, Therapontos C, Willson TM, Blanchard SG. Functional consequences of cysteine modification in the ligand binding sites of peroxisome proliferator activated receptors by GW9662. *Biochemistry.* 2002 May 28;41(21):6640-50.

- Lefebvre AM, Chen I, Desreumaux P, Najib J, Fruchart JC, Geboes K, Briggs M, Heyman R, Auwerx J. Activation of the peroxisome proliferator-activated receptor gamma promotes the development of colon tumors in C57BL/6J-APCMin/+ mice. *Nat Med*. 1998 Sep;4(9):1053-7.
- Lefebvre P, Chinetti G, Fruchart JC, Staels B. Sorting out the roles of PPAR alpha in energy metabolism and vascular homeostasis. *J Clin Invest*. 2006 Mar;116(3):571-80.
- Lehmann JM, Moore LB, Smith-Oliver TA, Wilkison WO, Willson TM, Kliewer SA. An antidiabetic thiazolidinedione is a high affinity ligand for peroxisome proliferator-activated receptor gamma (PPAR gamma). *J Biol Chem*. 1995 Jun 2;270(22):12953-6.
- Lim JH, Lee ES, You HJ, Lee JW, Park JW, Chun YS. Ras-dependent induction of HIF-1alpha785 via the Raf/MEK/ERK pathway: a novel mechanism of Ras-mediated tumor promotion. *Oncogene*. 2004 Dec 16;23(58):9427-31.
- Lin Q, Ruuska SE, Shaw NS, Dong D, Noy N. Ligand selectivity of the peroxisome proliferator-activated receptor alpha. *Biochemistry*. 1999 Jan 5;38(1):185-90.
- Liu Y, Meng Y, Liu H, Li J, Fu J, Liu Y, Chen X. Growth inhibition and differentiation induced by peroxisome proliferator activated receptor gamma ligand rosiglitazone in human melanoma cell line a375. *Med Oncol*. 2006;23(3):393-402.
- Luo Y, He DL, Ning L, Shen SL, Li L, Li X. Over-expression of Hypoxia-inducible factor 1alpha increases invasive potency of LNCaP cells in vitro *Zhonghua Yi Xue Za Zhi*. 2006 Aug 29;86(32):2285-8.
- MacDougald OA, Lane MD. Adipocyte differentiation. When precursors are also regulators. *Curr Biol*. 1995 Jun 1;5(6):618-21.
- Makino Y, Cao R, Svensson K, Bertilsson G, Asman M, Tanaka H, Cao Y, Berkenstam A, Poellinger L. Inhibitory PAS domain protein is a negative regulator of hypoxia-inducible gene expression. *Nature*. 2001 Nov 29;414(6863):550-4.

- Maltepe E, Schmidt JV, Baunoch D, Bradfield CA, Simon MC. Abnormal angiogenesis and responses to glucose and oxygen deprivation in mice lacking the protein ARNT. *Nature*. 1997 Mar 27;386(6623):403-7.
- Maxwell PH, Wiesener MS, Chang GW, Clifford SC, Vaux EC, Cockman ME, Wykoff CC, Pugh CW, Maher ER, Ratcliffe PJ. The tumour suppressor protein VHL targets hypoxia-inducible factors for oxygen-dependent proteolysis. *Nature*. 1999 May 20;399(6733):271-5.
- Mazure NM, Brahimi-Horn MC, Berta MA, Benizri E, Bilton RL, Dayan F, Ginouves A, Berra E, Pouyssegur J. HIF-1: master and commander of the hypoxic world. A pharmacological approach to its regulation by siRNAs. *Biochem Pharmacol*. 2004 Sep 15;68(6):971-80.
- McAdara, J. Drug targeting of nuclear hormone receptors intensifies functional studies. *The Scientist* 2000.14[11]:25.
- McIntyre TM, Pontsler AV, Silva AR, St Hilaire A, Xu Y, Hinshaw JC, Zimmerman GA, Hama K, Aoki J, Arai H, Prestwich GD. Identification of an intracellular receptor for lysophosphatidic acid (LPA):LPA is a transcellular PPARgamma agonist. *Proc Natl Acad Sci U S A*. 2003 Jan 7;100(1):131-6. Epub 2002 Dec 26.
- Melanoma Research Foundation Fact Sheet, http://www.melanoma.org/mrf_facts.pdf 2006.
- Metzen E, Berchner-Pfannschmidt U, Stengel P, Marxsen JH, Stolze I, Klinger M, Huang WQ, Wotzlaw C, Hellwig-Burgel T, Jelkmann W, Acker H, Fandrey J. Intracellular localisation of human HIF-1 alpha hydroxylases: implications for oxygen sensing. *J Cell Sci*. 2003 Apr 1;116(Pt 7):1319-26.
- Michaylira CZ, Nakagawa H. Hypoxic microenvironment as a cradle for melanoma development and progression. *Cancer Biol Ther*. 2006 May;5(5):476-9. Epub 2006 May 26.
- Minet E, Ernest I, Michel G, Roland I, Remacle J, Raes M, Michiels C. HIF-1A gene transcription is dependent on a core promoter sequence encompassing activating and inhibiting sequences located upstream from the transcription initiation site and cis

elements located within the 5'UTR. *Biochem Biophys Res Commun.* 1999 Aug 2;261(2):534-40.

Moore KJ, Rosen ED, Fitzgerald ML, Randow F, Andersson LP, Altshuler D, Milstone DS, Mortensen RM, Spiegelman BM, Freeman MW. The role of PPAR-gamma in macrophage differentiation and cholesterol uptake. *Nat Med.* 2001 Jan;7(1):41-7.

Mueller E, Sarraf P, Tontonoz P, Evans RM, Martin KJ, Zhang M, Fletcher C, Singer S, Spiegelman BM. Terminal differentiation of human breast cancer through PPAR gamma. *Mol Cell.* 1998 Feb;1(3):465-70.

Mukherjee R, Hoener PA, Jow L, Bilakovics J, Klausning K, Mais DE, Faulkner A, Croston GE, Paterniti JR Jr. A selective peroxisome proliferator-activated receptor-gamma (PPARgamma) modulator blocks adipocyte differentiation but stimulates glucose uptake in 3T3-L1 adipocytes. *Mol Endocrinol.* 2000 Sep;14(9):1425-33.

Murakami K, Ide T, Suzuki M, Mochizuki T, Kadowaki T. Evidence for direct binding of fatty acids and eicosanoids to human peroxisome proliferators-activated receptor alpha. *Biochem Biophys Res Commun.* 1999 Jul 14;260(3):609-13.

Nagasawa H, Mikamo N, Nakajima Y, Matsumoto H, Uto Y, Hori H. Antiangiogenic hypoxic cytotoxin TX-402 inhibits hypoxia-inducible factor 1 signaling pathway. *Anticancer Res.* 2003 Nov-Dec;23(6a):4427-34.

Nicol CJ, Yoon M, Ward JM, Yamashita M, Fukamachi K, Peters JM, Gonzalez FJ. PPARgamma influences susceptibility to DMBA-induced mammary, ovarian and skin carcinogenesis. *Carcinogenesis.* 2004 Sep;25(9):1747-55.

Nunez NP, Liu H, Meadows GG. PPAR-gamma ligands and amino acid deprivation promote apoptosis of melanoma, prostate, and breast cancer cells. *Cancer Lett.* 2006 May 8;236(1):133-41.

Oberfield JL, Collins JL, Holmes CP, Goreham DM, Cooper JP, Cobb JE, Lenhard JM, Hull-Ryde EA, Mohr CP, Blanchard SG, Parks DJ, Moore LB, Lehmann JM, Plunket K, Miller AB, Milburn MV, Kliewer SA, Willson TM. A peroxisome proliferator-activated receptor gamma ligand inhibits adipocyte differentiation. *Proc Natl Acad Sci U S A.*

1999 May 25;96(11):6102-6.

Oliver WR Jr, Shenk JL, Snaith MR, Russell CS, Plunket KD, Bodkin NL, Lewis MC, Winegar DA, Sznaidman ML, Lambert MH, Xu HE, Sternbach DD, Kliewer SA, Hansen BC, Willson TM. A selective peroxisome proliferator-activated receptor delta agonist promotes reverse cholesterol transport. *Proc Natl Acad Sci U S A*. 2001 Apr 24;98(9):5306-11.

Ozaki H, Yu AY, Della N, Ozaki K, Luna JD, Yamada H, Hackett SF, Okamoto N, Zack DJ, Semenza GL, Campochiaro PA. Hypoxia inducible factor-1alpha is increased in ischemic retina: temporal and spatial correlation with VEGF expression. *Invest Ophthalmol Vis Sci*. 1999 Jan;40(1):182-9.

Panigrahy D, Singer S, Shen LQ, Butterfield CE, Freedman DA, Chen EJ, Moses MA, Kilroy S, Duensing S, Fletcher C, Fletcher JA, Hlatky L, Hahnfeldt P, Folkman J, Kaipainen A. PPARgamma ligands inhibit primary tumor growth and metastasis by inhibiting angiogenesis. *J Clin Invest*. 2002 Oct;110(7):923-32.

Peng J, Zhang L, Drysdale L, Fong GH. The transcription factor EPAS-1/hypoxia-inducible factor 2alpha plays an important role in vascular remodeling. *Proc Natl Acad Sci U S A*. 2000 Jul 18;97(15):8386-91.

Peters JM, Lee SS, Li W, Ward JM, Gavrilova O, Everett C, Reitman ML, Hudson LD, Gonzalez FJ. Growth, adipose, brain, and skin alterations resulting from targeted disruption of the mouse peroxisome proliferator-activated receptor beta(delta). *Mol Cell Biol*. 2000 Jul;20(14):5119-28.

Peters JM, Cattley RC, Gonzalez FJ. Role of PPAR alpha in the mechanism of action of the nongenotoxic carcinogen and peroxisome proliferator Wy-14,643. *Carcinogenesis*. 1997 Nov;18(11):2029-33.

Pfaffl MW. A new mathematical model for relative quantification in real-time RT-PCR. *Nucleic Acids Res*. 2001 May 1;29(9):e45.

Pineda Torra I, Jamshidi Y, Flavell DM, Fruchart JC, Staels B. Characterization of the human PPARalpha promoter: identification of a functional nuclear receptor response

element. *Mol Endocrinol.* 2002 May;16(5):1013-28.

Placha W, Gil D, Dembinska-Kiec A, Laidler P. The effect of PPARgamma ligands on the proliferation and apoptosis of human melanoma cells. *Melanoma Res.* 2003 Oct;13(5):447-56.

Rajpurohit R, Koch CJ, Tao Z, Teixeira CM, Shapiro IM. Adaptation of chondrocytes to low oxygen tension: relationship between hypoxia and cellular metabolism. *J Cell Physiol.* 1996 Aug;168(2):424-32.

Ravi R, Mookerjee B, Bhujwalla ZM, Sutter CH, Artemov D, Zeng Q, Dillehay LE, Madan A, Semenza GL, Bedi A. Regulation of tumor angiogenesis by p53-induced degradation of hypoxia-inducible factor 1alpha. *Genes Dev.* 2000 Jan 1;14(1):34-44.

Ren D, Collingwood TN, Rebar EJ, Wolffe AP, Camp HS. PPARgamma knockdown by engineered transcription factors: exogenous PPARgamma2 but not PPARgamma1 reactivates adipogenesis. *Genes Dev.* 2002 Jan 1;16(1):27-32.

Richard DE, Berra E, Pouyssegur J. Angiogenesis: how a tumor adapts to hypoxia. *Biochem Biophys Res Commun.* 1999 Dec 29;266(3):718-22.

Richard DE, Berra E, Gothie E, Roux D, Pouyssegur J. p42/p44 mitogen-activated protein kinases phosphorylate hypoxia-inducible factor 1alpha (HIF-1alpha) and enhance the transcriptional activity of HIF-1. *J Biol Chem.* 1999 Nov 12;274(46):32631-7.

Rieusset J, Touri F, Michalik L, Escher P, Desvergne B, Niesor E, Wahli W. A new selective peroxisome proliferator-activated receptor gamma antagonist with antiobesity and antidiabetic activity. *Mol Endocrinol.* 2002 Nov;16(11):2628-44.

Roberts RA, James NH, Woodyatt NJ, Macdonald N, Tugwood JD. Evidence for the suppression of apoptosis by the peroxisome proliferator activated receptor alpha (PPAR alpha). *Carcinogenesis.* 1998 Jan;19(1):43-8.

Rosen ED, Hsu CH, Wang X, Sakai S, Freeman MW, Gonzalez FJ, Spiegelman BM. C/EBPalpha induces adipogenesis through PPARgamma: a unified pathway.

Genes Dev. 2002 Jan 1;16(1):22-6.

Rosenberger C, Mandriota S, Jurgensen JS, Wiesener MS, Horstrup JH, Frei U, Ratcliffe PJ, Maxwell PH, Bachmann S, Eckardt KU. Expression of hypoxia-inducible factor-1alpha and -2alpha in hypoxic and ischemic rat kidneys. *J Am Soc Nephrol.* 2002 Jul;13(7):1721-32.

Ryan HE, Lo J, Johnson RS. HIF-1 alpha is required for solid tumor formation and embryonic vascularization. *EMBO J.* 1998 Jun 1;17(11):3005-15.

Rybczynski PJ, Zeck RE, Dudash J Jr, Combs DW, Burris TP, Yang M, Osborne MC, Chen X, Demarest KT. Benzoxazinones as PPARgamma agonists. 2. SAR of the amide substituent and in vivo results in a type 2 diabetes model. *J Med Chem.* 2004 Jan 1;47(1):196-209.

Saez E, Rosenfeld J, Livolsi A, Olson P, Lombardo E, Nelson M, Banayo E, Cardiff RD, Izpisua-Belmonte JC, Evans RM. PPAR gamma signaling exacerbates mammary gland tumor development. *Genes Dev.* 2004 Mar 1;18(5):528-40.

Saez E, Tontonoz P, Nelson MC, Alvarez JG, Ming UT, Baird SM, Thomazy VA, Evans RM. Activators of the nuclear receptor PPARgamma enhance colon polyp formation. *Nat Med.* 1998 Sep;4(9):1058-61.

Saladin R, Fajas L, Dana S, Halvorsen YD, Auwerx J, Briggs M. Differential regulation of peroxisome proliferator activated receptor gamma1 (PPARgamma1) and PPARgamma2 messenger RNA expression in the early stages of adipogenesis. *Cell Growth Differ.* 1999 Jan;10(1):43-8.

Satyamoorthy K, Meier F, Hsu MY, Berking C, Herlyn M. Human xenografts, human skin and skin reconstructs for studies in melanoma development and progression. *Cancer Metastasis Rev.* 1999;18(3):401-5.

Schipani E, Ryan HE, Didrickson S, Kobayashi T, Knight M, Johnson RS. Hypoxia in cartilage: HIF-1alpha is essential for chondrocyte growth arrest and survival. *Genes Dev.* 2001 Nov 1;15(21):2865-76.

- Schoonjans K, Staels B, Auwerx J. The peroxisome proliferator activated receptors (PPARS) and their effects on lipid metabolism and adipocyte differentiation. *Biochim Biophys Acta*. 1996 Jul 26;1302(2):93-109.
- Semenza G. Signal transduction to hypoxia-inducible factor 1. *Biochem Pharmacol*. 2002 Sep;64(5-6):993-8.
- Semenza GL. Targeting HIF-1 for cancer therapy. *Nat Rev Cancer*. 2003 Oct;3(10):721-32.
- Semenza GL. Involvement of hypoxia-inducible factor 1 in human cancer. *Intern Med*. 2002 Feb;41(2):79-83.
- Shalev A, Siegrist-Kaiser CA, Yen PM, Wahli W, Burger AG, Chin WW, Meier CA. The peroxisome proliferator-activated receptor alpha is a phosphoprotein: regulation by insulin. *Endocrinology*. 1996 Oct;137(10):4499-502.
- Shao D, Rangwala SM, Bailey ST, Krakow SL, Reginato MJ, Lazar MA. Interdomain communication regulating ligand binding by PPAR-gamma. *Nature*. 1998 Nov 26;396(6709):377-80.
- Shappell SB, Gupta RA, Manning S, Whitehead R, Boeglin WE, Schneider C, Case T, Price J, Jack GS, Wheeler TM, Matusik RJ, Brash AR, Dubois RN. 15S-Hydroxyeicosatetraenoic acid activates peroxisome proliferator-activated receptor gamma and inhibits proliferation in PC3 prostate carcinoma cells. *Cancer Res*. 2001 Jan 15;61(2):497-503.
- Shibuya A, Wada K, Nakajima A, Saeki M, Katayama K, Mayumi T, Kadowaki T, Niwa H, Kamisaki Y. Nitration of PPARgamma inhibits ligand-dependent translocation into the nucleus in a macrophage-like cell line, RAW 264. *FEBS Lett*. 2002 Aug 14;525(1-3):43-7.
- Soengas MS, Lowe SW. Apoptosis and melanoma chemoresistance. *Oncogene*. 2003 May 19;22(20):3138-51.
- Spiegelman B, PPAR-gamma: adipogenic regulator and thiazolidinedione receptor.

Diabetes. 1998 Apr;47(4):507-14.

Suchanek KM, May FJ, Robinson JA, Lee WJ, Holman NA, Monteith GR, Roberts-Thomson SJ. Peroxisome proliferator-activated receptor alpha in the human breast cancer cell lines MCF-7 and MDA-MB-231. *Mol Carcinog*. 2002 Aug;34(4):165-71.

Sznajdman ML, Haffner CD, Maloney PR, Fivush A, Chao E, Goreham D, Sierra ML, LeGrumelec C, Xu HE, Montana VG, Lambert MH, Willson TM, Oliver WR Jr, Sternbach DD. Novel selective small molecule agonists for peroxisome proliferator-activated receptor delta (PPARdelta)--synthesis and biological activity. *Bioorg Med Chem Lett*. 2003 May 5;13(9):1517-21.

Tan NS, Shaw NS, Vinckenbosch N, Liu P, Yasmin R, Desvergne B, Wahli W, Noy N. Selective cooperation between fatty acid binding proteins and peroxisome proliferator-activated receptors in regulating transcription. *Mol Cell Biol*. 2002 Jul;22(14):5114-27. Erratum in: *Mol Cell Biol* 2002 Sep;22(17):6318.

Thieringer R, Fenyk-Melody JE, Le Grand CB, Shelton BA, Detmers PA, Somers EP, Carbin L, Moller DE, Wright SD, Berger J. Activation of peroxisome proliferator-activated receptor gamma does not inhibit IL-6 or TNF-alpha responses of macrophages to lipopolysaccharide in vitro or in vivo. *J Immunol*. 2000 Jan 15;164(2):1046-54.

Treins C, Giorgetti-Peraldi S, Murdaca J, Semenza GL, Van Obberghen E. Insulin stimulates hypoxia-inducible factor 1 through a phosphatidylinositol 3-kinase/target of rapamycin-dependent signaling pathway. *J Biol Chem*. 2002 Aug 2;277(31):27975-81.

Victor N, Ivy A, Jiang BH, Agani FH. Involvement of HIF-1 in invasion of Mum2B uveal melanoma cells. *Clin Exp Metastasis*. 2006;23(1):87-96.

Volm M, Koomagi R. Hypoxia-inducible factor (HIF-1) and its relationship to apoptosis and proliferation in lung cancer. *Anticancer Res*. 2000 May-Jun;20(3A):1527-33.

Wahli W. Peroxisome proliferator-activated receptors (PPARs): from metabolic control to epidermal wound healing. *Swiss Med Wkly*. 2002 Feb 23;132(7-8):83-91.

- Wang C, Fu M, Angeletti RH, Siconolfi-Baez L, Reutens AT, Albanese C, Lisanti MP, Katzenellenbogen BS, Kato S, Hopp T, Fuqua SA, Lopez GN, Kushner PJ, Pestell RG. Direct acetylation of the estrogen receptor alpha hinge region by p300 regulates transactivation and hormone sensitivity. *J Biol Chem*. 2001 May 25;276(21):18375-83
- Wang GL, Semenza GL. Purification and characterization of hypoxia-inducible factor 1. *J Biol Chem*. 1995 Jan 20;270(3):1230-7.
- Wang LH. Molecular signaling regulating anchorage-independent growth cancer cells. *Mt Sinai J Med*. 2004 Nov;71(6):361-7.
- Wang T, Xu J, Yu X, Yang R, Han ZC. Peroxisome proliferator-activated receptor gamma in malignant diseases. *Crit Rev Oncol Hematol*. 2006 Apr;58(1):1-14.
- Wenger RH, Kvietikova I, Rolfs A, Gassmann M, Marti HH. Hypoxia-inducible factor-1 alpha is regulated at the post-mRNA level. *Kidney Int*. 1997 Feb;51(2):560-3.
- Westergaard M, Henningsen J, Svendsen ML, Johansen C, Jensen UB, Schroder HD, Kratchmarova I, Berge RK, Iversen L, Bolund L, Kragballe K, Kristiansen K. Modulation of keratinocyte gene expression and differentiation by PPAR-selective ligands and tetradecylthioacetic acid. *J Invest Dermatol*. 2001 May;116(5):702-12.
- Westin S, Kurokawa R, Nolte RT, Wisely GB, McInerney EM, Rose DW, Milburn MV, Rosenfeld MG, Glass CK. Interactions controlling the assembly of nuclear receptor heterodimers and co-activators. *Nature*. 1998 Sep 10;395(6698):199-202.
- Wiesener MS, Maxwell PH. HIF and oxygen sensing; as important to life as the air we breathe? *Ann Med*. 2003;35(3):183-90.
- Willson TM, Cobb JE, Cowan DJ, Wiethe RW, Correa ID, Prakash SR, Beck KD, Moore LB, Kliwer SA, Lehmann JM. The structure-activity relationship between peroxisome proliferator-activated receptor gamma agonism and the antihyperglycemic activity of thiazolidinediones. *J Med Chem*. 1996 Feb 2;39(3):665-8.
- Wu RC, Smith CL, O'Malley BW. Transcriptional regulation by steroid receptor coactivator

phosphorylation. *Endocr Rev.* 2005 May;26(3):393-9.

Wu Z, Xie Y, Bucher NL, Farmer SR. Conditional ectopic expression of C/EBP beta in NIH-3T3 cells induces PPAR gamma and stimulates adipogenesis. *Genes Dev.* 1995 Oct 1;9(19):2350-63.

Xu HE, Lambert MH, Montana VG, Plunket KD, Moore LB, Collins JL, Oplinger JA, Kliewer SA, Gampe RT Jr, McKee DD, Moore JT, Willson TM. Structural determinants of ligand binding selectivity between the peroxisome proliferator-activated receptors. *Proc Natl Acad Sci U S A.* 2001 Nov 20;98(24):13919-24.

Yamakawa-Karakida N, Sugita K, Inukai T, Goi K, Nakamura M, Uno K, Sato H, Kagami K, Barker N, Nakazawa S. Ligand activation of peroxisome proliferator-activated receptor gamma induces apoptosis of leukemia cells by down-regulating the c-myc gene expression via blockade of the Tcf-4 activity. *Cell Death Differ.* 2002 May;9(5):513-26.

Yamauchi T, Waki H, Kamon J, Murakami K, Motojima K, Komeda K, Miki H, Kubota N, Terauchi Y, Tsuchida A, Tsuboyama-Kasaoka N, Yamauchi N, Ide T, Hori W, Kato S, Fukayama M, Akanuma Y, Ezaki O, Itai A, Nagai R, Kimura S, Tobe K, Kagechika H, Shudo K, Kadowaki T. Inhibition of RXR and PPARgamma ameliorates diet-induced obesity and type 2 diabetes. *J Clin Invest.* 2001 Oct;108(7):1001-13.

Yasinska IM, Sumbayev VV. S-nitrosation of Cys-800 of HIF-1alpha protein activates its interaction with p300 and stimulates its transcriptional activity. *FEBS Lett.* 2003 Aug 14;549(1-3):105-9.

Yin F, Wakino S, Liu Z, Kim S, Hsueh WA, Collins AR, Van Herle AJ, Law RE. Troglitazone inhibits growth of MCF-7 breast carcinoma cells by targeting G1 cell cycle regulators. *Biochem Biophys Res Commun.* 2001 Sep 7;286(5):916-22.

Zamir I, Zhang J, Lazar MA. Stoichiometric and steric principles governing repression by nuclear hormone receptors. *Genes Dev.* 1997 Apr 1;11(7):835-46.

Zhang C, Baker DL, Yasuda S, Makarova N, Balazs L, Johnson LR, Marathe GK, McIntyre TM, Xu Y, Prestwich GD, Byun HS, Bittman R, Tigyi G. Lysophosphatidic acid

induces neointima formation through PPARgamma activation. *J Exp Med.* 2004 Mar 15;199(6):763-74.

Zhang Q, Zhang ZF, Rao JY, Sato JD, Brown J, Messadi DV, Le AD. Treatment with siRNA and antisense oligonucleotides targeted to HIF-1alpha induced apoptosis in human tongue squamous cell carcinomas. *Int J Cancer.* 2004 Oct 10;111(6):849-57.

Zhang X, Kon T, Wang H, Li F, Huang Q, Rabbani ZN, Kirkpatrick JP, Vujaskovic Z, Dewhirst MW, Li CY. Enhancement of hypoxia-induced tumor cell death in vitro and radiation therapy in vivo by use of small interfering RNA targeted to hypoxia-inducible factor-1alpha. *Cancer Res.* 2004 Nov 15;64(22):8139-42.

Zhou YC, Waxman DJ. STAT5b down-regulates peroxisome proliferator-activated receptor alpha transcription by inhibition of ligand-independent activation function region-1 trans-activation domain. *J Biol Chem.* 1999 Oct 15;274(42):29874-82.

Zhu Y, Qi C, Calandra C, Rao MS, Reddy JK. Cloning and identification of mouse steroid receptor coactivator-1 (mSRC-1), as a coactivator of peroxisome proliferator-activated receptor gamma. *Gene Expr.* 1996;6(3):185-95.



Caroline Mills

Department of Biochemistry & Microbiology

1542 Spring Valley Drive

Huntington, West Virginia 25704

304-696-7287

EDUCATION

Marshall University:

- Ph.D. Candidate in Biomedical Sciences – July 2000 – March 2007

West Virginia University:

- B.S. Biology – August 1995 – December 1999

RESEARCH EXPERIENCE

- The function of Hypoxia Inducible Factor 1 α and HIF-1 α 785 in human melanoma progression, Marshall University, January 2005 - present
- The regulation and function of Peroxisome Proliferator Activated Receptors in human melanoma progression, Marshall University, July 2000 – May 2005
- Used recombinant DNA techniques to clone a gene inhibiting HIV replication into a mammalian expression vector, Undergraduate Research in Biochemistry, West Virginia University, Mentor: Dr. Vinay K. Pathak - Fall 1998

TECHNICAL SKILLS

- Laboratory:** Confocal Microscopy, Scanning Electron Microscopy, Florescence microscopy, western blotting, northern blotting (radioactive and digoxigenin), Quantigene (Genospectra) mRNA analysis, qPCR, RT-PCR, immunoprecipitation, immunohistochemistry, ³H-assay, tissue culture, tissue procurement from live animal (rat), cloning, site-directed mutagenesis, lentivirus production/titration/transduction
- Computer:** Very proficient in all Microsoft products, bioinformatics applications, SigmaStat/SigmaPlot, Adobe Photoshop, PathwayStudio

PRESENTATIONS

- Marshall University Center for African American Students Lecture Series
Huntington, WV, October 2005
 “The Road Less Traveled: My Experiences as a Minority in the Research Sciences”
- American Association of Cancer Research (AACR)
Anaheim, California, April 2005
 Poster Presentation: “Comparison of Peroxisome Proliferator-Activated Receptor- α expression and function in human melanoma and human melanocytes.”
 Caroline Mills, Zalfa Abdel-Malek, Richard M. Niles
- Melanoma Research Congress
Phoenix, Arizona, November 2004
 Poster Presentation: “Comparison of Peroxisome Proliferator-Activated Receptor Subtype Expression and Function in Human Melanoma and Human Melanocytes”
 Caroline Mills, Zalfa Abdel-Malek, Richard M. Niles
- Marshall University School of Medicine Seminar Series
Huntington, West Virginia, April 2004
 “Hypoxia, HIF-1, and Oxygen Sensing: A novel control mechanism for transcription factors”
- Marshall University School of Medicine Seminar Series
Huntington, West Virginia, May 2003
 “Stem Cells”

TEACHING EXPERIENCE

- Northern Blotting using Digoxigenin Labeled Probes. 2-three hour labs – BMS 670: Molecular Cloning Lab – Spring 2005 and Spring 2006
- TNF α Signaling. 50 minute course lecture. Marshall University, BIC 643: Molecular Signal Transduction – Fall 2002
- Methods of studying mRNA. 50 minute course lecture. Marshall University, BIC 638: Nucleic Acids and Protein Synthesis – Spring 2001

PUBLICATIONS

- Function and regulation of Peroxisome Proliferator Activated Receptors in mouse and human melanoma. **Caroline N. Mills**, Linda L. Eastham, Richard M. Niles. *Manuscript in preparation*
- HIF-1 α and HIF-1 α 785 in the progression of human melanoma. **Caroline N. Mills**, Sandeep Joshi, and Richard M. Niles. *Manuscript in preparation*
- Obesity and salt-sensitive hypertension in Zucker rats: Roles of Dietary and Genetic Factors. Ryan G. Morrison, **Caroline N. Mills**, Antoinette L. Moran, Chelsea E. Walton, Mohamed H. Sadek, Elsa I. Mangiarua, and Paulette S. Wehner, William D. McCumbee. *Manuscript in preparation*

AWARDS

- 2006 AACR Minority Scholar Award in Cancer Research – January 2006
- NIH Research Grant supplement for Underrepresented Minorities funded by the Comprehensive Minority Biomedical Branch, June 2002 – March 2005
- Storer Scholarship, West Virginia University, August 1995 – December 1999